



Final Report

**Department of Defense
Enhanced Particulate Matter Surveillance Program
(EPMSP)**

Prepared for:

**Enhanced Particulate Matter Surveillance Sub-Group
Particulate Matter Working Group
Deputy Assistant Secretary of Defense for Force Health Promotion and Readiness
Assistant Secretary of Defense for Health Affairs**

and

**Natural Environments Test Office
US Army Development Test Command
Yuma Proving Ground, Arizona**

Contract Number: W9124R-05-C-0135/SUBCLIN 000101-ACRN-AB

Prepared by:

**Drs. Johann P. Engelbrecht
Eric V. McDonald
John A. Gillies
Alan W. Gertler**

Desert Research Institute (DRI)
2215 Raggio Parkway
Reno, NV 89512-1095
tel: (775) 674 7027 • fax: (775) 674 7009 • e-mail: johann@dri.edu

With technical contributions from:

**Dr. R.K.M. (Jay) Jayanty, RTI International, Raleigh, NC
Gary Casuccio, RJ Lee Group, Inc., Monroeville, PA**

February, 2008

EXECUTIVE SUMMARY

Purpose

The purpose of the study was to provide US Central Command (USCENTCOM) with scientifically founded information on the chemical and physical properties of dust collected at deployment locations within their Area of Responsibility (AOR).

Results from this program are available to the Department of Defense's Occupational and Health Physicians, as well as environmental health professionals, to assist them in assessing the potential human health risks from exposure to ambient particulate matter at Middle East military bases. In addition, data on dust will allow for an assessment of its harmful effect on military equipment. Examples from this study of major and trace element chemistry as well as mineralogy and other physical properties of dust are presented in this report.

To fully understand mineral dusts, their chemical and physical properties as well as mineralogical interrelationships need to be understood. This Enhanced Particulate Matter Surveillance Program (EPMSP) demonstrates the benefits of integrating analytical results from complementary disciplines towards a better understanding of mineral dusts and other aerosols, as encountered at Forward Operating Bases and Forward Operating Sites (FOB/FOS).

Sampling and Analysis

Aerosol and bulk soil samples were collected during a period of approximately one year at 15 military sites—including Djibouti, Afghanistan (Bagram, Khowst), Qatar, United Arab Emirates, Iraq (Balad, Baghdad, Tallil, Tikrit, Taji, Al Asad), and Kuwait (Northern, Central, Coastal, and Southern regions).

Three collocated low volume particulate samplers, one each for total suspended (TSP), less than 10 μm in aerodynamic diameter (PM_{10}) and less than 2.5 μm in aerodynamic diameter ($\text{PM}_{2.5}$) particulates were deployed at each of the 15 sites. The three samplers were set to start and stop simultaneously, to provide filter sets for comparison of the three size fractions. A "1 in 6 day" sampling schedule was generally followed, and although the sites did sample at this frequency, not all sites sampled on the same sixth day.

The purpose of the chemical analysis was to measure levels of potentially harmful trace elements such as lead, arsenic, and other metals. The major element and ion chemistry provides an estimate of mineral components—such as quartz, clays, hematite, evaporites, etc.—which themselves may be hazardous to health or could be carriers of other toxic substances. X-ray diffractometry (XRD) provided a measure of the mineral content of dust, which is the main component of aerosols in these desert regions. Scanning Electron Microscopy (SEM) with Energy Dispersive Spectroscopy (EDS) was used to analyze chemical composition of small individual particles of relevance to understanding mineralogical interrelationships such as surface coatings, intergrowths and other particle features. Secondary electron images provided information on particle size and shape, which also can be linked with human health effects (e.g., shards of quartz or asbestos

fibers that cause physical injuries to lung tissue). Computer Controlled Scanning Electron Microscopy (CCSEM) was used for automated analysis of a large number of individual particles which provide data on particle size distributions and chemical compositions.

Of 2,308 (excluding blanks) Teflon® membrane and quartz fiber filters sampled in the field, 2207 (96%) were chemically analyzed, and after eliminating voided results, provided a filter recovery of 2022 (88%) for data analysis. Laboratory results from the Enhanced Particulate Matter Surveillance Program (EPMSP) study include 66,462 analyses on Teflon® membrane, 23,807 on quartz fiber, and several million single particle analyses on Nuclepore® filters.

Analytical results were recorded on spreadsheets and grouped by sampling site, analytical technique, and chemical species for a third level of data validation and analysis. All results, together with summary tables and more than 1,000 graphical representations are available on the Defense Occupational and Environmental Health Readiness System (DOEHRS) Occupational and Environmental Health Surveillance Portal (<https://doehportal.apgea.army.mil/doehrs-oehs/>).

Findings

Short-term dust events—exacerbated by dirt roads, agricultural activities, and disturbance of the desert floor by motorized vehicles—all contribute to exceedance of both PM₁₀ and PM_{2.5} mass exposure guidelines and standards. The highest annual average PM₁₀ levels were recorded at Tikrit, Tallil, and Central Kuwait. Elevated PM_{2.5} levels are a health concern, with means varying from 35 µg/m³ for Djibouti to as high as 103 µg/m³ for Baghdad and 114 µg/m³ for Tikrit. The USACHPPM 1-Year Military Exposure Guideline (MEG) values of 50 µg/m³ for PM₁₀, and of 15 µg/m³ for PM_{2.5} were exceeded at all 15 sites for the entire sampling period of approximately one year.

While the compositions of particulate matter (PM) from different regions vary, this study shows that PM concentrations from the Middle East are as much as ten times greater overall than those at both urban and rural southwestern U.S. air monitoring sites. Average PM_{2.5} mass and chemical concentration levels from the deployment sites are—except for a few species such as nitrate, sodium, and rubidium—greater than chemical abundances in PM_{2.5} samples measured at rural Interagency Monitoring of Protected Visual Environments (IMPROVE) and urban Speciation Trends Network (STN) sites in the southwestern U.S.

In each case, mineralogical content, chemical composition, as well as individual particle results of ambient and re-suspended soil bear the signature of that particular region's geology. Examples include the high quartz content of four Kuwait sites, high percentage of calcite of the United Arab Emirates (UAE) samples, high dolomite content of Al Asad samples, and titaniferous magnetite bearing soil of Djibouti.

Dust events result in elevated levels of soil-forming elements in aerosols—including magnesium (Mg), aluminum (Al), silicon (Si), potassium (K), calcium (Ca), titanium

(Ti), vanadium (V), manganese (Mn), iron (Fe), rubidium (Rb), strontium (Sr), zirconium (Zr), and barium (Ba).

In general, dusts from these Middle East sites were found to be similar to dust and rocks from other desert regions. Most dusts contain mixtures of silicate minerals, carbonates, oxides, sulfates, and salts in various proportions, as reflected by their chemistry and mineralogy. Differences among regions lie in the relative proportions of these minerals in soils. In comparison to the Sahara, China, and the U.S., the 15 Middle East sites have lower proportions of silicon (Si) and higher proportions of calcium (Ca) and magnesium (Mg). The last two components are largely contained in calcitic and dolomitic limestone, more evident in samples from UAE and Al Asad. Iron and manganese oxides occur in greater concentrations in dust from the Sahara, China, and the U.S., compared to those from Middle East samples. Aluminum (Al), a major component of clay minerals, is found to be similar for most dusts.

CCSEM combined with Backscattered Electron Image (BEI) results from this study show that quartz and other silicate minerals, and to a lesser extent carbonate particles, are often coated by Si-Al-Mg layers, which we interpret as being the clay minerals palygorskite and/or montmorillonite/illite. Mineral coatings are not unique to the USCENCOM study area and fine-grained clay minerals, with or without iron and manganese oxides, commonly occur as thin coatings on mineral grains and rock surfaces, in the latter instance referred to as “desert varnish” [Potter, 1977].

Interactive CCSEM and SEM analysis of the ultrafine (<0.5 μ m) particles show their chemistry and morphology to differ substantially from those of the coarser fractions. The former contains far less geological components (e.g., silicon, aluminum, iron, magnesium, calcium, or magnesium) than the coarser fractions. Ultrafines very often contain spheroidal particles of carbon, together with sulfur, sodium, and chlorine and, in a few instances lead, bromine and chlorine. Origin of the spheroids is uncertain, but it can be assumed from their carbon and sulfur content that many of these are from various oil, gasoline, and natural gas combustion processes, including motor vehicle tailpipe emissions.

Carbon chains, considered to be elemental carbon from combustion sources such as diesel vehicle emissions or possibly burn pits, were identified in small amounts at some sites. The highest concentrations on average of approximately 2.5% carbon by mass, as measured by CCSEM, were found at Bagram, Afghanistan and Baghdad, Iraq, and were substantially lower at the other sites.

Non-dust storm events resulted in elevated trace metal concentrations at Baghdad, Balad, and Taji. Metals concentrated in the fine (PM_{2.5}) size fractions at the three sites during these events include lead (Pb), arsenic (As), cadmium (Cd), antimony (Sb), and zinc (Zn). CCSEM results confirm that lead (Pb) is concentrated in the fine size (0.5–1.0 μ m) fraction. Comments on field data sheets imply that these events coincide with burn pit smoke impacting the monitoring sites. Open-pit burning is often used at FOB/FOS for residential trash, human, and medical waste disposal. In addition, tires, oil, plastic, and

metal objects (e.g., batteries, electronic circuit boards, and ammunition) could be burned in these pits, resulting in emission of trace metals into the atmosphere. Consistency in metal composition at all three sites points to a similar source type impacting the Baghdad-Balad-Taji metropolitan region, including the military bases. Secondary lead smelting together with lead acid and dry cell battery manufacturing facilities are known from these and other metropolitan areas of Iraq. A contribution to lead in the atmosphere is also from leaded gasoline used in the Middle East, electronic circuit board recycling, and detonation of ordnance to a much lesser extent.

Summary and Recommendations

This study clearly shows the three main air pollutant types to be geological dust, smoke from burn pits, and heavy metal condensates possibly from lead smelting and battery manufacturing facilities. The above findings can be synthesized under the following bullets:

- **Geological dust.** Little can be done about dust from regional dust storms. Dust at FOB/FOS, however, can be mitigated using best management practices (e.g., watering, spraying with dust suppressants, application of gravel, restricting movement, minimizing disturbance) to lower the local dust emission potential. Elevated PM_{2.5} levels are of health concern. We recommend that continuous PM_{2.5} monitors (beta gauges or similar) be installed at each of the military sites, including those sites not included in this study. This will provide information on the relationship between PM_{2.5} levels, potential health effects, and effectiveness of dust containment practices.
- **Burn pits.** Open burning results in a cloud of smoke hanging above these bases, more so during winter months. New incinerators were installed at Balad (Anaconda Times; June 20, 2007) and other sites, to take care of human and medical waste. Toxic metal objects plus other combustible products (e.g., wood, paint, plastic, tires, batteries, electronic circuit boards, ammunition, petrochemical products), however, may still end up in burn pits. To prevent dioxins, polycyclic aromatic compounds, volatile organic compounds, and toxic metals from being emitted, open burning should be discouraged.
- A likely source of lead (Pb) and associated zinc (Zn), cadmium (Cd), arsenic (As), and antimony (Sb) in the Baghdad-Balad-Taji region is the battery manufacturing industry. This points to emissions from secondary lead smelters (<http://www.cpa-iraq.org/business/industries/Battery%20Co.xls>.) and related battery manufacturing facilities, all impacting the health of the population. We recommend that these facilities be identified and moved outside heavy populated areas.
- Since Iraq uses leaded gasoline, gasoline vehicle emissions are a source of lead in the atmosphere. Lead from vehicle emissions previously deposited on dirt roads is also continually being re-suspended and may for many years be a source of aerosol lead.
- Electronic circuit board recycling may be a contributing source of lead, zinc, and cadmium in the atmosphere.

- Under fall to spring meteorological conditions, smoke and heavy metal pollutants become trapped within the atmospheric boundary layer and impact the population living along at least a 75 km stretch of the Tigris River valley.
- Research areas included looking for freshly fractured shards of quartz. Several hundred SEM secondary electron images of individual particles from all 15 sites provided no evidence of such freshly fractured quartz grains. In all instances, quartz grains had rounded edges and generally were coated by clay minerals and iron oxides.

Table of Contents

1	INTRODUCTION	1
2	SAMPLING	1
2.1	Sampling Sites	1
2.2	Sampling Equipment.....	2
2.3	Filter Media.....	2
2.4	Sampling Schedule.....	3
2.5	Bulk Samples	5
3	ANALYTICAL TECHNIQUES.....	5
3.1	Filter Analysis.....	5
3.1.1	Gravimetry	5
3.1.2	X-ray Fluorescence (XRF) Spectrometry	5
3.1.3	Inductively Coupled Plasma Mass Spectrometry (ICP-MS)	5
3.1.4	Ion Chromatography (IC)	6
3.1.5	Inductively Coupled Plasma Optical Emission Spectrometry (ICP-OES) .	6
3.1.6	Thermal Optical Transmission (TOT) Analysis	6
3.2	Individual Particle Analysis.....	6
3.2.1	Computer Controlled Scanning Electron Microscopy (CCSEM).....	6
3.2.2	Scanning Electron Microscopy (SEM)	6
3.3	Mineral Analysis by X-ray Diffraction (XRD).....	7
3.4	Data Processing and Storage.....	7
4	RESULTS	7
4.1	Gravimetry and Filter Chemistry	7
4.1.1	Gravimetry	7
4.1.2	Comparison to Air Quality and Health Standards	9
4.1.3	Comparison to Rural and Urban Sites in the U.S.	14
4.1.4	Trace Metals.....	15
4.1.5	Major Chemical Species	19
4.1.6	Organic and Elemental Carbon.....	22
4.2	Scanning Electron Microscopy (SEM)	23
4.2.1	Computer Controlled Scanning Electron Microscopy (CCSEM).....	24
4.2.2	Scanning Electron Microscopy of Ultrafines (<0.5µm)	25
4.2.3	Transmission Electron Microscopy (TEM)	25
4.2.4	Secondary Electron Images.....	25
4.2.5	Particle Size Distributions.....	37
4.3	Grab Soil Samples.....	38
4.3.1	Mineralogy of <38 µm Screened Soils	38
	Djibouti	38
	Afghanistan	39
	Qatar and the UAE.....	39
	Iraq	40
	Kuwait.....	41
4.3.2	Chemistry of Re-suspended Soils	41
	Major Element Chemistry	41
	Trace Element Chemistry	43

4.3.3	Scanning Electron Microscopy of Re-suspended Soils	44
4.3.4	Bulk Soil Chemistry.....	45
5	SUMMARY AND CONCLUSIONS	46
6	RECOMMENDATIONS	48
6.1	Remediation	49
6.2	Future Investigations.....	49
7	ACKNOWLEDGEMENTS	50
8	GLOSSARY	53
8.1	Acronyms and Mnemonics	53
8.2	Geological Terms.....	54
8.3	Sampling Sites, USCENCOM AOR	55
9	REFERENCES	56

List of Figures

Figure 2-1.	Locality map of 15 sampling sites at which ambient aerosol samples were collected during a period of approximately one year. Bulk surface soil samples for re-suspension in the laboratory and analysis were also collected at each site.	2
Figure 4-1.	Averaged particulate mass concentrations and uncertainties for TSP, PM ₁₀ , and PM _{2.5} on Teflon® filters for each of the 15 sites. Averaging period is approximately one year.....	8
Figure 4-2.	Location of Department of Defense (DoD) lands in the southwestern U.S. in relation to five rural IMPROVE sites (Dome Land NWA, Joshua Tree NP, Bosque del Apache NWR, Salt Creek, and San Andres NWR) and five urban STN sites (Las Vegas, Los Angeles, Tucson, Albuquerque, and El Paso).....	15
Figure 4-3.	Annual mean distributions of 12 trace metals for (a) TSP, (b) PM ₁₀ , and (c) PM _{2.5} size fractions for each of the 15 sites.....	16
Figure 4-4.	Time-series plot of trace metal concentrations from Baghdad, Iraq, showing corresponding elevated values for (a) lead, (b) zinc, (c) arsenic, and (d) cadmium on the 2006-10-19, 2006-11-30, and 2007-01-11 event days. These metals are concentrated in the PM _{2.5} size fraction.....	17
Figure 4-5	Comparative time series plots of lead concentrations for (a) Baghdad, (b) Balad, and (c) Taji. The events showing elevated lead levels occur on different days for the three sites and on days for which no major regional dust storms were measured, implying local point sources for lead (Pb) with fluctuating emission rates and/or variable meteorological conditions. High event days are listed in a table alongside the figures. Events recorded (R) or not recorded (NR) on field data sheets, together with their total TSP mass levels, are shown in adjacent tables.	18
Figure 4-6.	Major soil forming elements (a) silicon, (b) aluminum, (c) calcium, and (d) manganese as measured on Teflon® filters. Corresponding peak values represent dust blowing events on 2006-03-09, 2006-05-08, 2006-08-13, 2006-10-19, and 2006-11-30.	20
Figure 4-7	Annual mean major chemistry for (a) TSP, (b) PM ₁₀ , and (c) PM _{2.5} . Concentrations are expressed as mass fractions of oxides, sulfate (in gypsum), chloride (in salt), nitrate, and ammonium.....	21

Figure 4-8. Comparison of dust samples from the Middle East, Sahara, China, U.S., world average dust, and world rocks. In the case of the EPMS samples, mean TSP results are shown, from (a) Djibouti; (b) Bagram and Khowst in Afghanistan; (c) Qatar; (d) UAE; (e) Balad, Baghdad, Tallil, Tikrit, and Taji in Iraq; (f) Al Asad in Iraq; (g) Northern, Central, Coastal, and Southern Kuwait; (h) average Southern Sahara [Goudie, 2006]; (i) average Northern Sahara [Goudie, 2006]; (j) average China [Goudie, 2006]; (k) Arizona [Goudie, 2006]; (l) Western Texas [Labban, 2004]; (m) Utah Western Desert [Labban, 2004]; (n) average world dust [Goudie, 2006]; and average world crustal rocks [Clarke, 1916]...... 23

Figure 4-9. Composite of all CCSEM PM₁₀ results measured on Nuclepore® filters, grouped by site. All size fractions, from 0.5 to 10 µm diameter particles, are shown in (a) while the 0.5 to 1.0 µm diameter (fine fraction) subset is shown in (b), demonstrating that lead (Pb) is concentrated in this fine fraction. 26

Figure 4-10. SEM and CCSEM results of ultrafines (<0.5 µm diameter) measured on fifteen PM_{2.5} samples collected on Nuclepore® filters. Compositions of 100 particles analyzed for all species are shown in (a) while individual trace metals are shown on an expanded scale in (b). 27

Figure 4-11. Secondary Electron Images and EDS spectra of two particles on a Nuclepore® filter sampled in Balad, Iraq; (a) zinc (Zn)/lead (Pb) particle with carbon, possibly from a lead and dry cell battery smelting facility; (b) lead (Pb) particle from lead smelting. Dark circles in the field are approximately 0.4 µm pores in the Nuclepore® membrane filters..... 28

Figure 4-12. Secondary Electron Images and EDS spectra of two particles on a Nuclepore® filter sampled in Balad, Iraq. Both (a) and (b) are sections of carbon chains containing high concentrations of lead (Pb), bromine (Br), and chlorine (Cl)—tailpipe emissions from leaded gasoline vehicles. 29

Figure 4-13. Secondary Electron Images from Bagram (a), Bagram (b), Qatar (c), and United Arab Emirates (UAE) (d). Dark circles in the field are approximately 0.4 µm pores in the Nuclepore® membrane filters. 30

Figure 4-14. Secondary Electron Images from Baghdad (a), Baghdad (b), Baghdad (c) and Tikrit (d). Dark circles in the field are approximately 0.4 µm pores in the Nuclepore® membrane filters..... 31

Figure 4-15. Secondary Electron Images from Tikrit (a), Al Asad (b), and Central Kuwait (c and d). Dark circles in the field are approximately 0.4 µm pores in the Nuclepore® membrane filters..... 32

Figure 4-16. A polished section of sieved bulk dust sample from Coastal Kuwait showing compositional details of (a) a quartz grain and (b) its coating, consisting of a magnesium aluminum silicate clay, possibly montmorillonite and/or palygorskite..... 33

Figure 4-17. Secondary Electron Images and EDS spectra of two spherical ultrafine (approx. 0.2 µm diameter) particles on Nuclepore® filters: (a) carbon particle with sulfur from Southern Kuwait and (b) carbon particle with sodium and sulfur from Coastal Kuwait. Both particles may be from combustion of sulfur-rich oil, including diesel fuel.

Dark circles in the field are approximately 0.4 μm pores in the Nuclepore® membrane filters. 34

Figure 4-18. Secondary Electron Images and EDS spectra of two spheroids of ultrafine (approx. 0.5 μm diameter) particles on Nuclepore® filters: (a) carbon particle with sulfur from Al Asad and b) carbon particle from Tikrit in Iraq. Both particles may be from combustion of oil, including diesel fuel. Dark circles in the field are approximately 0.4 μm pores in the Nuclepore® membrane filters..... 35

Figure 4-19. Secondary Electron Images and EDS spectra of two spheroids of ultrafine approx. 0.4 μm diameter) particles on Nuclepore® filters: (a) carbon particle composed of smaller carbon particles from Taji, Iraq and (b) carbon-sodium-sulfur particle from Central Kuwait. Both particles may be from oil combustion processes. Dark circles in the field are approximately 0.4 μm pores in the Nuclepore® membrane filters. 36

Figure 4-20. Particle size distributions by mass percentage as measured by CCSEM, of TSP samples collected on Nuclepore® filters. 37

Figure 4-21. Mineralogical composition by XRD of <38 μm sieved soil samples collected in the vicinity of aerosol sampling sites. 39

Figure 4-22. Dust storm of October 8, 2004, originating from dry Hamoun Lake beds along the Iran-Afghanistan border and partly crossing the Makran Mountains into Pakistan and the Arabian Sea. A split off the plume moved in a northeasterly direction towards Kabul, Bagram, and Khowst. 40

Figure 4-23. Dust storm of January 21, 2006, originating at salt pans and wadis along the northern border of Iraq with Syria and Turkey. This specific storm crossed Iraq and Kuwait and continued on into the Arabian-Persian Gulf..... 41

Figure 4-24. Major element chemistry of PM_{10} (a) and $\text{PM}_{2.5}$ (b) re-suspended samples for each of the 15 sites. Concentration fractions are expressed as oxides, including CO_2 contained in carbonate minerals such as calcite and dolomite. 42

Figure 4-25. Trace element compositions of PM_{10} and $\text{PM}_{2.5}$ re-suspended samples as analyzed by P-MS for each of the 15 sites..... 43

Figure 4-26. CCSEM individual particle analysis on PM_{10} Nuclepore® filters of re-suspended soils..... 44

Figure 4-27. Compositional plot showing major elemental chemistry of fifteen <1000 μm sieved bulk samples. 45

Figure 5-1. Open burn pit typical of Forward Operating Bases and Forward Operating Sites (FOB/FOS) where trash, human and medical waste, and plastic are often burned acknowledgement: Major Dennis S. Palalay, USACHPPM, unclassified presentation, 15 May 2006). Tires, oil, and metal objects (e.g., batteries, electronic circuit boards, and ammunition) also can be burned resulting in emission of trace metals into the atmosphere. 47

List of Tables

Table 2-1. Summary of 1-in-6 day sampling schedule followed at each sampling site in theater. One shipment of 132 exposed filters was lost in transit, but these were replaced by adding sampling days to the end of the original sampling schedule. Analyzed filter days are those for which filter sets were collected for either chemical or CCSEM analysis.....	3
Table 2-2. Summary table of the approximate number of analyses performed on filter media and bulk samples, in the course of the EPMSP.....	4
Table 4-1. Mean mass concentrations for TSP, PM ₁₀ , and PM _{2.5} size fractions, as well as the TSP:PM ₁₀ :PM _{2.5} mass ratios for each of the 15 sites, as measured on Teflon® filters. For comparison, the mean STN (southwestern U.S. urban) and IMPROVE (southwestern U.S. rural) concentrations and ratios, from sites in the U.S. are given.	9
Table 4-2. Comparative table showing concentration ranges in micrograms per cubic meter (µg/m ³) of mean PM _{2.5} site concentrations, as well as various air quality and health standards.	11
Table 4-3. List of the number of Nuclepore® filters analyzed by CCSEM, for each sampled size fraction.....	24
Table 4-4. Particle size distributions by mass percentage, as measured by CCSEM on TSP Nuclepore® filters.....	38
Table 4-5. Trace element compositions of re-suspended PM _{2.5} samples for each of the 15 sites, as analyzed by ICP-MS. The highest trace metal concentrations for each site are shown in red.....	44

Appendices

- APPENDIX A: Tables of site statistics from each of the 15 sampling sites.
- APPENDIX B: RTI report of organic carbon artifact laboratory experiment.
- APPENDIX C: Scope of Work for EPMSP.
- APPENDIX D: DRI Soil Characterization Report.

1 INTRODUCTION

The purpose of the study was to provide USCENTCOM with information on chemical and physical properties of aerosols collected at 15 deployment locations within their Area of Responsibility (AOR). Results from this program are available to the Department of Defense's Occupational and Health Physicians, as well as environmental health professionals, to assist them in assessing potential human health risk from exposure to ambient particulate matter at their Middle East military bases. In addition, information on dust allows for an assessment of its potential harmful effect on military equipment. Examples of major and trace element chemistry, mineralogy, and other physical properties are presented.

A total of 3,136 filter samples were collected on a 1-in-6 day schedule, along with one-time bulk samples, at each of the 15 sites. Sample media included Teflon® membrane and quartz fiber filters for chemical analysis (71 species), and Nuclepore® filters for Scanning Electron Microscopy (SEM) and Computer Controlled Scanning Electron Microscopy (CCSEM). Re-suspension of bulk dust samples onto filters collected from each of the sites was performed by the Desert Research Institute (DRI). These filter samples underwent chemical, individual particle, and mineral analysis on DRI's X-ray diffractometer (XRD). To fully understand mineral dusts, their chemical and physical properties as well as mineralogical interrelationships need to be accurately established. The purpose of the chemical analysis was to determine levels of potentially harmful trace elements such as lead, arsenic, and other metals. The major element and ion chemistry provides an estimate of mineral components (e.g., quartz, clays, hematite, evaporates) which themselves may be hazardous to health or else could be carriers of other toxic substances. XRD provides a measure of mineral content of dust, being the main component of aerosols in these desert regions. Scanning Electron Microscopy (SEM) with Energy Dispersive Spectroscopy (EDS) analyzes chemical composition of small individual particles of relevance to understanding mineralogical interrelationships such as surface coatings, intergrowths, and other particle features. Secondary electron images provide information on particle size and shape, which also can be linked to human health effects (e.g., shards of quartz or asbestos fibers that cause physical injuries to lung tissue). The CCSEM is for automated analysis of a large number of individual particles which provides data on individual particle size distributions and chemical compositions.

2 SAMPLING

2.1 Sampling Sites

The 15 sampling localities are shown in Figure 2-1. These sites were selected to represent areas of potential exposure to military personnel. Sites included one in Djibouti, two in Afghanistan (Bagram and Khowst), one in Qatar, one in the United Arab Emirates (UAE), six in Iraq (Balad, Baghdad, Tallil, Tikrit, Taji, and Al Asad), and four in Kuwait (Northern, Central, Coastal, and Southern).

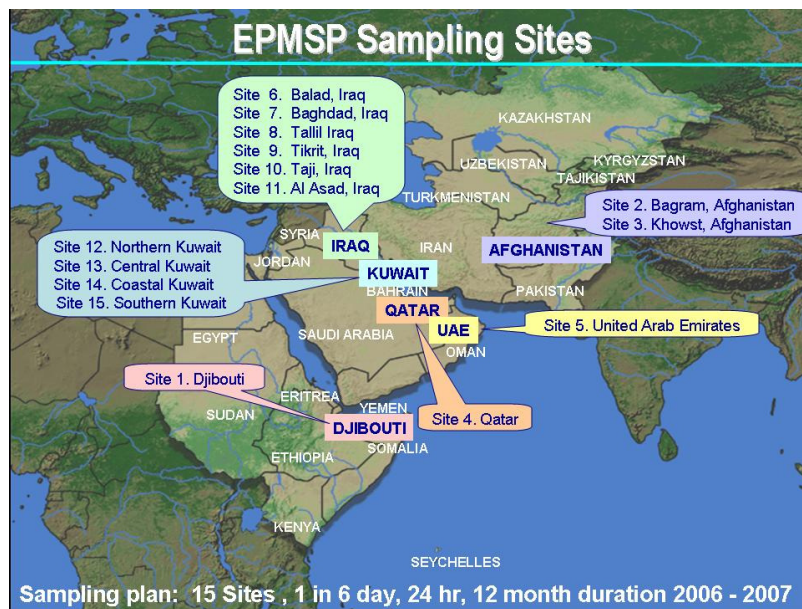


Figure 2-1. Locality map of 15 sampling sites at which ambient aerosol samples were collected during a period of approximately one year. Bulk surface soil samples for re-suspension in the laboratory and analysis were also collected at each site.

Three criteria were used for selection of the EPMSP sites. The first was the intent to collect air samples from the largest geographic dispersion within the AOR of USCENCOM. The second was to select locations where U.S. military forces were present, since they are the exposed population of concern for this study. Finally, the sites selected had to have Preventive Medicine or Military Public Health personnel stationed for the duration of the sampling campaign since they were the scientists, engineers, and technicians responsible for sample collection.

2.2 Sampling Equipment

Three dust sample sizes were collected using collocated low volume (5 liters/min) Airmetrics MiniVol[®] particulate samplers, one each for TSP, PM₁₀, and PM_{2.5}, deployed at each of the 15 sites. The three samplers were set to start and stop simultaneously, to provide filter sets for comparing the three size fractions.

2.3 Filter Media

The filter media (filters) were selected according to the following requirements for each analytical technique:

- The 47 mm diameter Teflon[®] filters were for gravimetry, XRF (40 elements), and ICP-MS (12 metals).
- The 47 mm diameter quartz fiber filters were for gravimetry, IC (4 anions, 1 cation), ICP-OES (4 cations), and TOT (2 carbon species).

- The 47 mm diameter Nuclepore® filters were for individual particle analysis by SEM (secondary electron images) and CCSEM (28 chemical species).

2.4 Sampling Schedule

Three different sample sets were collected on different sampling days, “Sample Set T” on Teflon membrane filters, “Sample Set Q” on quartz fiber filters, and “Sample Set N” on Nuclepore filters.

A 1-in-6 day sampling schedule generally was followed; and, although the sites did sample at this frequency, not all were sampled on the same sixth day. Each sampling day was either Teflon®, quartz fiber, or Nuclepore® filters. During a period of one month, there were two sampling days each for Teflon® and quartz fiber, and one sampling day for Nuclepore®. During the field campaign period, 40% each of the filter samples were Teflon® and quartz fiber and 20% Nuclepore®, so that during the period of the sampling year a maximum of 7% of the days were sampled by each of Teflon® and quartz fiber. For Teflon® and quartz fiber filters the run time was 24 hours. For Nuclepore® filters, the sampling period was two hours, so as to provide lightly loaded filters with dispersed single particles, as required for CCSEM analysis. A summary of sampling days and days for which filters were collected for analyses is in Table 2-1.

Table 2-1. Summary of 1-in-6 day sampling schedule followed at each sampling site in theater. One shipment of 132 exposed filters was lost in transit, but these were replaced by adding sampling days to the end of the original sampling schedule. Analyzed filter days are those for which filter sets were collected for either chemical or CCSEM analysis.

Site No.	Site Locality	Site ID	Start	End	Scheduled sampling days	Analyzed filter days
1	Djibouti	DJI-LEM	2005-12-05	2007-06-09	60	70
2	Bagram, Afghanistan	AFG_BAG	2005-12-07	2004-05-21	60	75
3	Khowst, Afghanistan	AFG_SAL	2006-04-28	2007-06-22	60	60
4	Qatar	QAT_UDE	2006-02-16	2007-02-06	60	60
5	United Arab Emirates	UAE_DHA	2006-02-18	2007-02-07	60	60
6	Balad, Iraq	IRQ_ANA	2006-01-15	2007-03-24	60	60
7	Baghdad, Iraq	IRQ_VIC	2006-01-08	2007-01-11	60	58
8	Iraq	IRQ_ADD	2006-01-15	2007-02-15	60	60
9	Tikrit, Iraq	IRQ_SPE	2006-01-12	2007-03-12	60	62
10	Taji, Iraq	IRQ_TAJ	2006-02-05	2007-02-11	60	60
11	Iraq, Al	IRQ_ALA	2006-01-08	2006-12-26	60	56
12	Northern Kuwait	KUW_BUE	2006-01-28	2007-02-04	60	59
13	Central Kuwait	KUW_AAS	2006-03-14	2007-03-19	60	60
14	Coastal Kuwait	KWT_SHU	2006-01-20	2007-03-20	60	61
15	Southern Kuwait	KUW_ARI	2006-01-21	2007-01-15	60	60
Total					900	921

The number of laboratory analyses performed in the course of the EPMS is summarized in Table 2-2, and includes 66,462 analyses on Teflon® membrane, 23,807 on quartz fiber, and several million single particle analyses on Nuclepore®. All results, together with summary tables and more than 1,000 graphical representations, are stored on the DOEHR Portal.

Table 2-2. Summary table of the approximate number of analyses performed on filter media and bulk samples, in the course of the EPMSF.

	Total Samples	Analytical method	Species/ parameters analyzed (Est.)	Samples/ Particles/Units	Total analyses (Estimate)
AMBIENT FILTER SAMPLES					
<i>Teflon filters</i>					
Mass	1224	Gravimetric	1	1,224	1,224
Elemental analysis	1224	XRF	40	1,224	48,960
Trace metal analysis	1224	ICP-MS	12	1,224	14,688
<i>Quartz fiber filters</i>					
Mass	1223	Gravimetric	1	1,223	1,223
Soluble anions and ammonium	1223	IC	5	1,223	6,115
Soluble cations	1223	ICP-OES	4	1,223	4,892
Carbon and carbonate	1223	TOT	9	1,223	11,007
<i>Nuclepore filters</i>					
Individual particle analysis 0.5-15 micron	243	CCSEM	28	256,334	7,177,352
Images & spectra	84	SEM	1	84	84
Ultrafines < 0.5micron	15	CCSEM	28	1,558	43,624
				Subtotal	7,309,169
RESUSPENDED DUST SAMPLES					
<i>Teflon filters</i>					
Mass	30	Gravimetric	1	30	30
Elemental analysis	30	XRF	40	30	1,200
Trace metal analysis	30	ICP-MS	12	30	360
<i>Quartz fiber filters</i>					
Mass	30	Gravimetric	1	30	30
Soluble anions	30	IC	4	30	120
Soluble cations	30	AA	4	30	120
Carbon and carbonate	30	TOR	9	30	270
Ammonium	30	AC	1	30	30
<i>Nuclepore filters</i>					
Individual particle analysis	15	CCSEM	28	14,900	417,200
				Subtotal	419,360
BULK DUST SAMPLES					
<i>Soil chemistry</i>					
Hydrogen-ion activity	15	pH	1	15	15
Carbonate content	15	Acid digestion	1	15	15
Electrical conductivity	15	EC	1	15	15
<i>Elemental and minerals analysis</i>					
Elemental analysis	15	XRF	13	15	195
Minerals analysis	15	XRD	12	15	180
<i>Particle-size analysis</i>					
Particle-size distribution (sand, silt, clay)	15	PSD	1	15	15
				Subtotal	435
				Total analyses	7,728,964

<u>Acronym</u>	<u>Analytical Method</u>	<u>Application</u>
AA	Atomic Absorption	Cation analysis
AC	Automated Colorimetry	Ammonium analysis
CCSEM	Computer Controlled Scanning Electron Microscopy	Individual particle size, shape and chemistry (0.5 - 15 micron)
EC	Electrical Conductivity	Salts in soil
IC	Ion Chromatography	Anion and ammonium analysis
ICP-MS	Inductively Coupled Plasma Mass Spectrometry	Trace metal analysis
ICP-OES	Inductively Coupled Plasma - Optical Emission Spectrometry	Cation analysis
PSD	Particle-size distribution	Particle-size distribution by laser diffraction
SEM	Scanning Electron Microscopy	Secondary electron particle image & XRF spectrum
TOR	Thermal Optical Reflectance	OC, EC and Carbonate analysis
TOT	Thermal Optical Transmission	OC, EC and Carbonate analysis
XRD	X-ray Diffraction	Mineral analysis
XRF	X-Ray Fluorescence Spectrometry	Major elemental analysis

2.5 Bulk Samples

Bulk soil samples were collected at each of the 15 sites. In each case, approximately 1 kg of soil from the top 10 mm at a previously undisturbed area near the aerosol sampling site was collected. The samples were air dried, and sample splits taken for soil analysis. Further sample splits were sieved to separate the <38 μm particle fractions that were subsequently re-suspended onto filters for chemical and mineralogical analysis.

3 ANALYTICAL TECHNIQUES

To fully understand their potential impact on human health, ambient aerosols and re-suspended soils were chemically, physically, and mineralogically characterized.

3.1 Filter Analysis

Analytical methods applied in this project are briefly described below.

3.1.1 Gravimetry

In total, 1124 Teflon® membrane and 1123 quartz fiber filters were conditioned and weighed prior to and after sampling, to measure the mass of particulate matter sampled in the field during each 24-hour sampling period¹. The way in which filters were handled is specified in the attached USCENTCOM Enhanced Particulate Matter Surveillance Protocol (APPENDIX C). From the flow volumes recorded on data sheets in the field and measured mass, particulate matter (PM) concentrations were calculated to micrograms per cubic meter ($\mu\text{g}/\text{m}^3$) of sampled air.

3.1.2 X-ray Fluorescence (XRF) Spectrometry

In the course of this study, 1124 Teflon® filters, including 92 field and 22 laboratory blanks were analyzed by Energy Dispersive X-ray Fluorescence Spectrometry (EDXRF) for 40 chemical elements including sodium (Na), magnesium (Mg), aluminum (Al), silicon (Si), phosphorus (P), sulfur (S), chlorine (Cl), potassium (K), calcium (Ca), titanium (Ti), vanadium (V), chromium (Cr), manganese (Mn), iron (Fe), cobalt (Co), nickel (Ni), copper (Cu), zinc (Zn), gallium (Ga), arsenic (As), selenium (Se), bromine (Br), rubidium (Rb), strontium (Sr), yttrium (Y), zirconium (Zr), molybdenum (Mo), palladium (Pd), silver (Ag), cadmium (Cd), indium (In), tin (Sn), antimony (Sb), barium (Ba), gold (Au), mercury (Hg), thallium (Tl), lead (Pb), lanthanum (La), and uranium (U). EDXRF is a non-destructive analytical technique performed on filter samples.

3.1.3 Inductively Coupled Plasma Mass Spectrometry (ICP-MS)

After completion and validation of the EDXRF results, the same 1124 Teflon® filters were dissolved in nitric/hydrochloric acid and the solutions analyzed by ICP-MS for 12 trace metals: antimony (Sb), arsenic (As), beryllium (Be), cadmium (Cd), chromium

¹ U.S. EPA Quality Assurance Guidance Document 2.12 – Monitoring $\text{PM}_{2.5}$ in Ambient Air Using Designated Reference or Class I Equivalent Methods, November 1998.

(Cr), lead (Pb), manganese (Mn), nickel (Ni), vanadium (V), zinc (Zn), mercury (Hg), and strontium (Sr).

3.1.4 Ion Chromatography (IC)

Water extractions were performed on one half of each of the 1123 quartz fiber filters, including 91 field and 20 laboratory blanks. Aliquots of the extractions were analyzed by IC for water soluble anions, sulfate (SO_4^{2-}), nitrate (NO_3^-), chloride (Cl^-), phosphate (PO_4^{3-}), and the ammonium (NH_4^+) cation.

3.1.5 Inductively Coupled Plasma Optical Emission Spectrometry (ICP-OES)

Further aliquots of the extractions were analyzed by ICP-OES, for water soluble cations, sodium (Na^+), potassium (K^+), calcium (Ca^{2+}), and magnesium (Mg^{2+}).

3.1.6 Thermal Optical Transmission (TOT) Analysis

Punches from the remaining half of each of the 1123 quartz fiber filters were analyzed for organic carbon (OC) and elemental carbon (EC) by the NIOSH method². Separate punches were acidified to dissolve carbonate ($\text{CO}_3^{=}$), and the latter was determined by the difference in total carbon (TC) between non-acidified and acidified punches.

3.2 Individual Particle Analysis

SEM individual particle analysis was performed on approximately 258 filters selected from approximately 555 sampled Nuclepore® filters. A dual approach was followed, the first being the CCSEM and the second, secondary electron imaging by high magnification SEM.

3.2.1 Computer Controlled Scanning Electron Microscopy (CCSEM)

CCSEM is a combination of Backscattered Electron Imagery (BEI) and Energy Dispersive Spectroscopy (EDS) which automatically analyzes in a cost effective fashion a large number (1,000–1,500) of individual particles, for particle size and chemical composition. The particles are grouped in “bins” by chemical composition and particle size. From these chemical measurements, mineralogy of individual particles can be inferred, for example Si particles being quartz and Ca particles being calcite. From each of the 15 sites, at least one TSP and one $\text{PM}_{2.5}$ Nuclepore® filter and between 3 and 10 PM_{10} filters were analyzed by CCSEM. Also, one $\text{PM}_{2.5}$ filter from each site was analyzed for its ultrafine (0.01 to 0.5 μm diameter) individual particle content. One PM_{10} Nuclepore® filter of each of the 15 re-suspensions was also analyzed by CCSEM

3.2.2 Scanning Electron Microscopy (SEM)

Although labor intensive, the field emission electron source allows for very high magnifications and sharp secondary electron images. This technique is for study of particle shape, surface coatings, and chemical composition. More than 100 secondary electron images representing all 15 sites were collected in this way.

² National Institute for Occupational Safety and Health (NIOSH) Method 5040 – ELEMENTAL CARBON (DIESEL PARTICULATE), Issue 3 (Interim); September 1999

3.3 Mineral Analysis by X-ray Diffraction (XRD)

XRD is the single most important non-destructive technique for characterization of minerals such as quartz, feldspars, calcite, dolomite, clay minerals, and iron oxides in fine dust. DRI's Bruker D8 XRD system with its highly sensitive detectors, monochromators, and sample spinner provided a system well suited for automated measurement of low concentrations of minerals in powder samples and on filter substrates. Quantitative mineral phase analysis by XRD is one of few techniques which is phase sensitive, rather than chemical sensitive as is the case with X-ray fluorescence (XRF) spectrometry. Quantitative software is part of DRI's system, and this and other software were applied for quantitative XRD analyses of fifteen <38µm screened dust samples [Caquineau, 1997; Chung F. H., 1974; Esteve, 1997; Esteve V., et al., 1997; Rietveld H.M., 1969; Sturges W.T., et al., 1989; Sturges, 1989].

3.4 Data Processing and Storage

Upon completion of analysis, filter results underwent a first level of quality assurance, before being uploaded to appropriate folders on the EPMSP Web page by each laboratory. DRI retrieved these files for second level quality assurance—including data validation, flagging, and compilation into folders for each site. Results were tabulated and graphically displayed as time series plots, pie-charts, and stacked bar-charts as part of a third level of quality assurance.

Chemical, mineralogical, and electron microscopic results of all analyzed filter and bulk soil samples for each of the 15 sites were submitted to the USACHPPM for archiving, following final quality assurance review and release by DRI.

4 RESULTS

All analytical results for each site—together with statistics, tables, and graphical representations—are available on the DOEHS Portal. Of 2,308 (excluding blanks) Teflon® membrane and quartz fiber filters sampled in the field, 2207 (96%) were chemically analyzed, and after eliminating voided results, provided a filter recovery of 2022 (88%), for subsequent data analysis. The following results include some sites and key chemical species that highlight areas of potential concern to the U.S. Department of Defense. To keep this report concise, only some results that demonstrate potential problem areas are shown.

4.1 Gravimetry and Filter Chemistry

Time series plots for TSP, PM₁₀, and PM_{2.5} 24-hour gravimetric and chemical abundances from Teflon® and quartz fiber filters were compiled for each of the 15 sites.

4.1.1 Gravimetry

Averaged concentration levels (Fig. 4-1, Table 4-1) show highest particulate matter concentrations for TSP at Tikrit (600 µg/m³) and PM₁₀ at Tallil (303 µg/m³). Differences among sites for PM_{2.5} total mass concentrations are less, with Tikrit giving the highest annual average PM_{2.5} concentration of 114 µg/m³. Although both Teflon® and quartz

fiber filters were weighed, gravimetric results from the latter were often found to be unreliable.

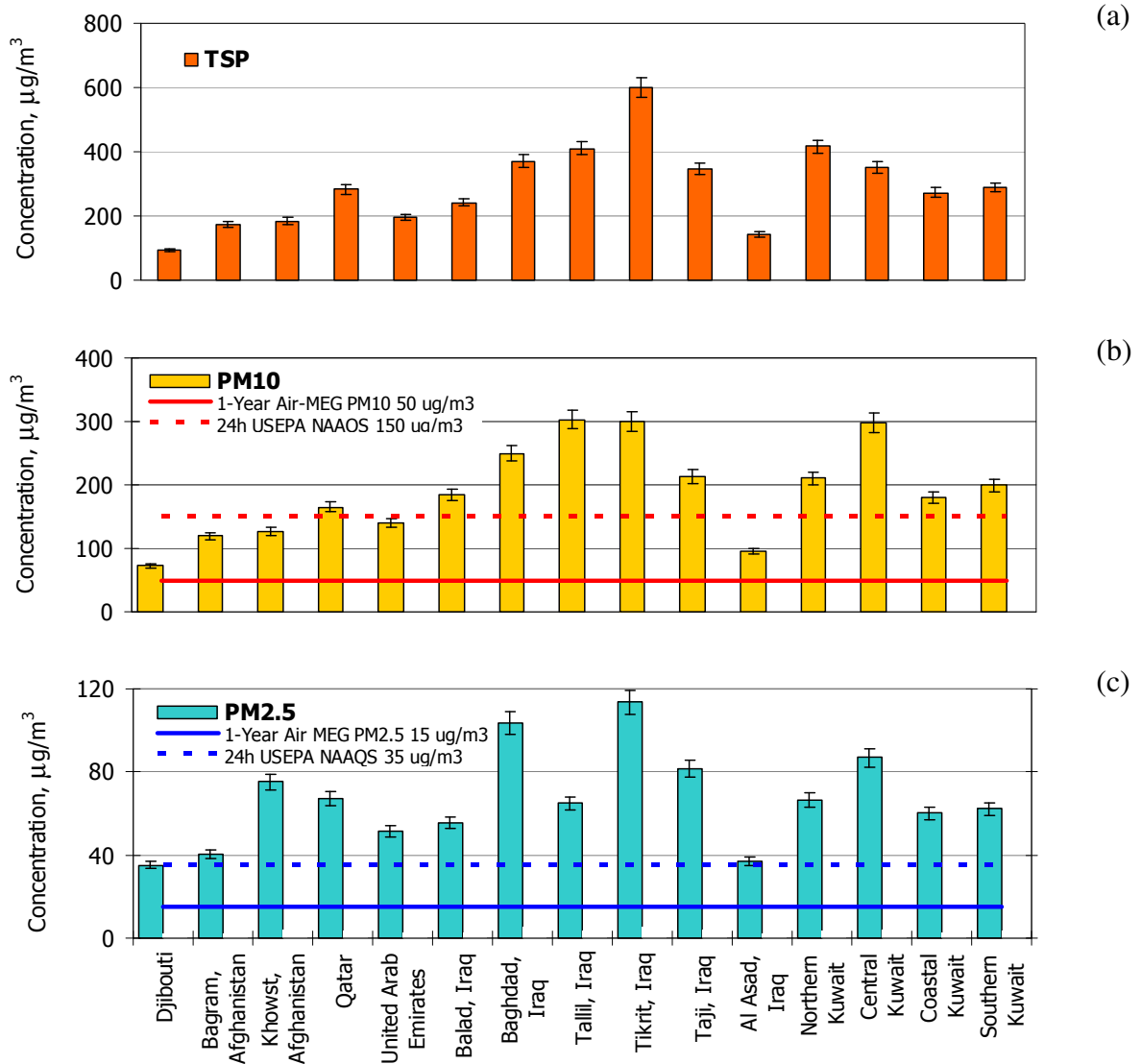


Figure 4-1. Averaged particulate mass concentrations and uncertainties for TSP, PM_{10} , and $\text{PM}_{2.5}$ on Teflon® filters for each of the 15 sites. Averaging period is approximately one year.

This is due to the brittle nature of the glass fiber filter medium and subsequent loss of mass from small bits of fiber breaking off edges of the filters. In some instances, this was negligible but, in other cases, it resulted in underestimation of the PM mass collected on quartz fiber filters. Gravimetric results from both Teflon® and quartz fiber filters were processed and are available on the DOEHRS Portal.

The high average particulate matter (TSP, PM_{10} , and $\text{PM}_{2.5}$) levels from each site are to a large extent determined by the number and intensity of dust-blowing events. Differences in PM measurements among Baghdad, Taji, Balad, and Tikrit (all within 200 km of each other along the Tigris River valley) can be ascribed to varying contributions from local

dust sources including dirt and paved roads, agriculture, and disturbances of the desert floor by motorized vehicles.

The $PM_{2.5}/PM_{10}$ mass ratios vary substantially among the 15 sites, from 0.21 for Tallil, Iraq to 0.60 for Khowst, depending on the fraction of coarse dust in the air. For the Iraq and Kuwait sites, the average $PM_{2.5}/PM_{10}$ mass ratio is 0.36, which is similar to the average ratio for the rural southwestern U.S. (Table 4-1). This signifies that on average the $PM_{2.5}/PM_{10}$ particulate mass distribution of sampled areas in the Middle East are similar to those of the drier parts of the southwestern U.S. This low value is typical of regions dominated by geological dust, in contrast to rural areas where combustion processes such as coal or wood burning dominate [Engelbrecht, 2001], and where the $PM_{2.5}/PM_{10}$ ratios are on average as high as 0.85.

Although no longer monitored in the U.S. or considered a health standard, TSP was measured as part of the EPMSP because of the impact of coarse dust on military equipment. Average TSP/ PM_{10} mass ratios vary from 1.18 for Central Kuwait to as high as 2.09 for Tikrit, Iraq (Table 4-1), also emphasizing dominance by coarse dust at the latter site.

Table 4-1. Mean mass concentrations for TSP, PM_{10} , and $PM_{2.5}$ size fractions, as well as the TSP: PM_{10} : $PM_{2.5}$ mass ratios for each of the 15 sites, as measured on Teflon® filters. For comparison, the mean STN (southwestern U.S. urban) and IMPROVE (southwestern U.S. rural) concentrations and ratios, from sites in the U.S. are given.

Site No.	Site Location	Concentration			Ratio		
		TSP $\mu\text{g}/\text{m}^3$	PM_{10} $\mu\text{g}/\text{m}^3$	$PM_{2.5}$ $\mu\text{g}/\text{m}^3$	TSP PM_{10}	$PM_{2.5}$	
Site 1	Djibouti	94	72	33	1.29	1	0.46
Site 2	Bagram, Afghanistan	174	120	40	1.45	1	0.34
Site 3	Khowst, Afghanistan	185	126	75	1.47	1	0.60
Site 4	Qatar	282	166	67	1.70	1	0.41
Site 5	United Arab Emirates	196	140	52	1.40	1	0.37
Site 6	Balad, Iraq	242	183	56	1.32	1	0.30
Site 7	Baghdad, Iraq	371	250	103	1.48	1	0.41
Site 8	Tallil, Iraq	411	303	65	1.36	1	0.21
Site 9	Tikrit, Iraq	628	300	114	2.09	1	0.38
Site 10	Taji, Iraq	348	213	81	1.63	1	0.38
Site 11	Al Asad, Iraq	142	96	38	1.48	1	0.39
Site 12	Northern Kuwait	416	211	67	1.98	1	0.32
Site 13	Central Kuwait	352	298	117	1.18	1	0.39
Site 14	Coastal Kuwait	264	180	60	1.47	1	0.33
Site 15	Southern Kuwait	290	199	62	1.45	1	0.31
STN	US SW Urban (City)		40	12		1	0.30
IMPROVE	US SW Rural (Desert)		13	5		1	0.36

4.1.2 Comparison to Air Quality and Health Standards

Table 4-2 provides a summary of concentration levels measured in the course of the EPMSP as well as U.S. and international health standards. It should be noted that the air quality standards listed in Table 4-2 have qualifiers regarding the way in which samples are to be collected, analytical methods applied, as well as chemical species to be

considered or excluded. References for each air quality and health standard are listed as a footnote to Table 4-2. For this study, tabled values serve as indicators only. Because of health risks associated with the finer fraction, only PM_{2.5} levels are presented in this report. It will be shown that trace metals—such as lead (Pb), arsenic (As), cadmium (Cd), antimony (Sb), and zinc (Zn)—are concentrated in the PM_{2.5} fraction (Figs. 4-3, 4-4, 4-5, 4-9[b]). Also, fine aluminum silicate minerals such as clays are concentrated in the fine fraction.

Averaged for the sampling period of approximately one year, all sites exceed the USACHPPM 1-Year Air-MEG value of 50 µg/m³ for PM₁₀ as well as the USACHPPM 1-Year MEG value of 15 µg/m³ for PM_{2.5}. Other standards that were exceeded are the U.S. Environmental Protection Agency (USEPA) annual National Ambient Air Quality Standards (NAAQS) for PM₁₀ (annual NAAQS for PM₁₀ of 50 µg/m³ revoked in December, 2006) and the World Health Organization's guidelines for particulate matter (20 µg/m³ for PM₁₀, 10 µg/m³ for PM_{2.5}). Of note is that USEPA's 24-hour standard for PM₁₀ (150 µg/m³) is exceeded at 10 sites and for PM_{2.5} (35 µg/m³) at all 15 sites (Fig. 4-1).

Depending on the analytical method and standard or guideline applied, the chemical species aluminum (Al), cadmium (Cd), and lead (Pb) were noted as possible exceedances. The USACHPPM 1-year interim Air-MEG of 3.42 µg/m³ for aluminum (Al) was on average exceeded at all 15 sites. We assume that this guideline may be for aluminum metal or soluble aluminum salts. Since aluminum measured in samples from all 15 sites was identified as inert aluminum silicates (i.e., part of the crystalline mineral structure) including feldspars, micas, or clays, this guideline should not apply. The Occupational Safety and Health Administration (OSHA) 8-hour guideline value of 5000 µg/m³ for respirable alumina (aluminum oxide) as shown in Table 4-2 was not exceeded.

Although the USACHPPM 1-year Air-MEG for cadmium (Cd) of 0.244 µg/m³ was not exceeded, the World Health Organization (WHO) guideline value of 0.005 µg/m³ was exceeded at all 15 sites, as measured by XRF. As measured by the more sensitive ICP-MS method, however, all 15 sites had average measured values below this WHO guideline.

Mean lead (Pb) levels for all 15 sites fall within the USACHPPM 1-year MEG of 1.5 µg/m³. The average level for Baghdad, Iraq exceeds the WHO guideline of 0.5 µg/m³, as analyzed by both XRF and ICP-MS. Demonstrated below, this is largely due to a single metals emitting event on 2006-11-30, possibly from lead smelters or a nearby burn pit.

Short-term health guidelines such as the USACHPPM 8-hour MEG, as well as National Institute of Occupational Safety and Health (NIOSH) and OSHA standards should be considered for such short-term events.

Table 4-2. Comparative table showing concentration ranges in micrograms per cubic meter ($\mu\text{g}/\text{m}^3$) of mean $\text{PM}_{2.5}$ site concentrations, as well as various air quality and health standards.

Symbol	Name	Mnemonic	Method	(a)	(b)	(c)	(d)	(e)	(f)	(g)	(h)	(i)	(j)	(k)	(l)
				Range of Annual Mean of 15 Sites		Site Ranking			USACHPPM	USACHPPM	US EPA	US EPA	WHO	NIOSH	OSHA
				PM _{2.5} Annual Mean	Min	Max	Highest	2nd Highest	3rd Highest	8-hour Air-MEG $\mu\text{g}/\text{m}^3$	1-Year Air-MEG $\mu\text{g}/\text{m}^3$	Annual NAAQS $\mu\text{g}/\text{m}^3$	24hr NAAQS $\mu\text{g}/\text{m}^3$	TWA annual $\mu\text{g}/\text{m}^3$	REL: TWA (10-hr day 40-h workweek) $\mu\text{g}/\text{m}^3$
Particulate Matter Mass Concentrations															
TSP	TSP Mass Teflon	TMAC	Grav	91.815	599.632	IRQ_SPE	KUW_BUE	IRQ_ADD							
PM10	PM ₁₀ Mass Teflon	TMAC	Grav	72.451	303.004	IRQ_ADD	IRQ_SPE	KUW_AAS		50		150	20		
PM2.5	PM _{2.5} Mass Teflon	TMAC	Grav	35.271	113.521	IRQ_SPE	IRQ_VIC	KUW_AAS		15	15	35	10		
PM_{2.5} Chemical Concentrations															
Cl ⁻	Chloride	CLIC	IC	0.149	0.854	IRQ_VIC	UAE_DHA	IRQ_TAJ							
NO ₃ ⁻	Nitrate	N3IC	IC	0.586	2.064	KWT_SHU	IRQ_VIC	AFG_BAG							
PO ₄ ³⁻	Phosphate	PHIC	IC	0.047	0.166	AFG_SAL	IRQ_VIC	IRQ_ALA							
SO ₄ ²⁻	Sulfate	S4IC	IC	2.138	11.915	QAT_UDE	KWT_SHU	KUW_ARI							
NH ₄ ⁺	Ammonium	N4IC	IC	0.865	3.629	QAT_UDE	KWT_SHU	KUW_ARI							
Ca ²⁺	Calcium	CAEC	ICP-OES	0.247	3.574	IRQ_VIC	IRQ_SPE	IRQ_ALA							
K ⁺	Potassium	KPEC	ICP-OES	0.086	0.250	IRQ_TAJ	AFG_SAL	IRQ_VIC							
Mg ²⁺	Magnesium	MGEC	ICP-OES	0.036	0.260	KUW_AAS	UAE_DHA	IRQ_VIC							
Na ⁺	Sodium	NAEC	ICP-OES	0.057	0.310	UAE_DHA	DJI_LEM	IRQ_VIC							
CO ₃	Carbonate carbon	C3TC	TOT	0.855	2.241	IRQ_VIC	IRQ_ALA	IRQ_SPE							
C	Elemental carbon	ECTNIC	TOT	1.152	5.085	KUW_ARI	KWT_SHU	IRQ_VIC							5000
OC	Organic carbon	OCTNIC	TOT	1.373	9.864	AFG_BAG	AFG_SAL	IRQ_TAJ							
TOC	Total carbon	TCTC	TOT	3.400	14.750	IRQ_VIC	AFG_SAL	AFG_BAG							
Ag	Silver	AGXC	XRF	0.009	0.016	IRQ_SPE	AFG_SAL	DJI_LEM						10	10
Al	Aluminum	ALXC	XRF	0.465	3.302	IRQ_SPE	KUW_AAS	IRQ_VIC						5000	5000
As	Arsenic	ASXC	XRF	0.002	0.056	IRQ_VIC	IRQ_TAJ	IRQ_ANA		1.11					10
Au	Gold	AUXC	XRF	0.003	0.016	AFG_SAL	DJI_LEM	IRQ_VIC							
Ba	Barium	BAXC	XRF	0.007	0.066	IRQ_VIC	KUW_AAS	QAT_UDE		3.42					500
Br	Bromine	BRXC	XRF	0.003	0.019	IRQ_VIC	IRQ_ANA	KUW_ARI	63					700	700
Ca	Calcium	CAXC	XRF	0.549	6.491	IRQ_SPE	IRQ_VIC	KUW_AAS							5000
Cd	Cadmium	CDXC	XRF	0.012	0.020	IRQ_SPE	KUW_ARI	DJI_LEM		0.244			0.005		5
Cl	Chlorine	CLXC	XRF	0.044	0.799	IRQ_VIC	DJI_LEM	IRQ_TAJ	1500						
Co	Cobalt	COXC	XRF	0.001	0.001	IRQ_SPE	IRQ_TAJ	KUW_ARI						50	50
Cr	Chromium	CRXC	XRF	0.001	0.002	IRQ_SPE	IRQ_TAJ	KUW_ARI		12.2				500	1000
Cu	Copper	CUXC	XRF	0.001	0.010	IRQ_VIC	IRQ_ANA	KWT_SHU						1000	1000
Fe	Iron	FEXC	XRF	0.420	2.919	IRQ_SPE	KUW_AAS	IRQ_VIC							
Ga	Gallium	GAXC	XRF	0.002	0.007	IRQ_VIC	IRQ_SPE	IRQ_TAJ							
Hg	Mercury	HGXC	XRF	0.005	0.009	IRQ_SPE	AFG_SAL	IRQ_TAJ		0.205			1	10	10
In	Indium	INXC	XRF	0.015	0.029	IRQ_SPE	AFG_SAL	IRQ_TAJ						100	100
K	Potassium	KPXC	XRF	0.211	1.074	IRQ_VIC	IRQ_SPE	IRQ_TAJ							
La	Lanthanum	LAXC	XRF	0.005	0.060	IRQ_VIC	KUW_AAS	KUW_BUE							

Table 4-2 continued

Symbol	Name	Mnemonic	Method	(a) Range of Annual Mean of 15 Sites		(c) Site Ranking			(f) USACHPPM	(g) USACHPPM	(h) US EPA	(i) US EPA	(j) WHO	(k) NIOSH	(l) OSHA
				PM _{2.5} Annual Mean		Highest	2nd Highest	3rd Highest	8-hour Air-MEG	1-Year Air-MEG	Annual NAAQS	24hr NAAQS	TWA annual	REL: TWA (10-hr day 40-h workweek)	PEL: TWA (8-hr day 40-h workweek)
				Min	Max				μg/m ³	μg/m ³					
PM_{2.5} Chemical Concentrations															
Mg	Magnesium	MGXC	XRF	0.175	1.529	IRQ_SPE	KUW_AAS	IRQ_VIC							
Mn	Manganese	MNXC	XRF	0.006	0.048	IRQ_SPE	IRQ_VIC	KUW_AAS		0.342			0.15	1000	
Mo	Molybdenum	MOXC	XRF	0.006	0.010	IRQ_SPE	IRQ_TAJ	KUW_ARI							10000
Na	Sodium	NAXC	XRF	0.112	0.496	IRQ_VIC	DJI_LEM	UAE_DHA							
Ni	Nickel	NIXC	XRF	0.002	0.012	AFG_SAL	IRQ_SPE	IRQ_VIC		4.9					1000
P	Phosphorus	PHXC	XRF	0.034	0.333	IRQ_SPE	IRQ_VIC	KUW_AAS	100						
Pb	Lead	PBXC	XRF	0.005	0.581	IRQ_VIC	IRQ_TAJ	IRQ_ANA		1.5	1.5		0.5	50	50
Pd	Palladium	PDXC	XRF	0.007	0.013	IRQ_SPE	DJI_LEM	IRQ_TAJ							
Rb	Rubidium	RBXC	XRF	0.002	0.005	IRQ_SPE	IRQ_TAJ	AFG_SAL							
S	Sulfur	SUXC	XRF	0.712	3.727	QAT_UDE	UAE_DHA	KUW_BUE							
Sb	Antimony	SBXC	XRF	0.027	0.074	IRQ_ANA	IRQ_SPE	DJI_LEM		12				500	500
Se	Selenium	SEXC	XRF	0.001	0.003	IRQ_SPE	IRQ_VIC	IRQ_TAJ						200	200
Si	Silicon	SIXC	XRF	1.182	9.124	IRQ_SPE	KUW_AAS	IRQ_VIC						5000	5000
Sn	Tin	SNXC	XRF	0.022	0.037	IRQ_SPE	IRQ_VIC	QAT_UDE						2000	2000
Sr	Strontium	SRXC	XRF	0.004	0.030	UAE_DHA	IRQ_VIC	QAT_UDE		1510					
Ti	Titanium	TIXC	XRF	0.020	0.155	KUW_AAS	IRQ_SPE	AFG_SAL							
Tl	Thallium	TLXC	XRF	0.003	0.006	IRQ_VIC	IRQ_SPE	IRQ_TAJ							
U	Uranium	URXC	XRF	0.021	0.037	IRQ_SPE	IRQ_TAJ	KUW_ARI						200	250
V	Vanadium	VAXC	XRF	0.012	0.108	IRQ_SPE	IRQ_VIC	KUW_AAS		0.72					500
Y	Yttrium	YTXC	XRF	0.002	0.003	IRQ_SPE	IRQ_TAJ	KUW_AAS						1000	1000
Zn	Zinc	ZNXC	XRF	0.014	0.043	IRQ_TAJ	IRQ_VIC	KWT_SHU		720					
Zr	Zirconium	ZRXC	XRF	0.003	0.011	IRQ_VIC	IRQ_SPE	KUW_AAS						5000	5000
As	Arsenic	ASMC	ICP-MS	0.002	0.004	IRQ_VIC	IRQ_SPE	IRQ_TAJ		1.11					10
Be	Beryllium	BEMC	ICP-MS	0.000	0.001	IRQ_SPE	IRQ_TAJ	KUW_ARI		0.014					2
Cd	Cadmium	CDMC	ICP-MS	0.000	0.002	IRQ_ANA	IRQ_VIC	IRQ_TAJ		0.244			0.005		5
Cr	Chromium	CRMC	ICP-MS	0.003	0.013	IRQ_SPE	AFG_SAL	KUW_AAS		12.20					
Hg	Mercury	HGMC	ICP-MS	0.000	0.001	IRQ_SPE	IRQ_ADD	UAE_DHA		0.205			1	10	10
Mn	Manganese	MNMC	ICP-MS	0.011	0.056	IRQ_SPE	KUW_AAS	AFG_SAL		0.342			0.15	1000	
Ni	Nickel	NIMC	ICP-MS	0.002	0.014	AFG_SAL	IRQ_SPE	IRQ_VIC		36.7					1000
Pb	Lead	PBMC	ICP-MS	0.007	0.546	IRQ_VIC	IRQ_TAJ	IRQ_ANA		1.5	1.5		0.5	50	50
Sb	Antimony	SBMC	ICP-MS	0.001	0.050	IRQ_ANA	IRQ_VIC	AFG_BAG		12				500	500
Sr	Strontium	SRMC	ICP-MS	0.002	0.019	QAT_UDE	IRQ_VIC	UAE_DHA		1510					
V	Vanadium	VAMC	ICP-MS	0.001	0.009	IRQ_SPE	IRQ_VIC	KWT_SHU		0.72					500
Zn	Zinc	ZNMC	ICP-MS	0.028	0.069	IRQ_TAJ	KWT_SHU	IRQ_ANA		720					

Footnote to Table 4-2:

- (a), (b) The range in annual mean concentration values among the 15 sites. Mean concentrations calculated for each chemical species and each site on the PM_{2.5} size fraction unless stated otherwise.
- (c), (d) (e) Three sites with the highest, second highest, and third highest annual mean concentration per species. Site mnemonics are (1) DJI_LEM = Djibouti, (2) AFG_BAG = Afghanistan Bagram, (3) AFG_SAL = Afghanistan Khowst, (4) QAT_UDE = Qatar, (5) UAE_DHA = United Arab Emirates, (6) IRQ_ANA = Iraq Balad, (7) IRQ_VIC = Iraq Baghdad (8) IRQ_ADD = Iraq Tallil, (9) IRQ_SPE = Iraq Tikrit, (10) IRQ_TAJ = Iraq Taji, (11) IRQ_ALA = Iraq Al Asad, (12) KUW_BUE = Northern Kuwait, (13) KUW_AAS = Central Kuwait, (14) KWT_SHU = Coastal Kuwait, (15) KUW_ARI = Southern Kuwait
- (f) (g) USACHPPM 8-hour and 1-year Air-MEGs: USACHPPM Military Exposure Guidelines (MEG) for Deployed Military Personnel, Tabel 1. Military Exposure Guidelines for Air - January 2004 TG 230 Addendum, <http://chppm-www.apgea.army.mil/documents/TG/TECHGUID/TG230.pdf>
- (h), (i) US EPA NAAQS: United States Environmental Protection Agency Ambient Air Quality Standards, annual and 24 hour, <http://www.epa.gov/air/criteria.html>
- (j) WHO TWA annual: World Health Organization (WHO) annual time-weighted average (TWA), Air quality guidelines - global update 2005, http://www.who.int/phe/health_topics/outdoorair_aqg/en/index.html
- (k) NIOSH REL TWA: National Center for Disease Control (CDC), National Institute for Occupational Safety and Health (NIOSH), recommended exposure limit (REL), 10-hour time-weighted average (TWA), 40-hour workweek, <http://www.cdc.gov/niosh/npg/npgd0022.html> , INDEX of Chemical Abstracts Service Registry Numbers (CAS No.), <http://www.cdc.gov/niosh/npg/npgdcas.html>
- (l) OSHA PEL TWA: Occupational Safety and Health Administration standards, permissible exposure limit (PEL), time-weighted average (TWA) 8-hour day, Regulations (Standards - 29 CFR), TABLE Z-1, Limits for Air Contaminants, http://www.osha.gov/pls/oshaweb/owadisp.show_document?p_table=STANDARDS&p_id=9992

4.1.3 Comparison to Rural and Urban Sites in the U.S.

To provide perspective on results from the 15 Middle Eastern sites, we compared these to five rural and five urban PM_{2.5} sites in the southwestern U.S. (Fig. 4-2; APPENDIX A). The 10 U.S. sites were selected because of their proximity to military bases in drier regions of the U.S. Average particulate matter and chemical values were calculated for the period 2002–2006.

The five rural sites are at Dome Land National Wildlife Area (NWA), Joshua Tree National Park, Bosque del Apache National Wildlife Refuge (NWR), Salt Creek NWR, and San Andres NWR, which form part of the Interagency Monitoring of Protected Visual Environments (IMPROVE) air quality monitoring network (<http://vista.cira.colostate.edu/improve/>).

The five urban sites are in Las Vegas, Nevada; Los Angeles, California; Tucson, Arizona; Albuquerque, New Mexico; and El Paso, Texas and form part of USEPA's Speciation Trends Network (STN) monitoring program: (<http://www.epa.gov/ttn/airs/airsaqs/detaildata/downloadaqsdta.htm>).

Average PM_{2.5} mass and chemical concentration levels from the deployment sites are — except for a few species such as nitrate, sodium, and rubidium — greater than chemical abundances in PM_{2.5} samples measured at rural Interagency Monitoring of Protected Visual Environments (IMPROVE) and urban Speciation Trends Network (STN) sites in the southwestern U.S.

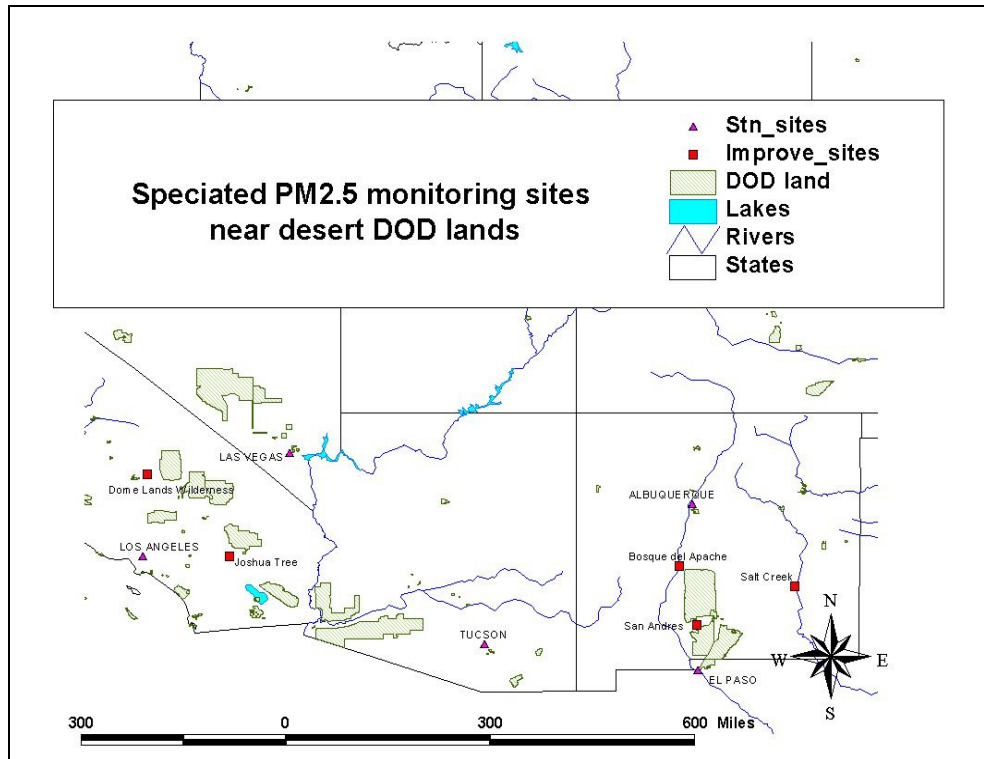


Figure 4-2. Location of Department of Defense (DoD) lands in the southwestern U.S. in relation to five rural IMPROVE sites (Dome Land NWA, Joshua Tree NP, Bosque del Apache NWR, Salt Creek, and San Andres NWR) and five urban STN sites (Las Vegas, Los Angeles, Tucson, Albuquerque, and El Paso).

4.1.4 Trace Metals

Annual mean ICP-MS trace metal results of 12 chemical species were compiled per size-cut (TSP, PM₁₀, PM_{2.5}) and sampling site (Figure 4-3). Lead (Pb) is the most abundant trace species found in Baghdad aerosol and also contributes substantially to measured trace metals at Taji and Balad. Of note is that for all sites the lead concentrations (in $\mu\text{g}/\text{m}^3$) are nearly identical for the three size fractions (TSP, PM₁₀, PM_{2.5}). Since PM₁₀ is contained in TSP and PM_{2.5} in PM₁₀, this implies that most, if not all the lead occurs in the PM_{2.5} size fraction. Most combustion products (elemental carbon and particulate organic compounds) also occur in the fine (PM_{2.5}) and ultra-fine fractions, and some lead may be a component of combustion products for these locations. Fine lead and zinc, together with other associated metals, also are generated from condensed fumes emitted by metallurgical processes such as lead-zinc smelters or backyard electronic circuit board smelting operations. Lead also occurs as an additive in leaded gasoline and is emitted with gasoline vehicle emissions.

A major lead emitting event, far exceeding the USACHPPM 1-year Air-MEG value of $1.5 \mu\text{g}/\text{m}^3$ was recorded at the Baghdad site on 2006-11-30, with a smaller spike on 2007-1-11, and a few other days (Fig. 4-4 [a]). Similar elevated concentration levels also were recorded for zinc (Fig. 4-4 [b]), arsenic (Fig 4-4 [c]), and cadmium (Fig 4-4 [d]) on the same days. This implies that these (and antimony) trace metals were emitted by the same or a collocated source.

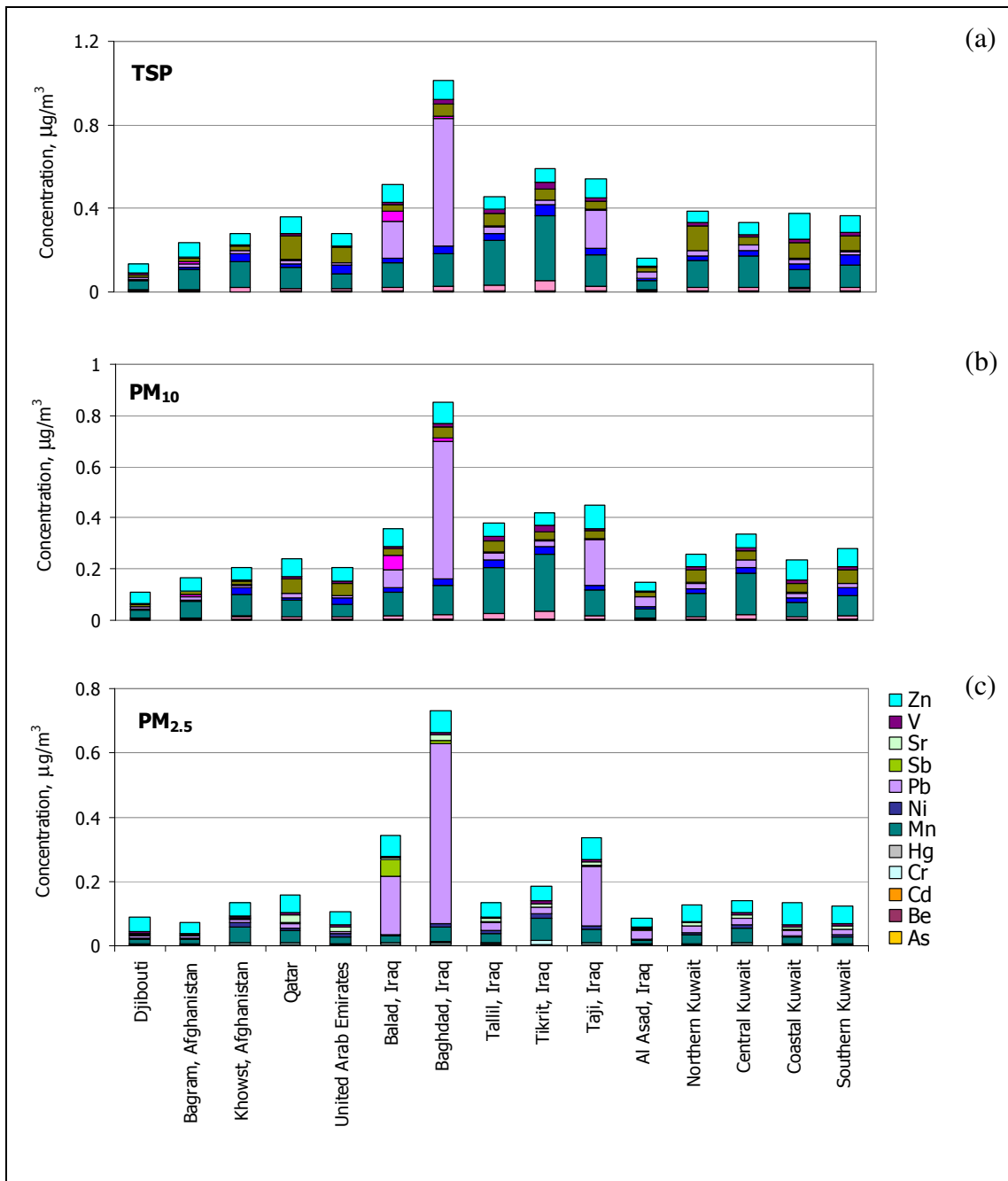


Figure 4-3. Annual mean distributions of 12 trace metals for (a) TSP, (b) PM_{10} , and (c) $\text{PM}_{2.5}$ size fractions for each of the 15 sites.

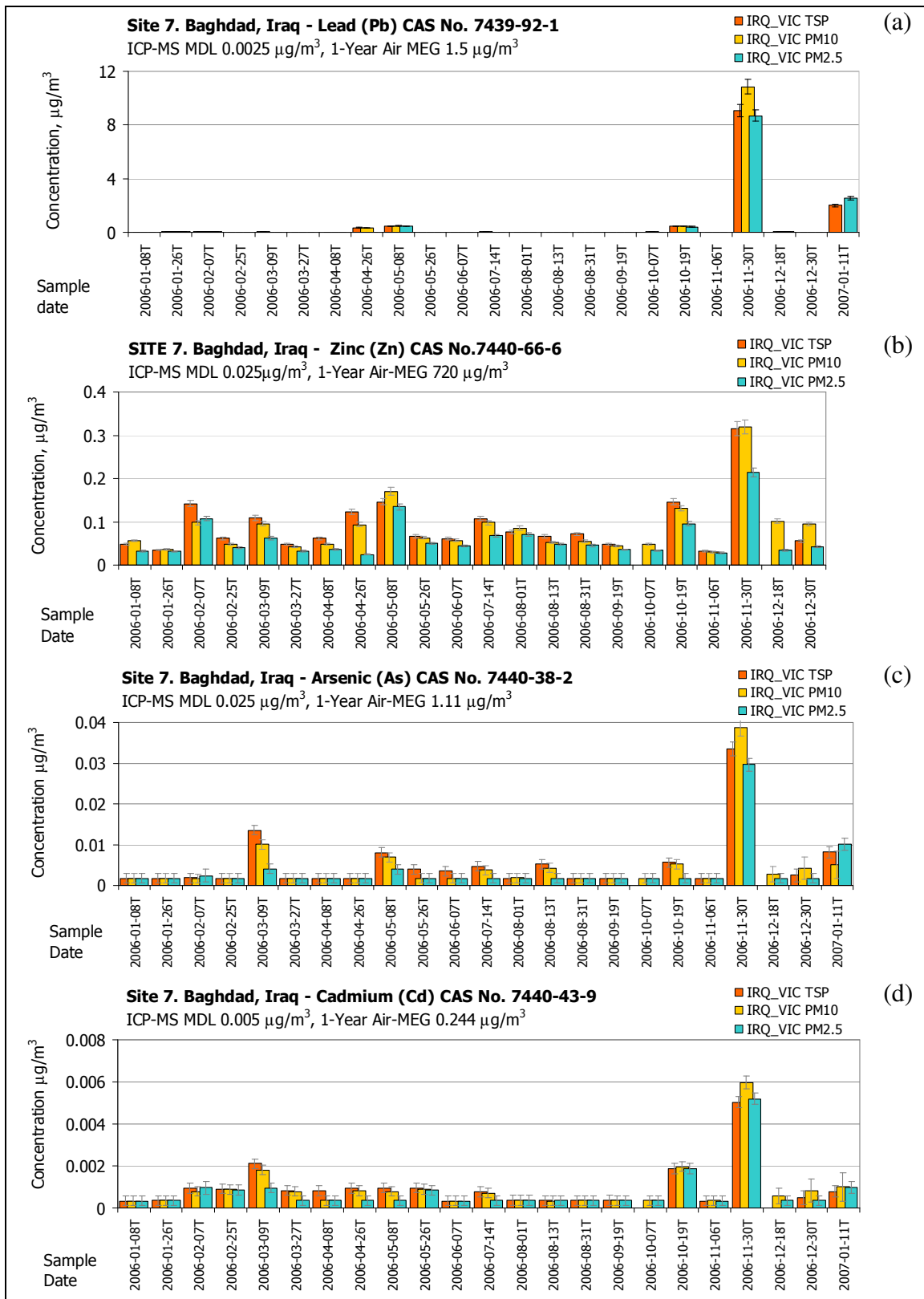
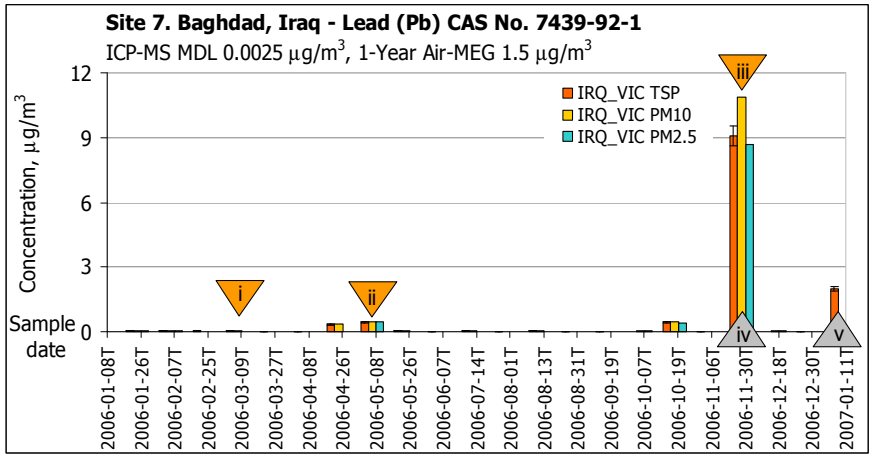


Figure 4-4. Time-series plot of trace metal concentrations from Baghdad, Iraq, showing corresponding elevated values for (a) lead, (b) zinc, (c) arsenic, and (d) cadmium on the 2006-10-19, 2006-11-30, and 2007-01-11 event days. These metals are concentrated in the PM_{2.5} size fraction.

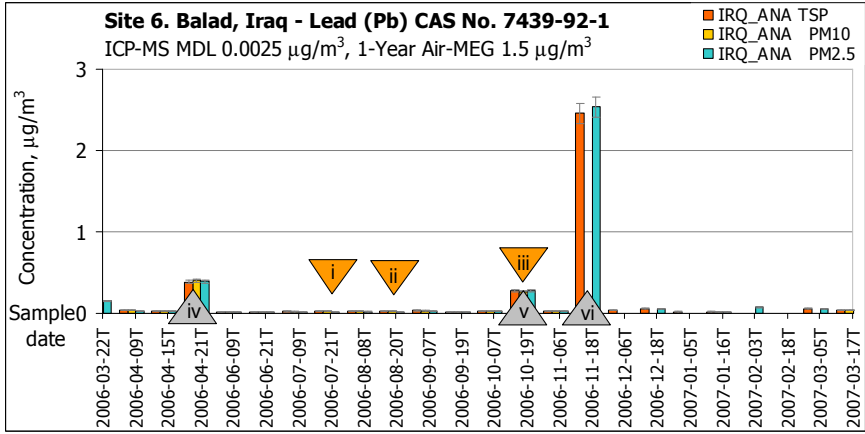


(a) Site 7. Baghdad, Iraq

Major events reported and/or measured

Sample date	TSPmass $\mu\text{g}/\text{m}^3$
<u>Dust event</u>	
(i) 2006-03-09*	1909 R
(ii) 2006-05-08*	975 R
(iii) 2006-11-30	662 R
<u>Lead event</u>	
(iv) 2006-11-30	662 R
(v) 2007-01-11	85 NR

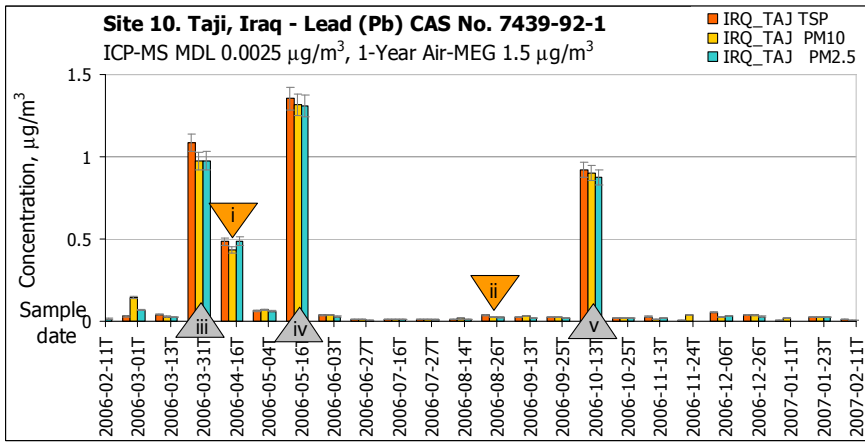
* - dust storm reported
NR - not reported



(b) Site 6. Balad, Iraq

Major events reported and/or measured

Sample date	TSPmass $\mu\text{g}/\text{m}^3$
<u>Dust event</u>	
(i) 2006-07-21	404 R
(ii) 2006-08-20	593 R
(iii) 2006-10-19	312 NR
<u>Lead event (year round burn pit)</u>	
(iv) 2006-04-21	158 R
(v) 2006-01-11	312 R
(vi) 2006-11-18	266 R



(c) Site 10. Taji, Iraq

Major events reported and/or measured

Sample date	TSPmass $\mu\text{g}/\text{m}^3$
<u>Dust event</u>	
(i) 2006-04-16	1086 R
(ii) 2006-08-26	2034 NR
<u>Lead event</u>	
(iii) 2006-03-31	270 NR
(iv) 2006-05-16	495 NR
(v) 2006-10-13	249 NR

Figure 4-5 Comparative time series plots of lead concentrations for (a) Baghdad, (b) Balad, and (c) Taji. The events showing elevated lead levels occur on different days for the three sites and on days for which no major regional dust storms were measured, implying local point sources for lead (Pb) with fluctuating emission rates and/or variable meteorological conditions. High event days are listed in a table alongside the figures. Events recorded (R) or not recorded (NR) on field data sheets, together with their total TSP mass levels, are shown in adjacent tables.

Very low concentration levels of arsenic and cadmium also were measured in TSP and PM₁₀, and in lower concentrations in PM_{2.5}, on 2006-03-09 and 2006-05-08—most likely associated with dust events on those two days. Similar associations among lead (Pb), arsenic (As), cadmium (Cd), and antimony (Sb) were measured at Balad and Taji, pointing to a similar source type, such as secondary lead battery and electronic circuit board smelters impacting all three sites. The relationship between known dust events and lead emissions for the three sites at Baghdad, Taji, and Balad are shown in Figures 4-5 (a), (b), and (c). The table alongside each time series plot shows the recorded high dust days and corresponding measured TSP levels. There is little coincidence between the high dust and high lead days, pointing to two distinct but different sources—one for geological dust and the other for trace metals (lead, arsenic, cadmium, antimony, zinc). Lead spikes occur on different days for each of the three monitoring sites, indicating different wind directions for point sources in relation to the monitoring sites, as well as variable meteorological conditions. The presence of individual particles of zinc and lead as well as lead in vehicle emissions, from the Balad-Baghdad-Taji region were confirmed by SEM/EDS (Figs. 4-11, 4-12).

A further trace element of interest is manganese, which was highest at Tikrit (Fig. 4-3). The highest manganese concentrations occurred in TSP and PM₁₀, and in low concentrations in the PM_{2.5} fraction. This means that manganese is associated with the coarse fraction of dust corresponding to days of high particulate matter concentrations and also to recorded dust events (Fig. 4-6 [d]).

4.1.5 Major Chemical Species

Elevated levels of major chemical species occur during dust events at all 15 sites. In the case of Baghdad, major dust events were recorded on 2006-03-09, 2006-05-08, 2006-08-13, 2006-10-19, and 2006-11-30. This is reflected by the time series plots for silicon, aluminum, calcium, and manganese (Fig. 4-6) which are similar for iron, magnesium, potassium, and sodium. The large mass differences between the TSP and PM₁₀ as well as PM₁₀ and PM_{2.5} soil-forming components show that these chemical species are largely in coarse dust fractions. As previously shown (Table 4-1), the coarse nature of minerals contain the major chemical species; the proportion of mineral dust in the PM_{2.5} fraction is small.

Total particulate matter distribution (Fig. 4-1) is reflected in the total major element distribution patterns—with Tikrit, Tallil, and Central Kuwait having the highest average total major element concentrations. The mass fractions of major chemical species are graphically presented as oxides, nitrate, sulfate, ammonium, and chloride (Fig. 4-7). Although there are differences among some sites, there is consistency among the three size fractions: TSP and PM₁₀ were very similar for all 15 sites. Mass fractions of SiO₂ are least in PM_{2.5} due to this mineral being largely contained in hard and coarse mineral quartz. The SiO₂ content is the highest at Khowst in Afghanistan for all size fractions which can be ascribed to a high percentage of SiO₂ rich silt in dust. Similarly, CaO and CO₂, which are both contained in the carbonate mineral calcite, have slightly higher mass fractions in TSP and PM₁₀.

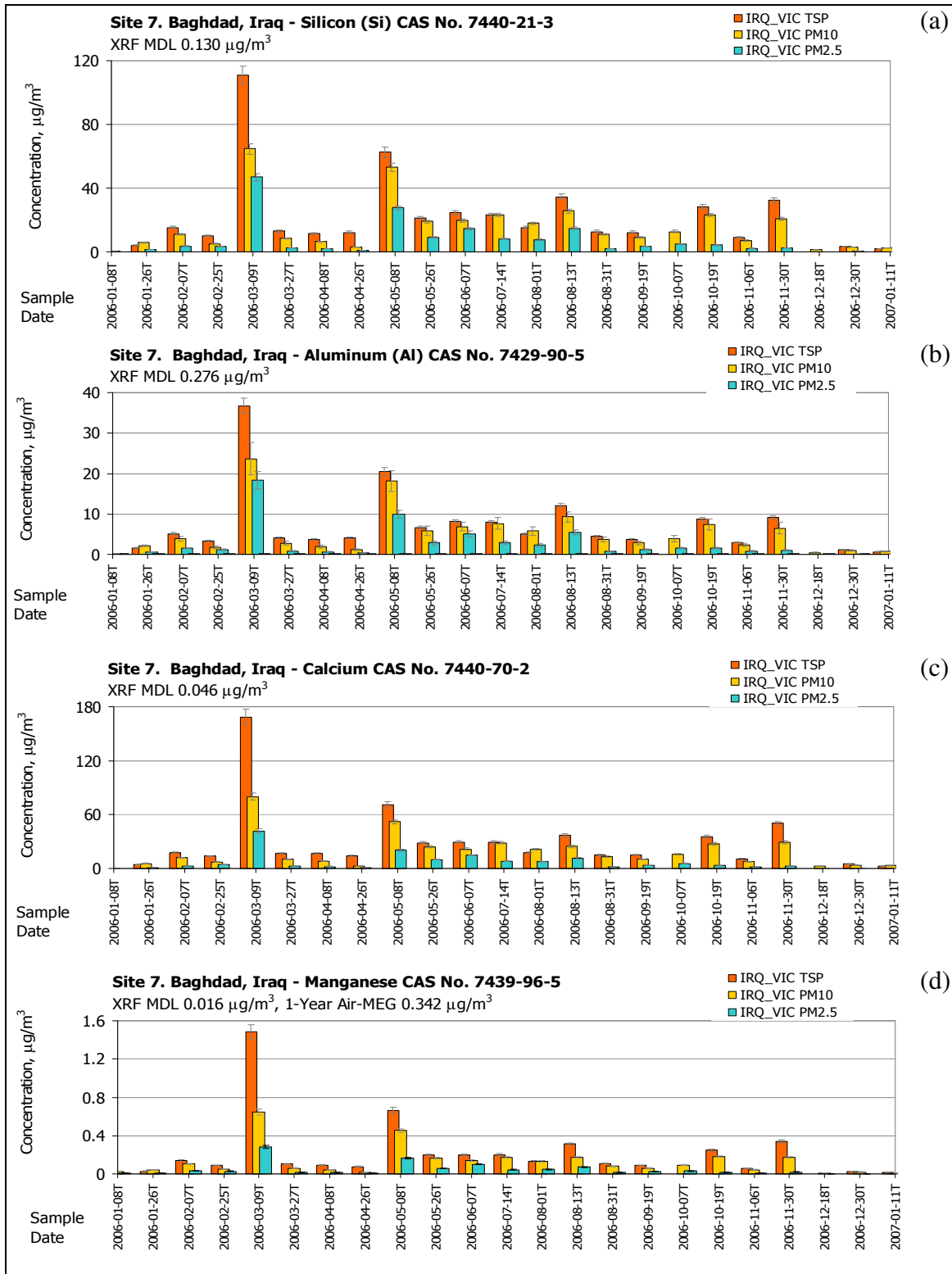


Figure 4-6. Major soil forming elements (a) silicon, (b) aluminum, (c) calcium, and (d) manganese as measured on Teflon® filters. Corresponding peak values represent dust blowing events on 2006-03-09, 2006-05-08, 2006-08-13, 2006-10-19, and 2006-11-30.

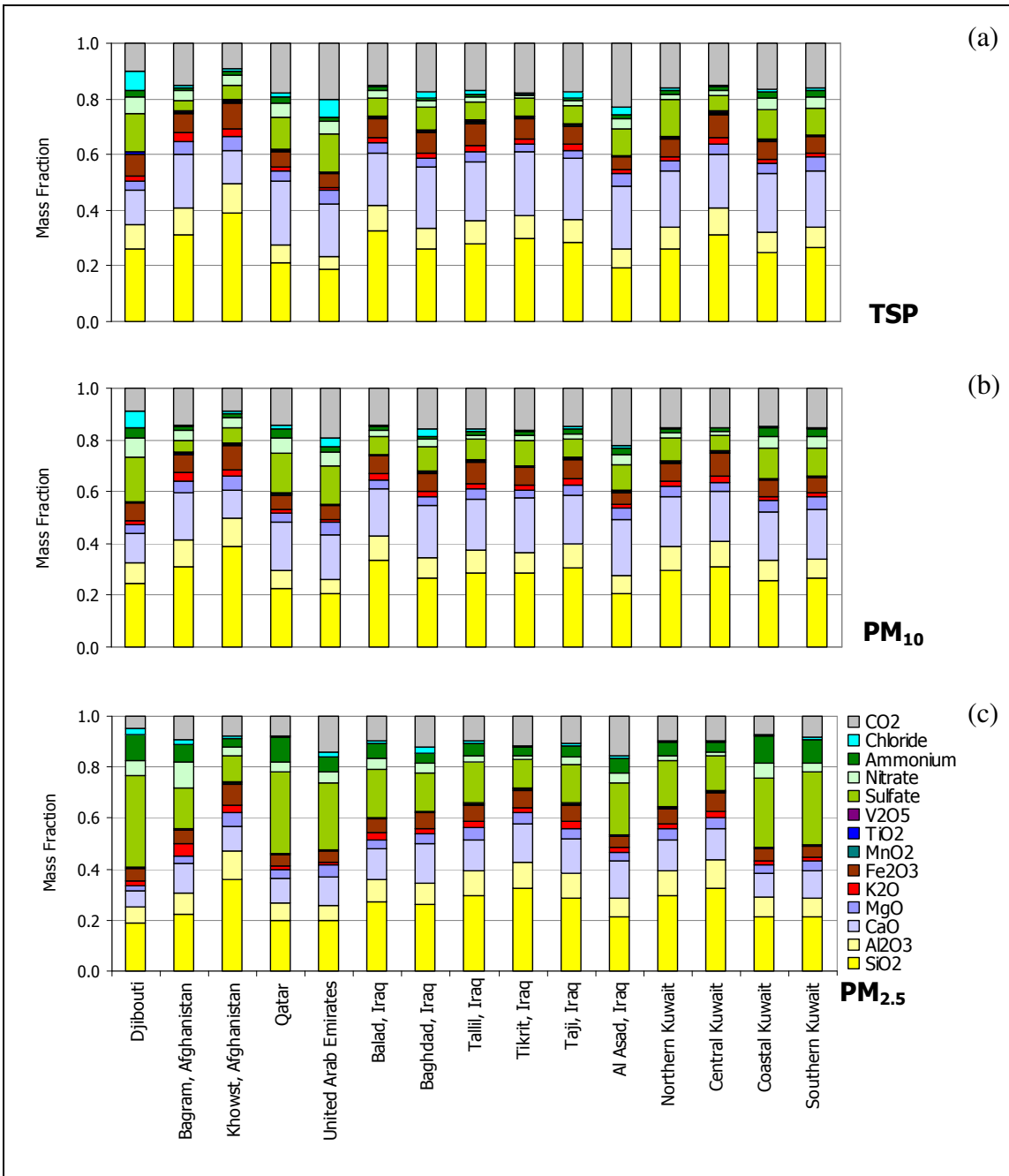


Figure 4-7 Annual mean major chemistry for (a) TSP, (b) PM₁₀, and (c) PM_{2.5}. Concentrations are expressed as mass fractions of oxides, sulfate (in gypsum), chloride (in salt), nitrate, and ammonium.

Chloride from sea salt was found in TSP and PM₁₀ at Djibouti, a site on the Gulf of Aden. Sulfate, largely as secondary ammonium sulfate and to a lesser extent in gypsum, was concentrated in the PM_{2.5} size fraction. High concentrations of secondary ammonium sulfate were found in PM_{2.5} at Djibouti, Qatar, UAE as well as Coastal and Southern Kuwait. Ammonium sulfate was in all likelihood from sulfur dioxide emissions from petrochemical and other industries in the Middle East. Compared to the other sites, UAE and Al Asad samples had slightly higher CaO, MgO, and CO₂ contents representing contributions from calcite and dolomite soils in these two regions.

In general, analyzed dust from these 15 Middle East sites are not considered to be out of the ordinary. A comparison of TSP filter chemistry from this program with dust from various parts of the southwestern U.S., Sahara, and China is given in Figure 4-8. Most dust samples contain mixtures of silicate minerals, carbonates, oxides, sulfates, and salts, in various proportions, as reflected by their chemistry. Differences lie in the relative proportions of these minerals and subsequent chemical components. Compared to the Sahara, China, U.S., and world dusts, Middle East samples had lower proportions of SiO₂ and higher proportions of CaO and MgO. The last two components are contained in the carbonate minerals calcite and dolomite and were found in higher concentrations at the UAE and Al Asad sites. Fe₂O₃ and MnO occur as various iron-manganese minerals, found in greater concentrations in the Sahara, China and U.S. when compared to the Middle East sample sets. Al₂O₃, a major constituent of clay minerals and other silicates, was found to be similar for most dusts. Sodium generally occurs as salt (NaCl) from evaporated sea water as well as saline desert areas.

4.1.6 Organic and Elemental Carbon

Because of unreliable results based on a sampling issue, discussion of OC and EC is not included in this report. Low concentrations of carbon measured by CCSEM and SEM on Nuclepore® filters supports our assumption that carbon in ambient air is overestimated when measured on quartz fiber filters. CCSEM measured carbon-rich particle concentrations varied from 0.3% for Tallil to as high as 1.2% for Djibouti. On the other hand, mean total carbon measured by TOT on quartz fiber filters is substantially higher, 3.5% on the low end for UAE to as high as 18.1% for Baghdad. Time series plots for OC and EC fluctuate greatly and are unrelated to distribution patterns for any other chemical species.

Quartz fiber strongly adsorbs volatile and semi-volatile organic compounds from its immediate environment, resulting in major OC artifacts on the filters [Olson, 2005]. This is exacerbated by temperature fluctuations, time period of exposure, and presence of volatile organic compounds in the immediate environment. To minimize this effect, quartz fiber filters should be transported and stored at sub-zero temperatures and analyzed soon after exposure. For practical reasons, both these conditions were violated in the EPSMP, resulting in variable, often high concentrations of artifacts on the quartz fiber filters from the 15 sites. An experiment to confirm this phenomenon is attached as APPENDIX B to this report. Demonstrated is that a significant OC artifact developed on quartz fiber filters by heating in their plastic “mailers” to 40°C for several hours. It is evident that out-gassing of the plastic and other packaging materials as well as adsorption

of emitted volatile organic compounds on the quartz fiber were responsible for variable and often high OC values on the Middle East filters. Out of practical necessity, these filters were subjected to elevated and variable ambient temperatures for several months before being analyzed.

Similar OC artifacts were found on unexposed “trip blanks” that were dispatched to the Middle East and back but were not exposed to the ambient atmosphere in theater.

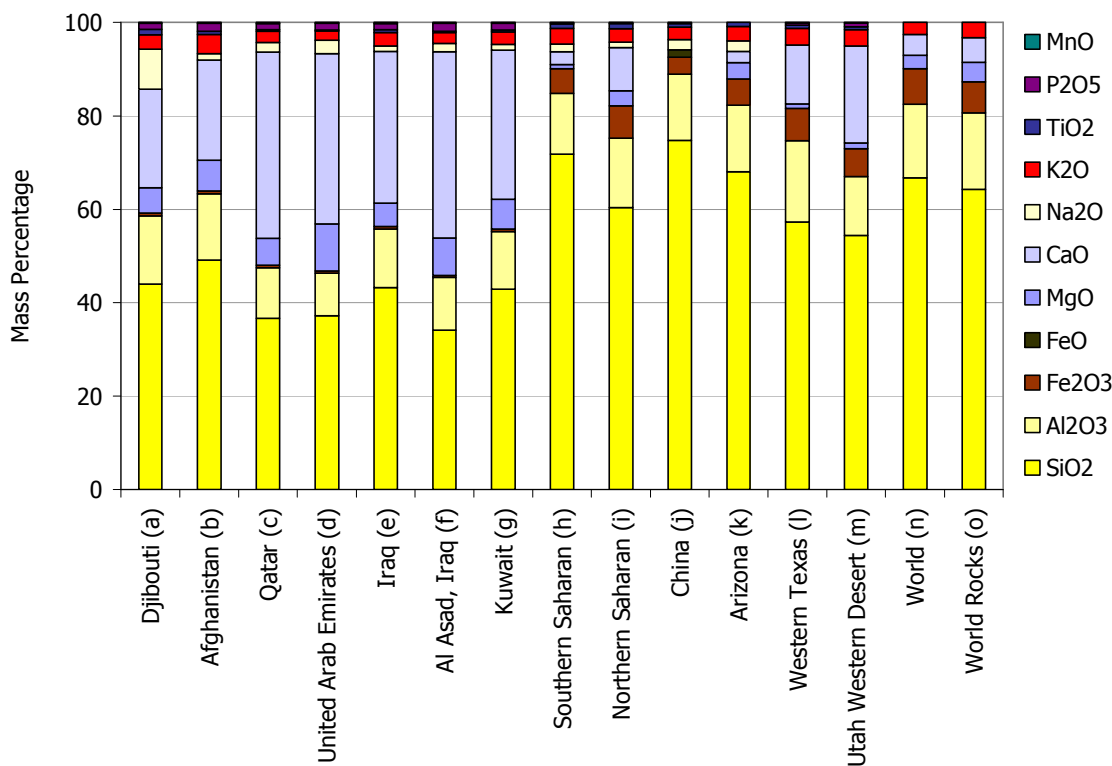


Figure 4-8. Comparison of dust samples from the Middle East, Sahara, China, U.S., world average dust, and world rocks. In the case of the EPMS samples, mean TSP results are shown, from (a) Djibouti; (b) Bagram and Khowst in Afghanistan; (c) Qatar; (d) UAE; (e) Balad, Baghdad, Tallil, Tikrit, and Taji in Iraq; (f) Al Asad in Iraq; (g) Northern, Central, Coastal, and Southern Kuwait; (h) average Southern Sahara [Goudie, 2006]; (i) average Northern Sahara [Goudie, 2006]; (j) average China [Goudie, 2006]; (k) Arizona [Goudie, 2006]; (l) Western Texas [Labban, 2004]; (m) Utah Western Desert [Labban, 2004]; (n) average world dust [Goudie, 2006]; and average world crustal rocks [Clarke, 1916].

4.2 Scanning Electron Microscopy (SEM)

SEM provided chemical and morphological information about individual particles collected on Nuclepore® filters at each of the 15 sites. Chemical compositions of the individual particles show a similarity to chemical results from Teflon® and quartz fiber filter samples collected in the ambient atmosphere at these sites.

4.2.1 Computer Controlled Scanning Electron Microscopy (CCSEM)

CCSEM provided chemical and morphological analyses of approximately 1000 particles per filter measured on a total of 243 Nuclepore® filters (Table 4-3).

Table 4-3. List of the number of Nuclepore® filters analyzed by CCSEM, for each sampled size fraction.

Site No.	Site Locality	Site ID	TSP	PM ₁₀	PM _{2.5}	Total
1	Djibouti	DJI_LEM	2	9	4	15
2	Bagram, Afghanistan	AFG_BAG	2	9	6	17
3	Khowst, Afghanistan	AFG_SAL	1	10	5	16
4	Qatar	QAT_UDE	1	10	5	16
5	United Arab Emirates	UAE_DHA	3	8	7	18
6	Balad, Iraq	IRQ_ANA	1	10	5	16
7	Baghdad, Iraq	IRQ_VIC	2	7	7	16
8	Tallil, Iraq	IRQ_ADD	2	9	7	18
9	Tikrit, Iraq	IRQ_SPE	2	3	4	9
10	Taji, Iraq	IRQ_TAJ	2	8	7	17
11	Al Asad, Iraq	IRQ_ALA	2	9	9	20
12	Northern Kuwait	KUW_BUE	1	8	7	16
13	Central Kuwait	KUW_AAS	1	8	5	14
14	Coastal Kuwait	KWT_SHU	1	10	5	16
15	Southern Kuwait	KUW_ARI	2	9	8	19
Total			25	127	91	243

Figure 4-9 (a) presents results of three to 10 compounded PM₁₀ Nuclepore® filters from each of the 15 sampling sites. Particles were classed into chemical “bins” some of which were interpreted as minerals, based on XRD measurements of <38 µm sieved soil samples (Fig 4-21). (*Note: “Bin” size data tables for each site and Nuclepore® filter as well as composited filters are available on the DOEHRs Portal*). In this fashion, we interpreted Ca-Mg particles as dolomite, Ca-rich as calcite, Si-Al-Mg rich as clay, Si-rich as quartz, etc. The “bin” with the highest concentrations by mass at all 15 sites is Si-Al-Mg (clay), varying from 27% for UAE to 59% for Tallil. Except for UAE and Al Asad, which have higher concentrations of carbonate (calcite and dolomite respectively) and the UAE which has a higher Si-Mg content, there is similarity among the sites. What is evident from these CCSEM results is the low percentage of Si-rich (quartz) particles, considering substantial amounts of quartz were measured by XRD (Fig. 4-21) and supported by XRF results (Figs. 4-7, 4-24, 4-27). Direct comparisons cannot be made in all instances, since XRD was performed on the <38 µm sieved fraction and chemical analysis on the <1000 µm sieved soil samples. In general, the proportion of quartz decreases toward the finer dust fractions, with an increase in the softer clay minerals. Interpretation of the CCSEM measurements is that quartz and other silicate minerals, as well as dolomite, and calcite particles to a limited degree, are often coated by clay minerals such as palygorskite and montmorillonite/illite. The CCSEM provides good measurements of surface coatings on quartz and other mineral grains, but the coated mineral grains result in underestimation of the total particle mineralogy using this analytical technique.

Figure 4-9 (b) presents the 0.5–1.0 μm size subset from the Figure 4-9(a) data set. As with trace metal results, this demonstrates that lead-bearing (Pb-rich) aerosol particles are concentrated in the finer fraction on Nuclepore® filters.

4.2.2 Scanning Electron Microscopy of Ultrafines (<0.5 μm)

Summary plots of the ultrafine fractions, as measured by SEM are graphically presented in Figure 4-10. A total of 100 particles of less than 0.5 μm in diameter were analyzed on Nuclepore® membrane filters, one PM_{2.5} filter from each of the 15 sites. Because of the small particle sizes, 50 particles less than 0.2 μm from each filter were manually analyzed by SEM and another 50 particles 0.2 μm to 0.5 μm in diameter by interactive CCSEM. The purpose was to establish if trace metals or particles of concern are concentrated in this size fraction. From particle-size distribution patterns (Fig. 4-20), total mass in the ultrafine size fraction was estimated to be far less than 1% of total mass on the filters.

Chemistry and morphology of the ultrafines were found to differ substantially from those of the coarser fractions. The former contains far less geological components (e.g., silicon, aluminum, iron, magnesium, calcium, or magnesium) than the coarser fractions. Ultrafines very often contain spheroidal particles of carbon, together with sulfur, sodium, and chlorine (Figs. 4-17 to 4-19) and, in a few instances lead, bromine and chlorine (Figs. 4-12). Origin of the spheroids is uncertain, but it can be assumed from their carbon and sulfur content that many of these are from various oil, gasoline, and natural gas combustion processes, including motor vehicle tailpipe emissions. Chromium and vanadium rich particles typical of igneous rocks from the Rift Valley region were analyzed in ultrafines from Djibouti (Fig. 4-10[b]). Trace amounts of nickel from Bagram, as well as titanium and nickel from Southern Kuwait also may be of geological origin. Lead measured in the Balad sample is likely to be from lead smelters and gasoline vehicle emissions. Lead on the Bagram filter likely is from gasoline vehicle emissions.

4.2.3 Transmission Electron Microscopy (TEM)

Transmission Electron Microscope (TEM) measurements for airborne asbestos were performed on one Nuclepore® filter from each site. No asbestos fibers were found by this method [Yamate, 1984].

4.2.4 Secondary Electron Images

Figures 4-11 to 4-19 are high resolution secondary electron images of mineral grains from selected sampling sites. These show a variety of crystal forms, including dolomite and calcite, as well as aggregates and coatings of clay minerals. Although detailed clay mineral analysis was not performed on these samples, several references on the clays of the Middle East [Al-Awadhi, 2005; Al-Juboury, 2006; Çagatay, 1990; Kahlaf, 1985], as well as the CCSEM and secondary electron images, are evidence for Mg-Al-Si particles being a clay phase. We interpret rods and fibers as palygorskite (Figs. 4-14 [d], 4-15 [c]) and the platelets as montmorillonite/illite mixed layers or kaolinite (Figs. 4-13 [c], 4-14 [b], 4-15 [d]).

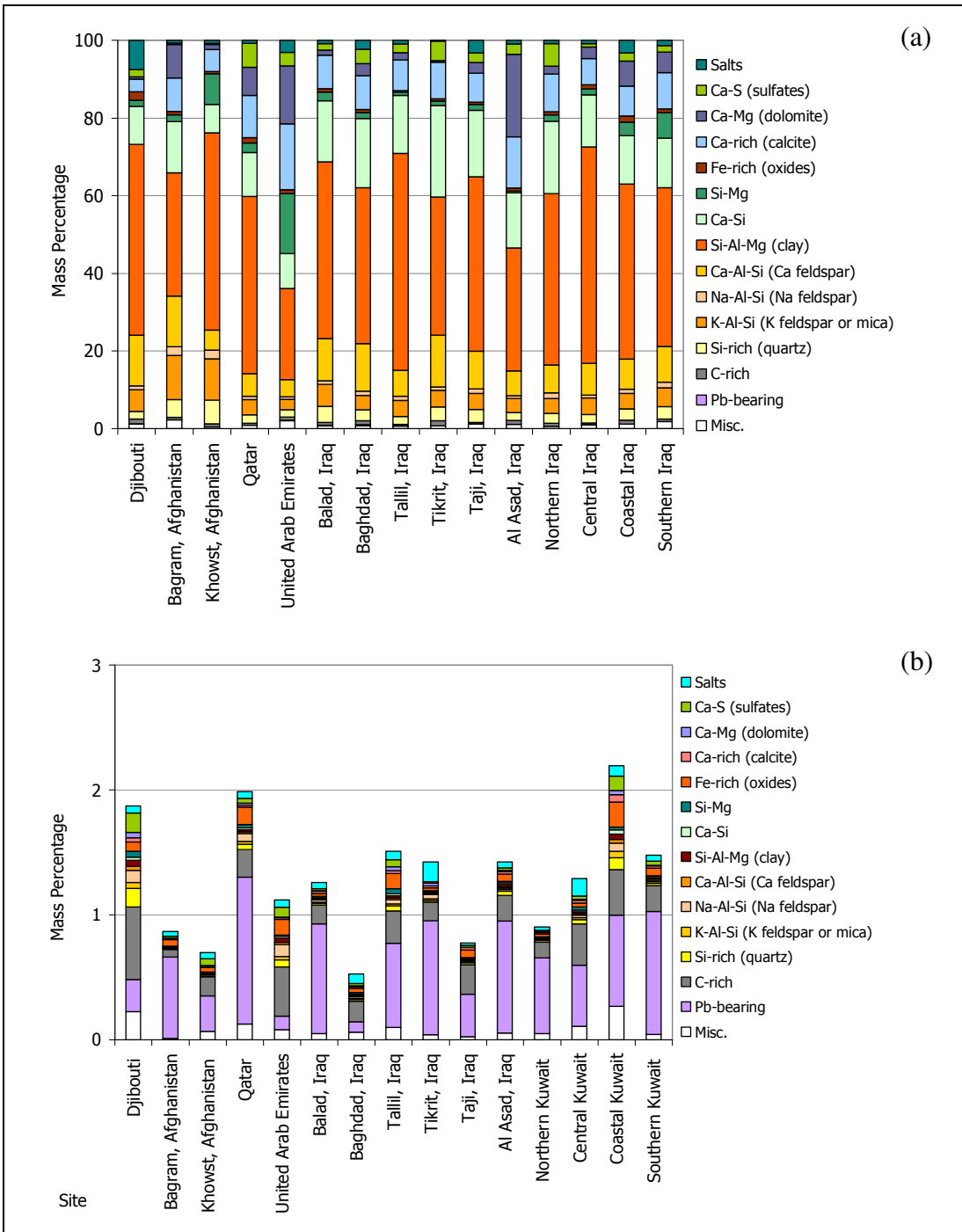


Figure 4-9. Composite of all CCSEM PM₁₀ results measured on Nuclepore® filters, grouped by site. All size fractions, from 0.5 to 10 µm diameter particles, are shown in (a) while the 0.5 to 1.0 µm diameter (fine fraction) subset is shown in (b), demonstrating that lead (Pb) is concentrated in this fine fraction.

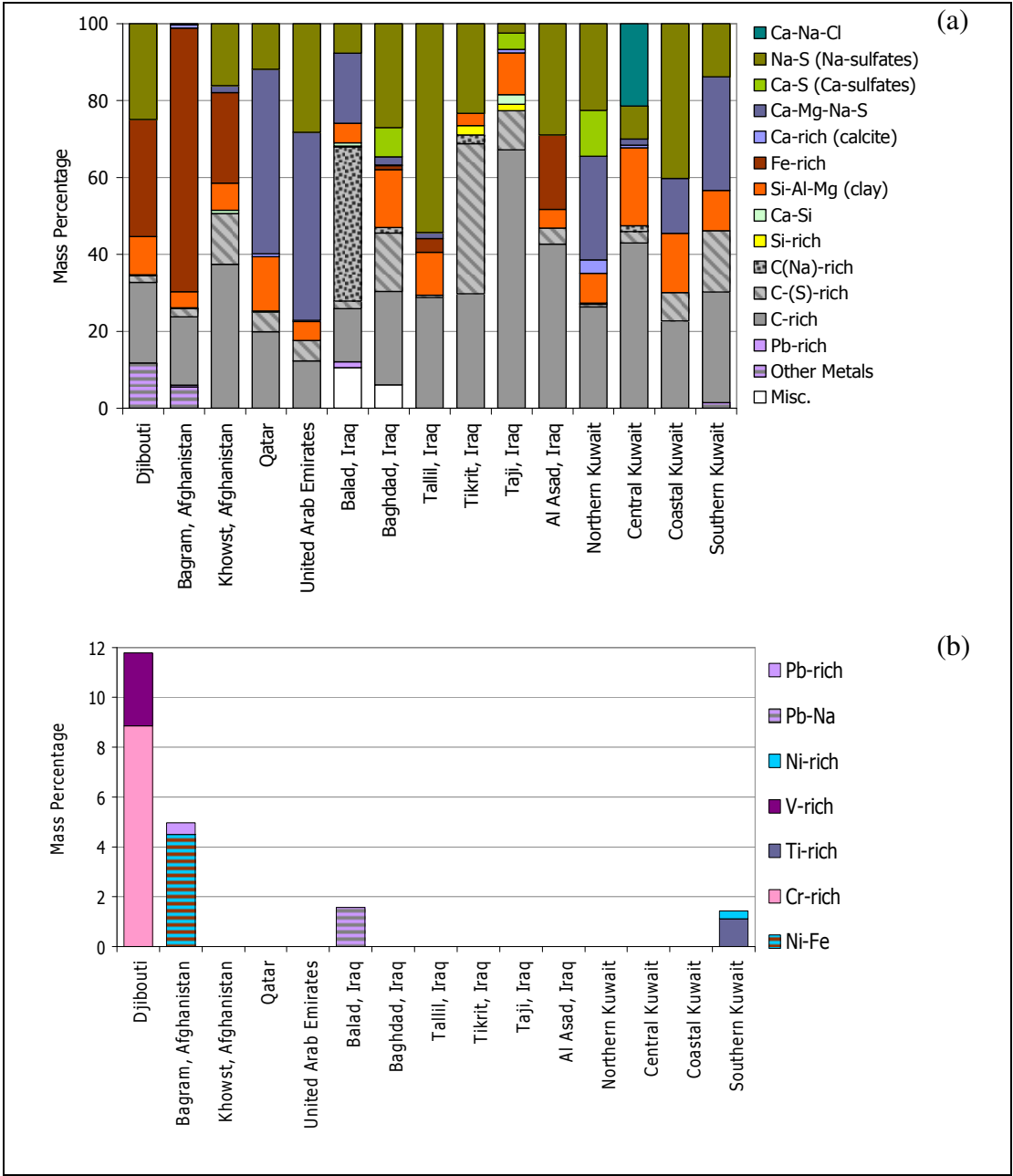


Figure 4-10. SEM and CCSEM results of ultrafines (<0.5 μm diameter) measured on fifteen PM_{2.5} samples collected on Nuclepore® filters. Compositions of 100 particles analyzed for all species are shown in (a) while individual trace metals are shown on an expanded scale in (b).

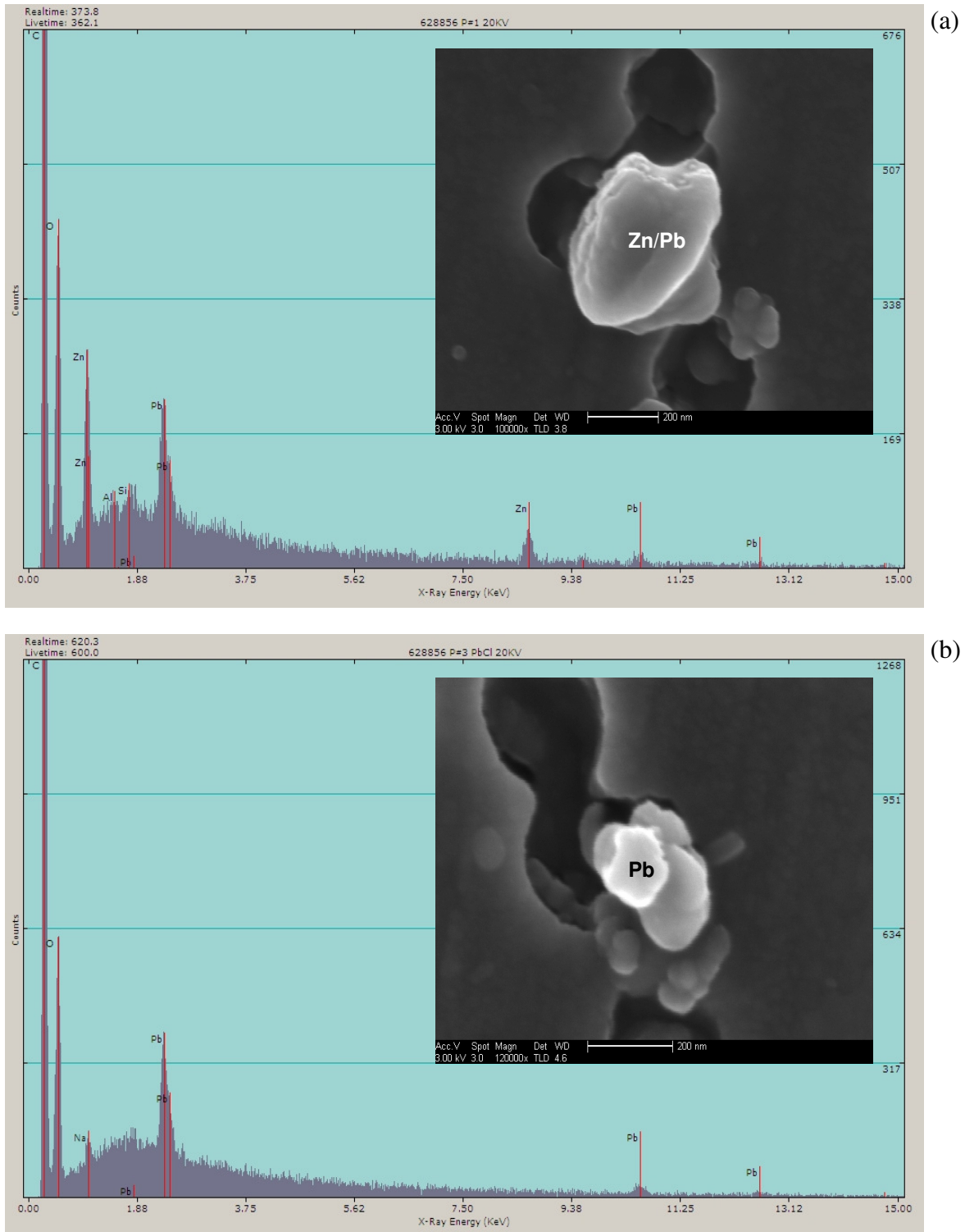


Figure 4-11. Secondary Electron Images and EDS spectra of two particles on a Nuclepore® filter sampled in Balad, Iraq; (a) zinc (Zn)/lead (Pb) particle with carbon, possibly from a lead and dry cell battery smelting facility; (b) lead (Pb) particle from lead smelting. Dark circles in the field are approximately 0.4 μm pores in the Nuclepore® membrane filters.

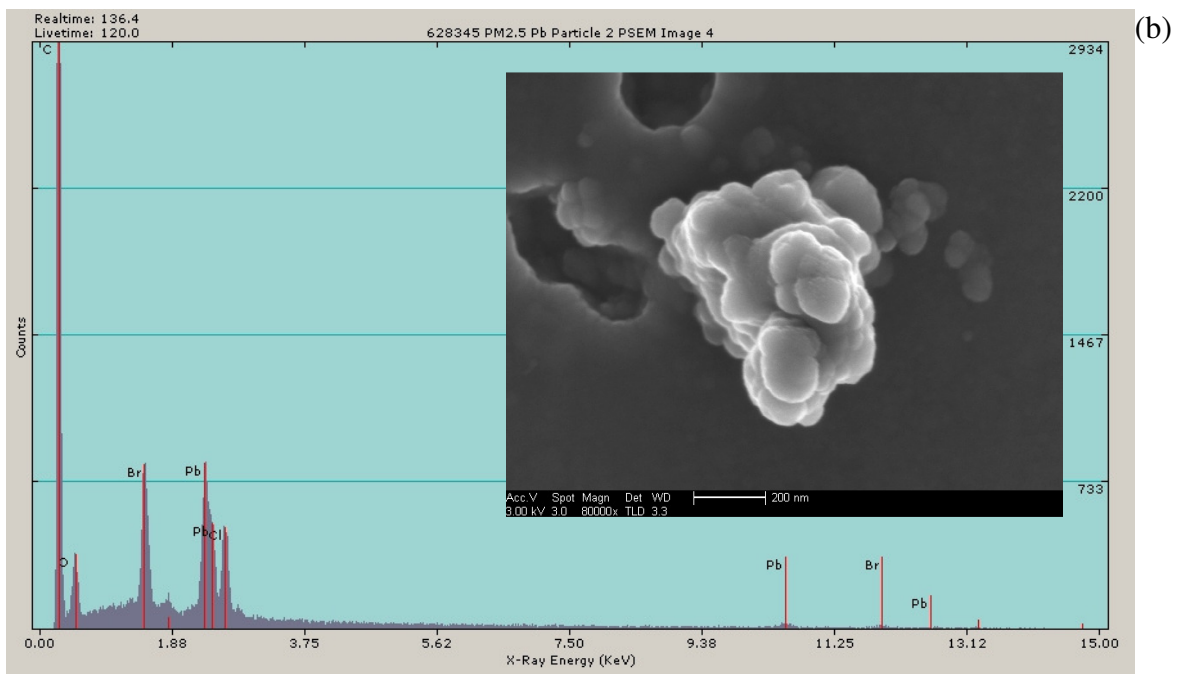
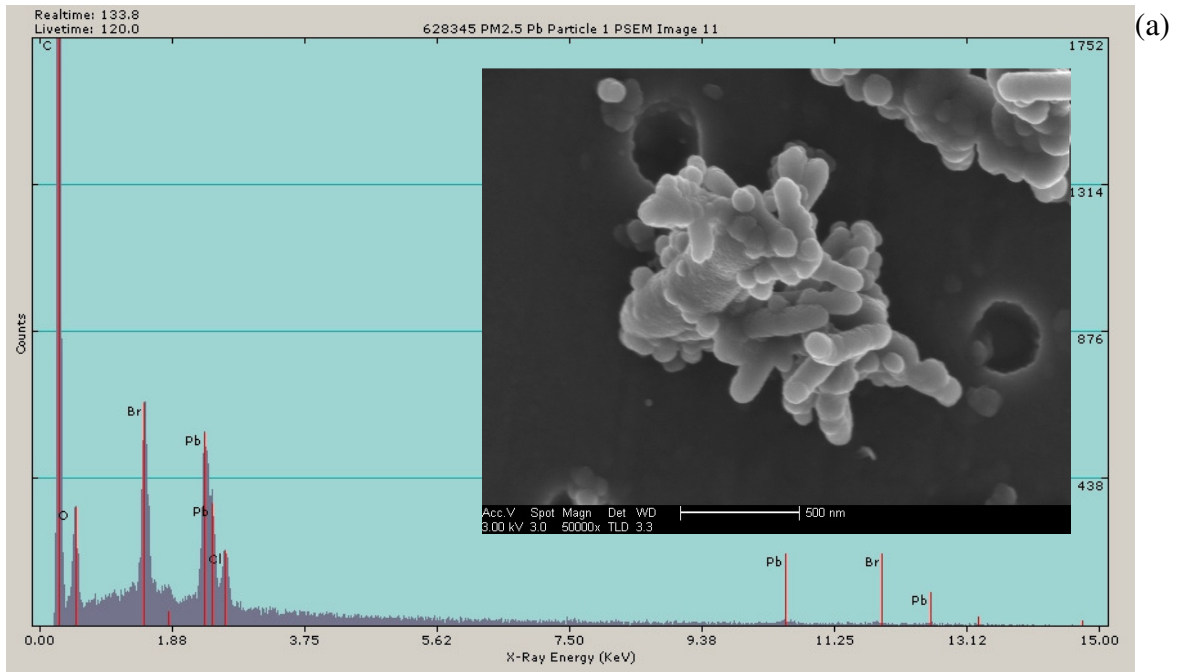


Figure 4-12. Secondary Electron Images and EDS spectra of two particles on a Nuclepore® filter sampled in Balad, Iraq. Both (a) and (b) are sections of carbon chains containing high concentrations of lead (Pb), bromine (Br), and chlorine (Cl)—tailpipe emissions from leaded gasoline vehicles.

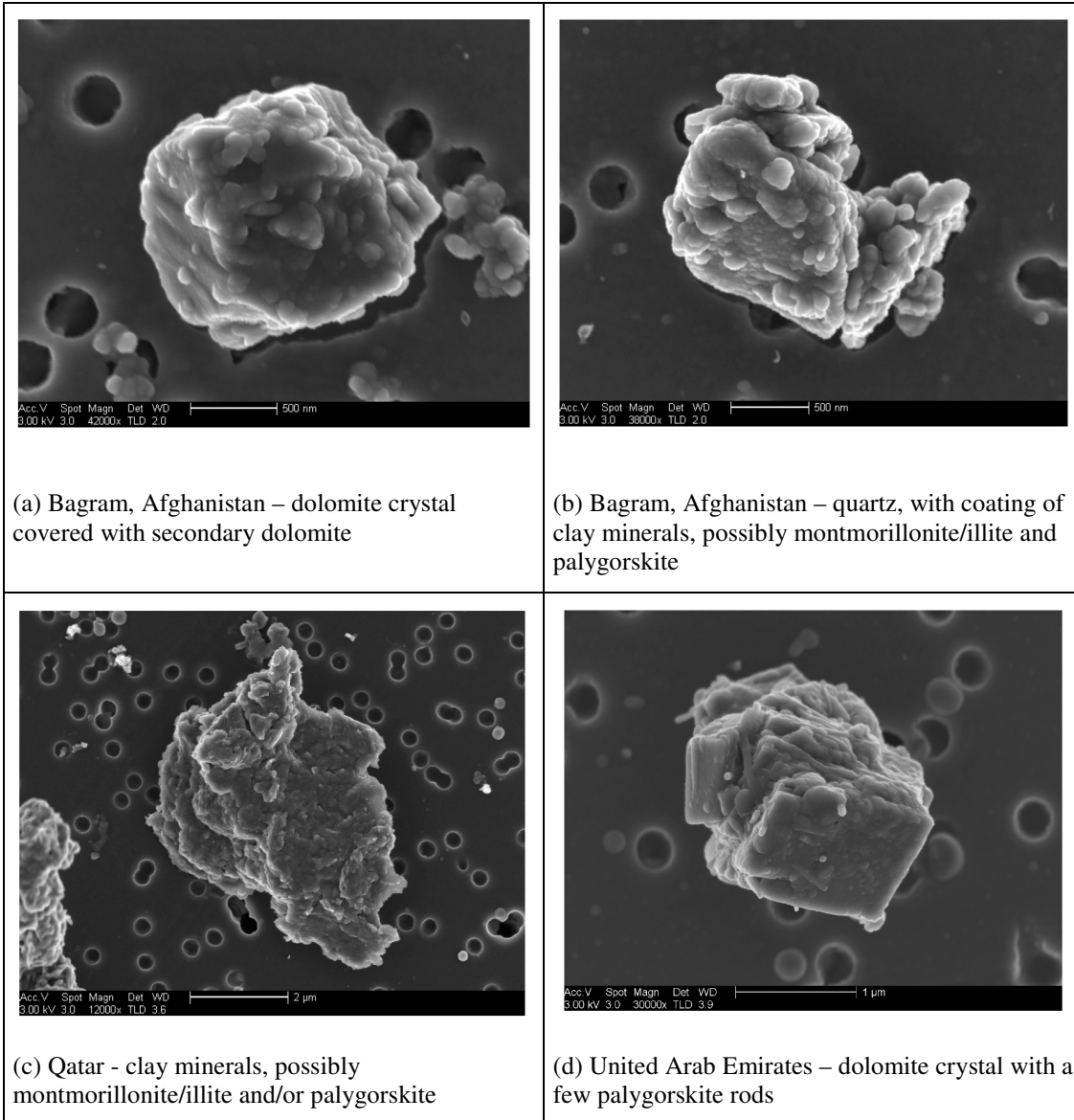


Figure 4-13. Secondary Electron Images from Bagram (a), Bagram (b), Qatar (c), and United Arab Emirates (UAE) (d). Dark circles in the field are approximately 0.4 μm pores in the Nuclepore® membrane filters.

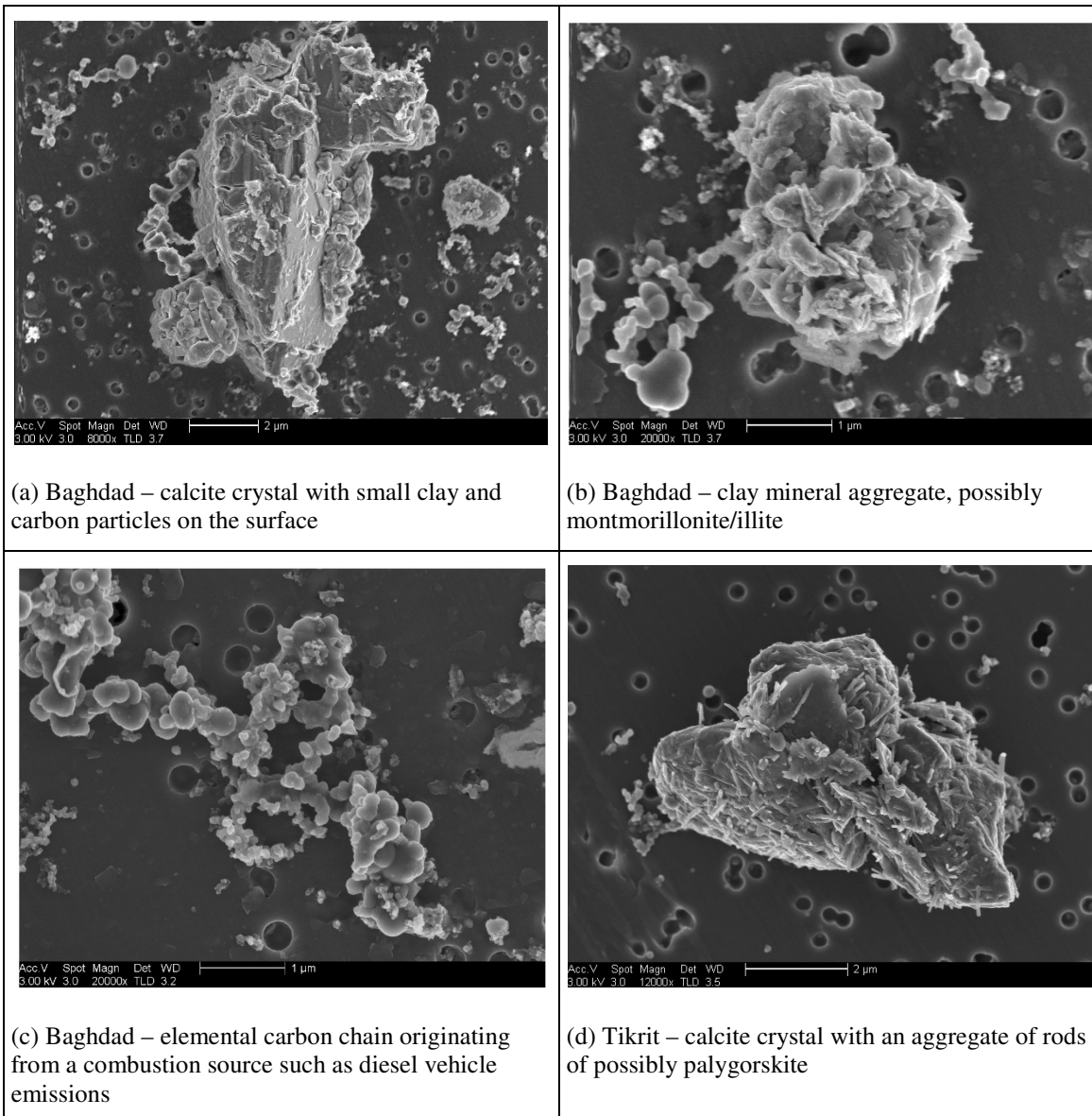


Figure 4-14. Secondary Electron Images from Baghdad (a), Baghdad (b), Baghdad (c) and Tikrit (d). Dark circles in the field are approximately 0.4 μm pores in the Nuclepore® membrane filters.

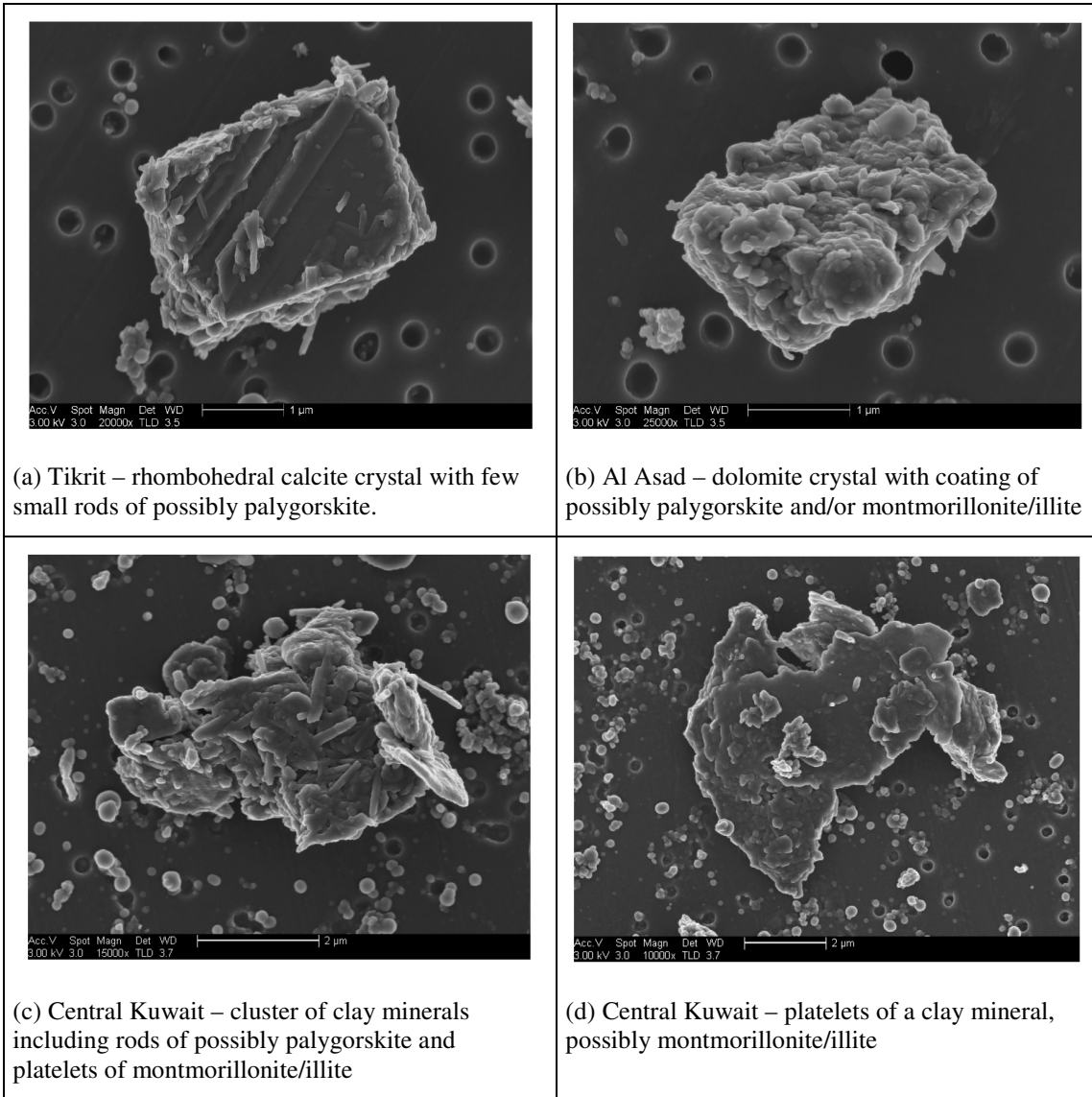


Figure 4-15. Secondary Electron Images from Tikrit (a), Al Asad (b), and Central Kuwait (c and d). Dark circles in the field are approximately 0.4 μm pores in the Nuclepore® membrane filters.

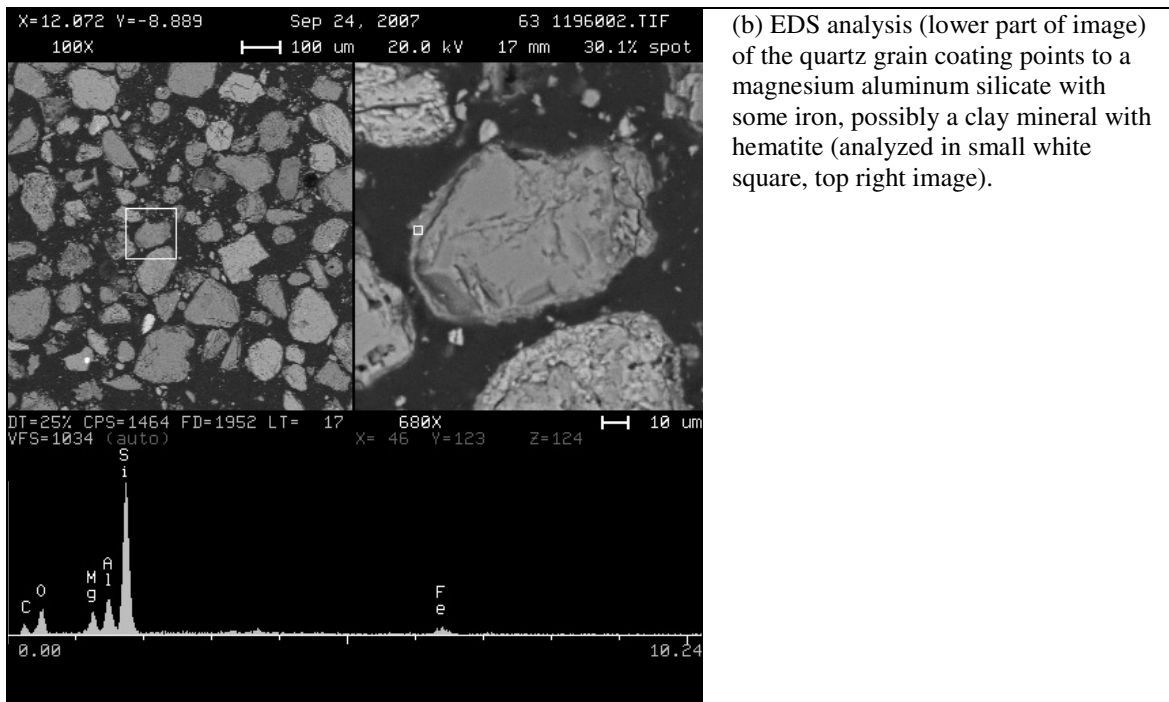
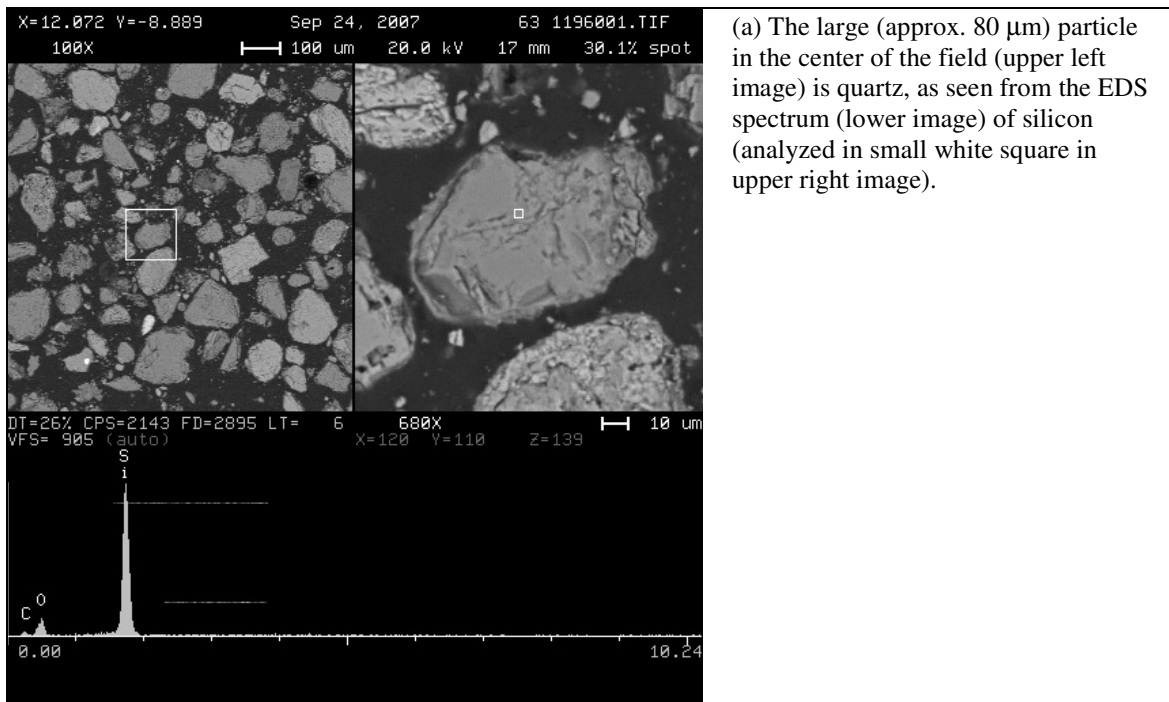


Figure 4-16. A polished section of sieved bulk dust sample from Coastal Kuwait showing compositional details of (a) a quartz grain and (b) its coating, consisting of a magnesium aluminum silicate clay, possibly montmorillonite and/or palygorskite.

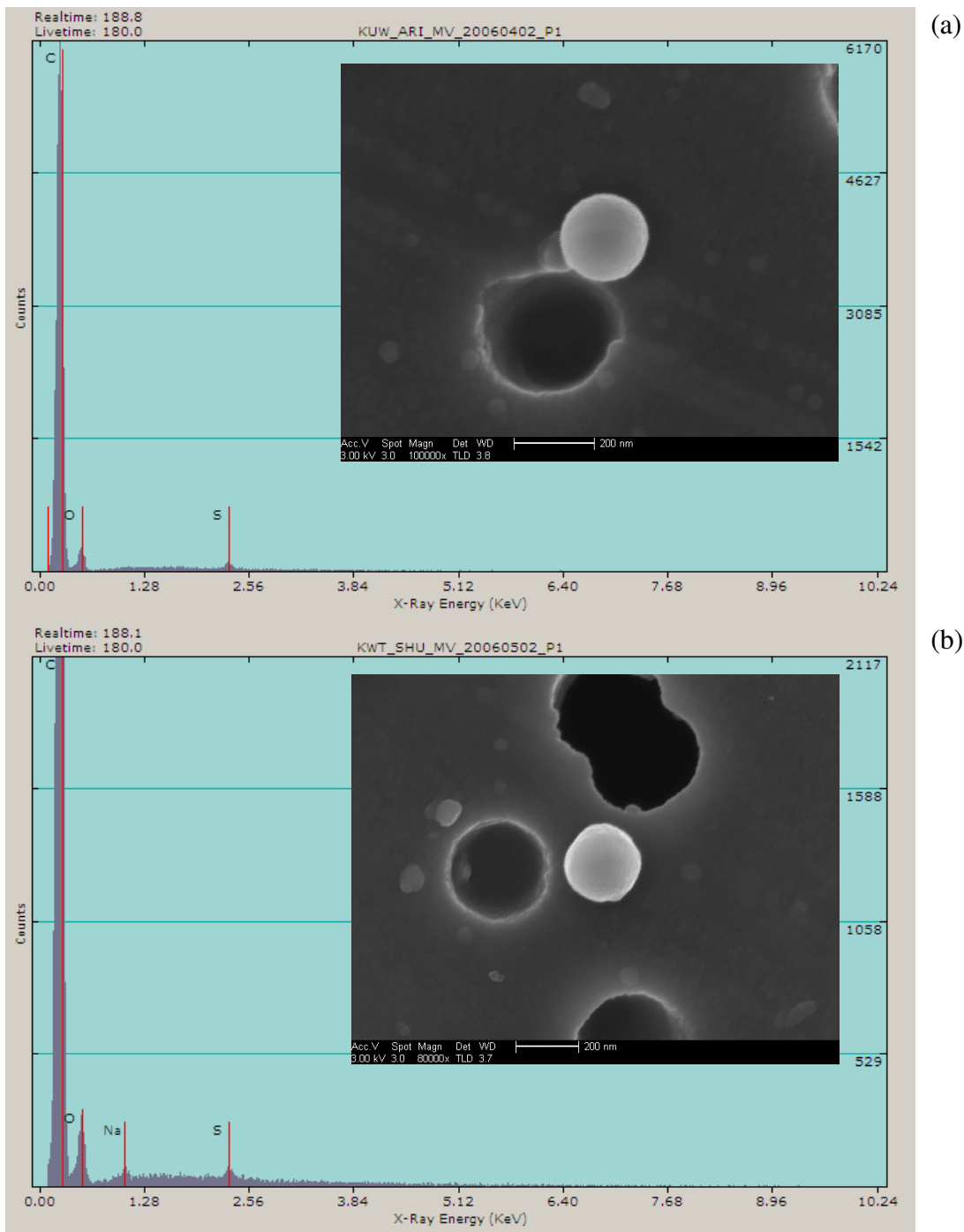


Figure 4-17. Secondary Electron Images and EDS spectra of two spherical ultrafine (approx. 0.2 μm diameter) particles on Nuclepore® filters: (a) carbon particle with sulfur from Southern Kuwait and (b) carbon particle with sodium and sulfur from Coastal Kuwait. Both particles may be from combustion of sulfur-rich oil, including diesel fuel. Dark circles in the field are approximately 0.4 μm pores in the Nuclepore® membrane filters.

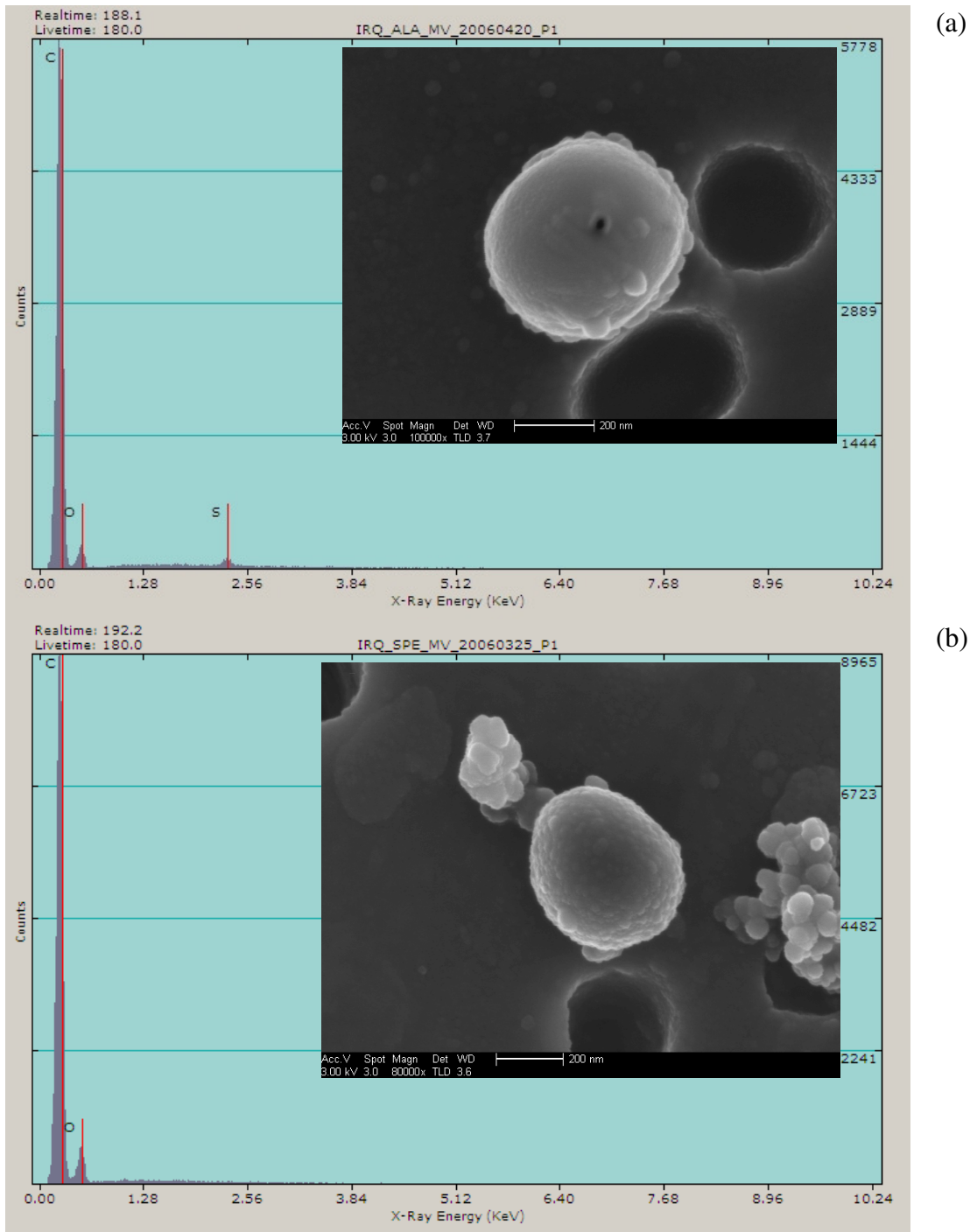


Figure 4-18. Secondary Electron Images and EDS spectra of two spheroids of ultrafine (approx. 0.5 μm diameter) particles on Nuclepore® filters: (a) carbon particle with sulfur from Al Asad and (b) carbon particle from Tikrit in Iraq. Both particles may be from combustion of oil, including diesel fuel. Dark circles in the field are approximately 0.4 μm pores in the Nuclepore® membrane filters.

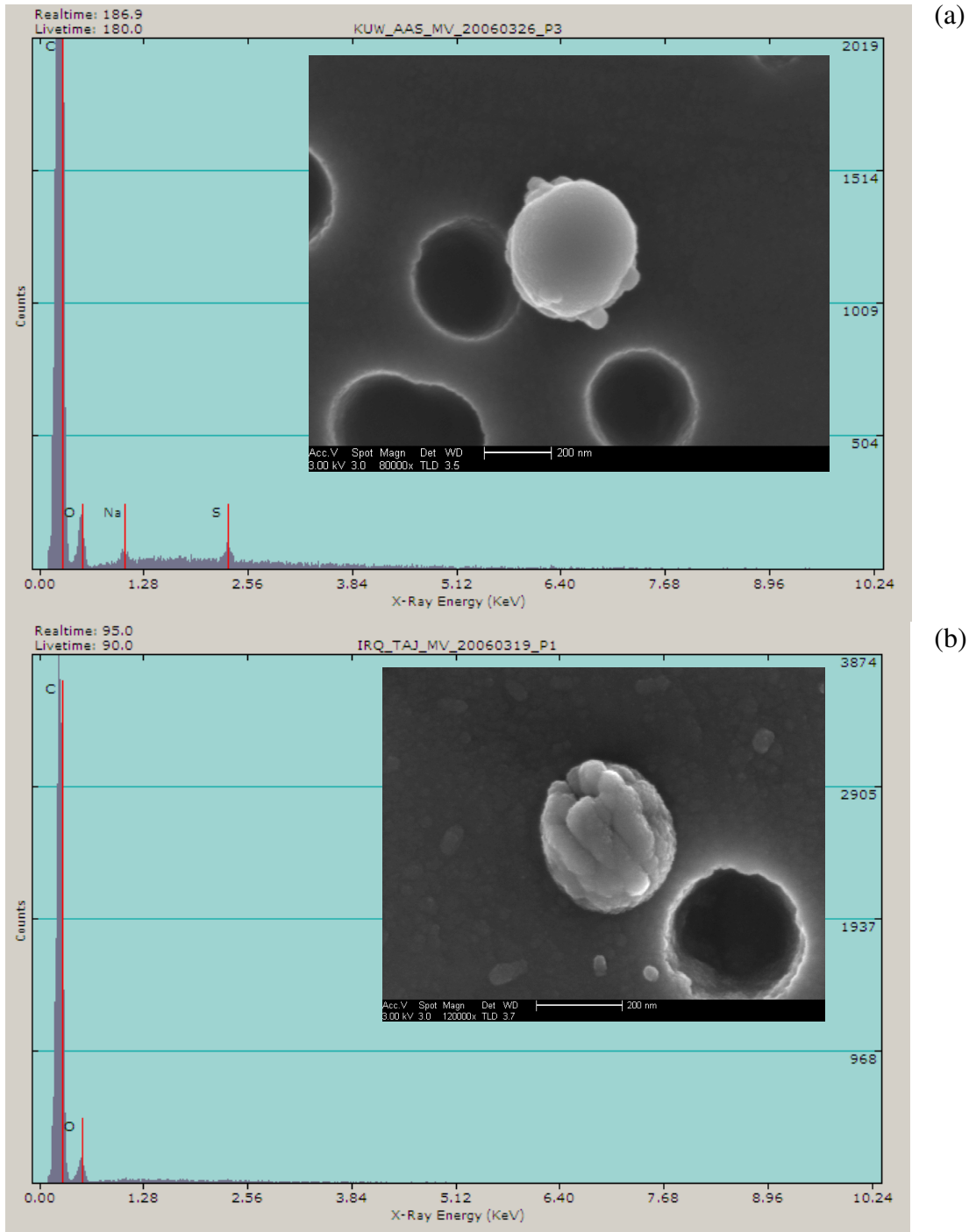


Figure 4-19. Secondary Electron Images and EDS spectra of two spheroids of ultrafine approx. 0.4 μm diameter) particles on Nuclepore® filters: (a) carbon particle composed of smaller carbon particles from Taji, Iraq and (b) carbon-sodium-sulfur particle from Central Kuwait. Both particles may be from oil combustion processes. Dark circles in the field are approximately 0.4 μm pores in the Nuclepore® membrane filters.

4.2.5 Particle Size Distributions

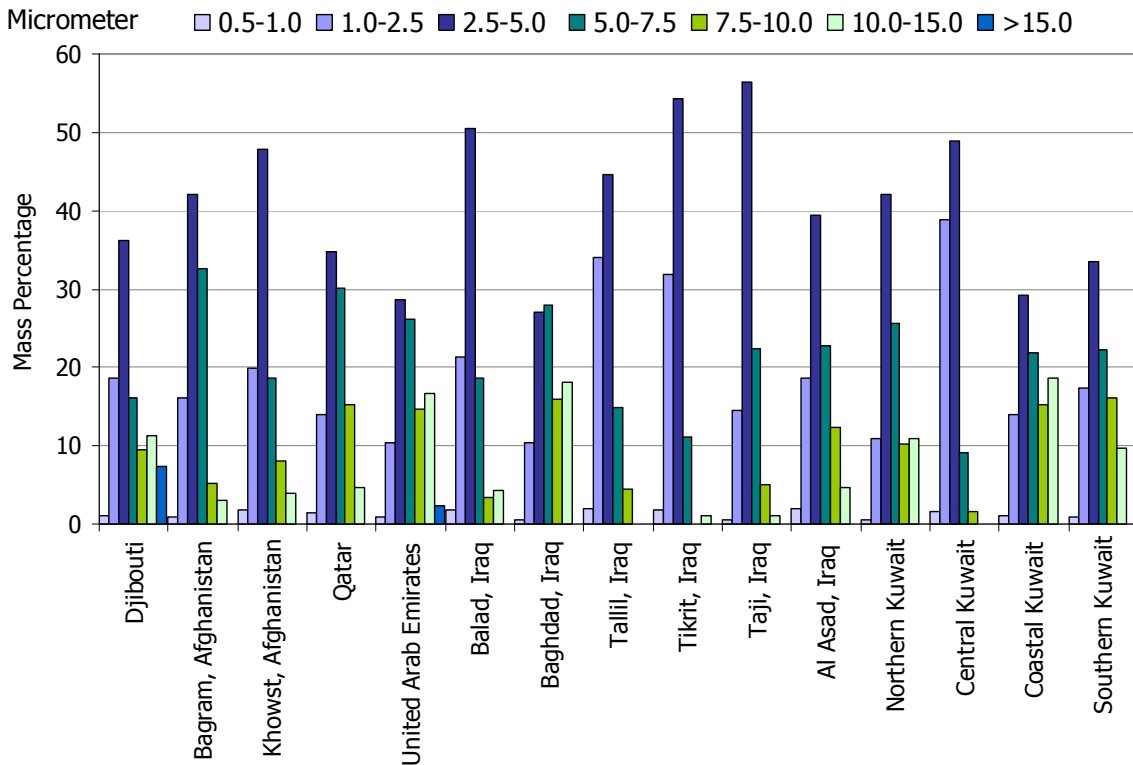


Figure 4-20. Particle size distributions by mass percentage as measured by CCSEM, of TSP samples collected on Nuclepore® filters.

A particle size distribution for each of the 15 sites was compiled from the composite (1 to 3 filters) TSP Nuclepore® samples. All sites show a positive skewed distribution, and all except Baghdad have a distinct maximum in the 2.5 to 5.0 μm size range (Fig. 4-20, Table 4-4). Distributions of Djibouti, UAE, Balad, Baghdad, Northern Kuwait, and Coastal Kuwait have a slightly bimodal concentration, with a minor peak in the 10 to 15 μm size range. We ascribe these to wind-blown dust events producing large particles.

Table 4-4. Particle size distributions by mass percentage, as measured by CCSEM on TSP Nuclepore® filters.

Bin Size			0.5-1 µm	1-2.5 µm	2.5-5 µm	5-7.5 µm	7.5-10 µm	10-15 µm	>15 µm
Site No.	Site Locality	Site ID	%	%	%	%	%	%	%
1	Djibouti	DJI_LEM	1.2	18.6	36.2	16.1	9.5	11.2	7.3
2	Bagram, Afghanistan	AFG_BAG	0.9	16.1	42.1	32.6	5.2	3.1	0.0
3	Khowst, Afghanistan	AFG_SAL	1.8	19.8	47.8	18.6	8.1	3.9	0.0
4	Qatar	QAT_UDE	1.3	14.0	34.7	30.1	15.2	4.7	0.0
5	United Arab Emirates	UAE_DHA	0.8	10.4	28.6	26.2	14.8	16.7	2.4
6	Balad, Iraq	IRQ_ANA	1.9	21.2	50.5	18.6	3.5	4.4	0.0
7	Baghdad, Iraq	IRQ_VIC	0.6	10.3	27.0	28.0	15.9	18.1	0.0
8	Tallil, Iraq	IRQ_ADD	1.9	34.1	44.7	14.8	4.5	0.0	0.0
9	Tikrit, Iraq	IRQ_SPE	1.7	31.8	54.2	11.2	0.0	1.1	0.0
10	Taji, Iraq	IRQ_TAJ	0.6	14.6	56.5	22.3	5.1	1.0	0.0
11	Al Asad, Iraq	IRQ_ALA	2.0	18.6	39.4	22.8	12.4	4.7	0.0
12	Northern Kuwait	KUW_BUE	0.5	11.0	42.0	25.5	10.1	10.8	0.0
13	Central Kuwait	KUW_AAS	1.7	38.8	48.8	9.0	1.6	0.0	0.0
14	Coastal Kuwait	KUW_SHU	1.1	13.9	29.2	21.9	15.3	18.7	0.0
15	Southern Kuwait	KUW_ARI	1.0	17.4	33.6	22.2	16.2	9.7	0.0

Of note is that except for small percentages at Djibouti and UAE, no particles were recorded in the >15 µm size “bin.”

4.3 Grab Soil Samples

Representative surface soil samples were collected at each of the 15 aerosol sampling sites. To be representative of wind-blown dust at the site, we sampled the top 1 cm of soil. A sample split was screened to separate the <38 µm particles for mineralogical analysis by XRD and re-suspension onto Teflon®, quartz fiber, and Nuclepore® filters, similar to the ambient filter samples collected in the field. Analysis of sieved bulk samples allowed us to compare particles that were present in the soil which have the potential to become airborne and those that were observed in ambient dust.

A second sample split of each was screened to <1000 µm for analysis of particle size, carbonate content, electrical conductivity, pH, and elemental analysis by XRF. These results provided a comparison between the Middle East dust samples and soil samples collected in other parts of the world. (*Note: a complete set of results is posted on the DOEHS Portal.*)

4.3.1 Mineralogy of <38 µm Screened Soils

In general, mineralogy of the <38 µm screened bulk samples (Figure 4-21) is a reflection of both regional geology and wind-transported dust that deposits to local soils.

Djibouti

Djibouti lies in the Afar triangle which is part of the African continental rift zone, underlain by basaltic lava flows and associated sediments. Igneous minerals in the <38 µm screened dust sample include pyroxene, amphibole, olivine, plagioclase, ilmenite, and magnetite. The nearly 10% calcite in the sample is possibly from raised coral reefs in that area.

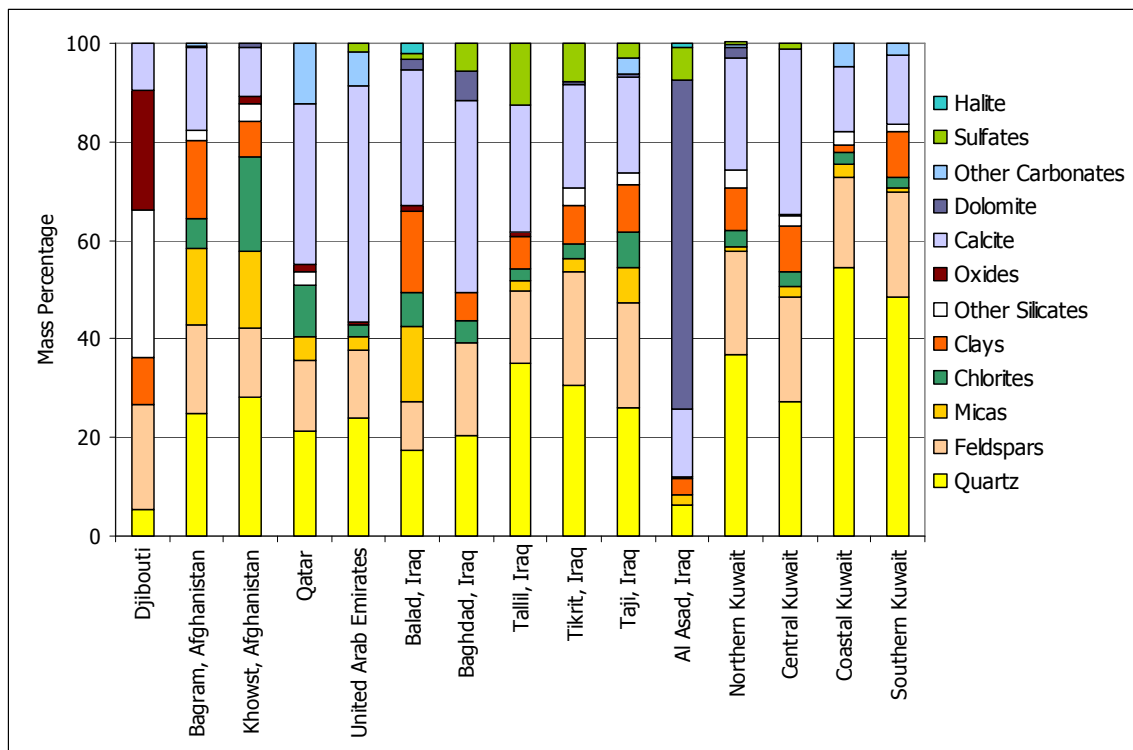


Figure 4-21. Mineralogical composition by XRD of <38 μm sieved soil samples collected in the vicinity of aerosol sampling sites.

Afghanistan

Both the Bagram and Khowst sites are in eastern Afghanistan, the latter in the mountainous region close to the Pakistan border. Dust storms (Fig. 4-22) originating in the southwestern part of the country move in a counter-clockwise direction, funneling some windblown dust toward Kabul, Bagram, and Khowst. The Bagram site is underlain by loess (wind deposited silt), sand and clay, and Khowst by alluvium containing gravel, sand, silt, and clay. The two screened samples are mineralogically similar, both containing major amounts of quartz, feldspar, mica, calcite, and smaller amounts of chlorite. The sample from Bagram contains 14% clay minerals.

Qatar and the UAE

Both Qatar and the UAE are impacted by dust from the Arabian Peninsula, Iraq, and Kuwait. Samples from both sites contain large amounts of calcite (28-41%), quartz, and feldspar and lesser amounts of chlorite and clay minerals. Qatar also contains small amounts of hornblende and ilmenite, probably transported from weathered volcanics in Saudi Arabia to the west of the sampling site.

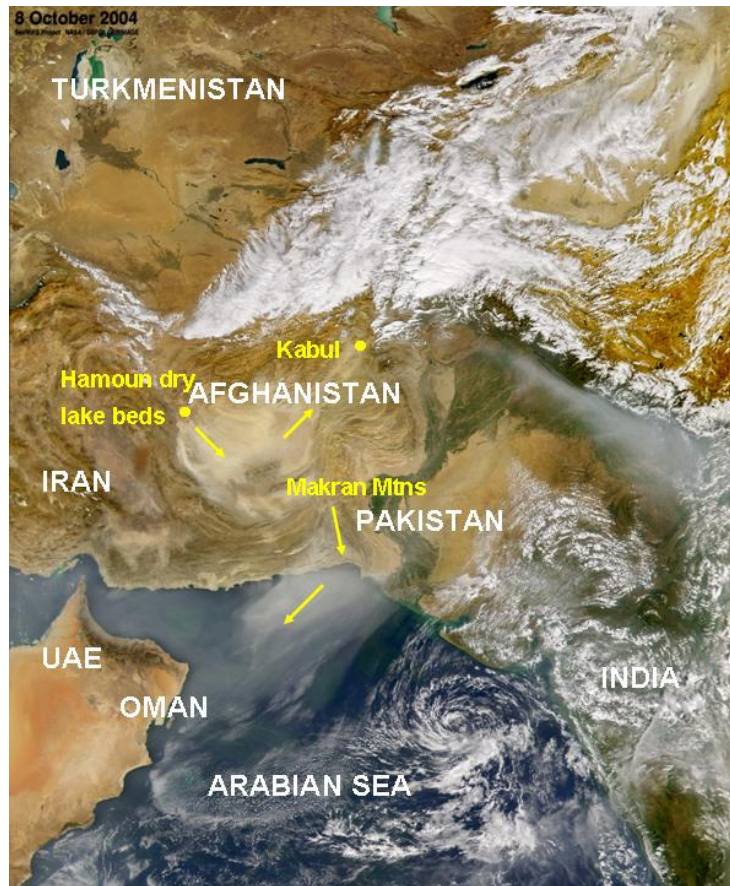


Figure 4-22. Dust storm of October 8, 2004, originating from dry Hamoun Lake beds along the Iran-Afghanistan border and partly crossing the Makran Mountains into Pakistan and the Arabian Sea. A split off the plume moved in a northeasterly direction towards Kabul, Bagram, and Khowst.

Iraq

Satellite imagery shows dust storms (Fig. 4-23) blowing across Iraq and Kuwait, storms that originated at salt pans and wadis along the border with Turkey and Syria.

The Baghdad site as well as the three sites further north and close to the Tigris River (i.e., Taji, Balad, and Tikrit) contain major amounts of quartz, calcite, and feldspar with smaller amounts of gypsum, micas, and clays. The Tallil sample, collected further to the south and close to the Tigris-Euphrates river confluence, contains about 11% sulfate as the mineral gypsum. This sampling site is on poorly drained river basin soils, and gypsum could be from windblown dust off the gypsiferous desert immediately to the southwest of this site. Al Asad, closer to the Euphrates River and 200 km to the west of Baghdad, differs from the other five Iraq sites in that it contains about 59% dolomite, 6% gypsum, and only 5% quartz. That region is underlain by soils containing gypsum, limestone, and sandstone [Buringh, 1960]. XRD analysis of the <38 µm sieved dust samples confirms that the limestone in this region is largely dolomite instead of calcite, as at the other five Iraq sampling sites.

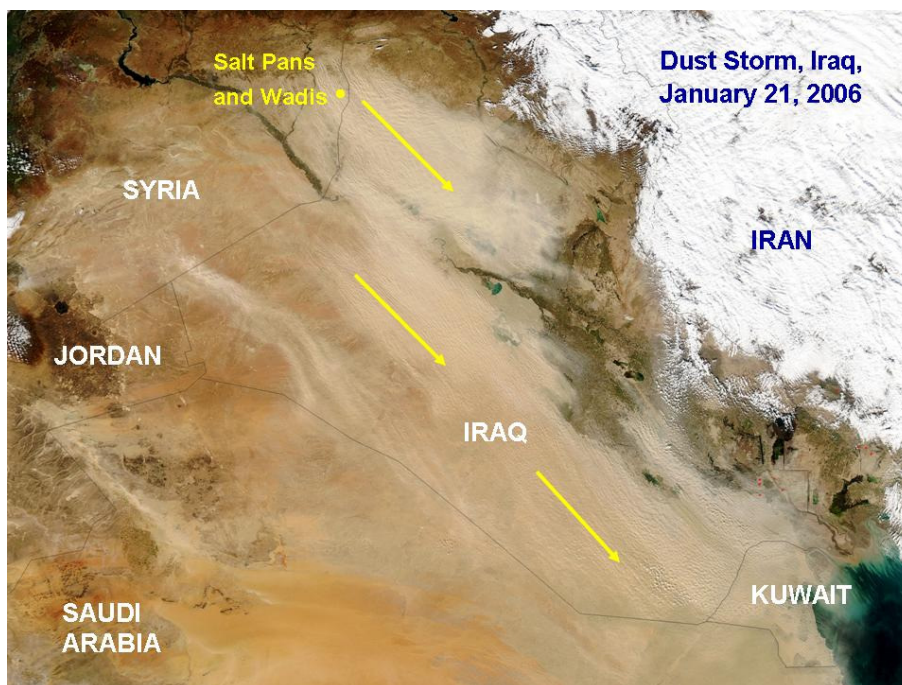


Figure 4-23. Dust storm of January 21, 2006, originating at salt pans and wadis along the northern border of Iraq with Syria and Turkey. This specific storm crossed Iraq and Kuwait and continued on into the Arabian-Persian Gulf.

Kuwait

The four samples from Kuwait contain higher percentages of silt than those from adjacent Iraq, with 25% to 48% quartz. Samples from all four sites also contain approximately 18% feldspar, mostly plagioclase, as well as calcite and clay minerals. Previous studies on fallout dust in Kuwait [Al-Awadhi, 2005] showed that the clay minerals are palygorskite, together with illite-montmorillonite and a smaller proportion of kaolinite. Al-Awadhi [2005] and Kahlaf [1985] suggested that most of the dust in Kuwait was transported from the dry Mesopotamian floodplain in southern Iraq and other parts of the Arabian peninsula.

4.3.2 Chemistry of Re-suspended Soils

The fifteen <math><38\ \mu\text{m}</math> screened soil samples were re-suspended onto Teflon® and quartz fiber filters, providing two filter sample sets for chemical analysis, one each of PM₁₀ and PM_{2.5}. We followed the same chemical analysis procedures for filter samples from re-suspensions as for ambient samples.

Major Element Chemistry

Major oxide chemistry for both PM₁₀ (Fig. 4-24 [a]) and PM_{2.5} (Fig. 4-24 [b]) are shown below. In all instances, samples contain major amounts of SiO₂, mainly in the mineral quartz, as well as variable amounts of CaO, in the minerals calcite, dolomite, and to a limited extent plagioclase feldspar. The MgO is largely contained in dolomite and to a lesser extent in clay minerals such as palygorskite and/or montmorillonite.

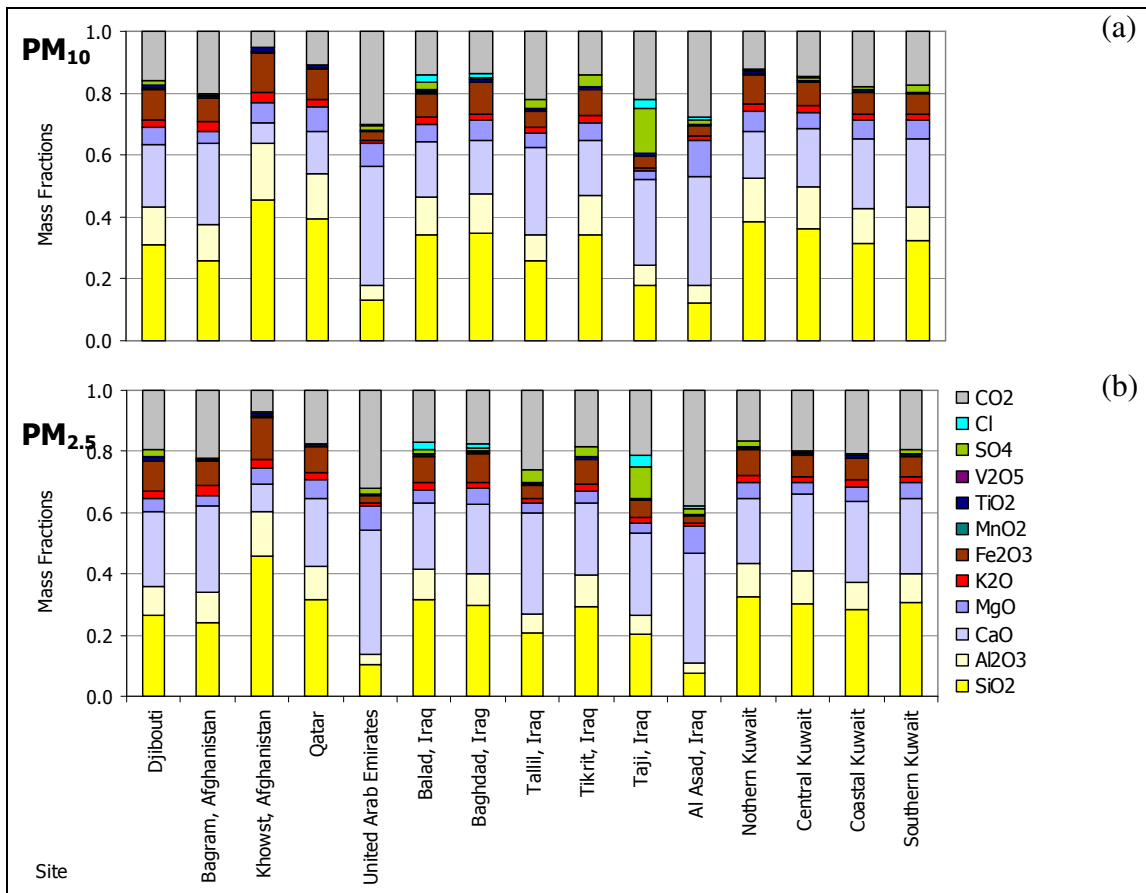


Figure 4-24. Major element chemistry of PM_{10} (a) and $PM_{2.5}$ (b) re-suspended samples for each of the 15 sites. Concentration fractions are expressed as oxides, including CO_2 contained in carbonate minerals such as calcite and dolomite.

In the case of Djibouti, the above mentioned oxides are largely in silicate minerals such as pyroxene, amphibole, and feldspar. For the four Kuwait sites, parts of the Al_2O_3 and CaO are contained in plagioclase feldspar. The UAE sample contains a higher fraction of CaO, in the carbonate mineral calcite while Al Asad has a high percentage of MgO in the carbonate mineral dolomite. Khowst also differs from the other sites in that it contains a high fraction of SiO_2 in silt, less CaO in calcite, and slightly more Al_2O_3 in clay than the other sites. The four Kuwait re-suspensions are chemically very similar to each other. Chloride (Cl) in both the PM_{10} and $PM_{2.5}$ size fractions at Taji, Balad and Baghdad point to soil salinization in the general region along the Tigris River valley.

The $PM_{2.5}$ samples differ marginally in composition from the PM_{10} samples. PM_{10} contains more SiO_2 in mineral quartz.

Major chemistry results from the 15 re-suspended dust samples are for each site similar to the ambient samples, as seen in Figures 4-7 (b), (c). This implies that part of the wind-blown dust is locally generated and local surface soil could have formed from previous deposition of wind-blown dust. Ambient samples contain higher proportions of sulfate, possibly ammonium sulfate and/or gypsum ($CaSO_4 \cdot 2H_2O$).

Trace Element Chemistry

Figure 4-25 presents trace element results of the 15 re-suspended soil samples.

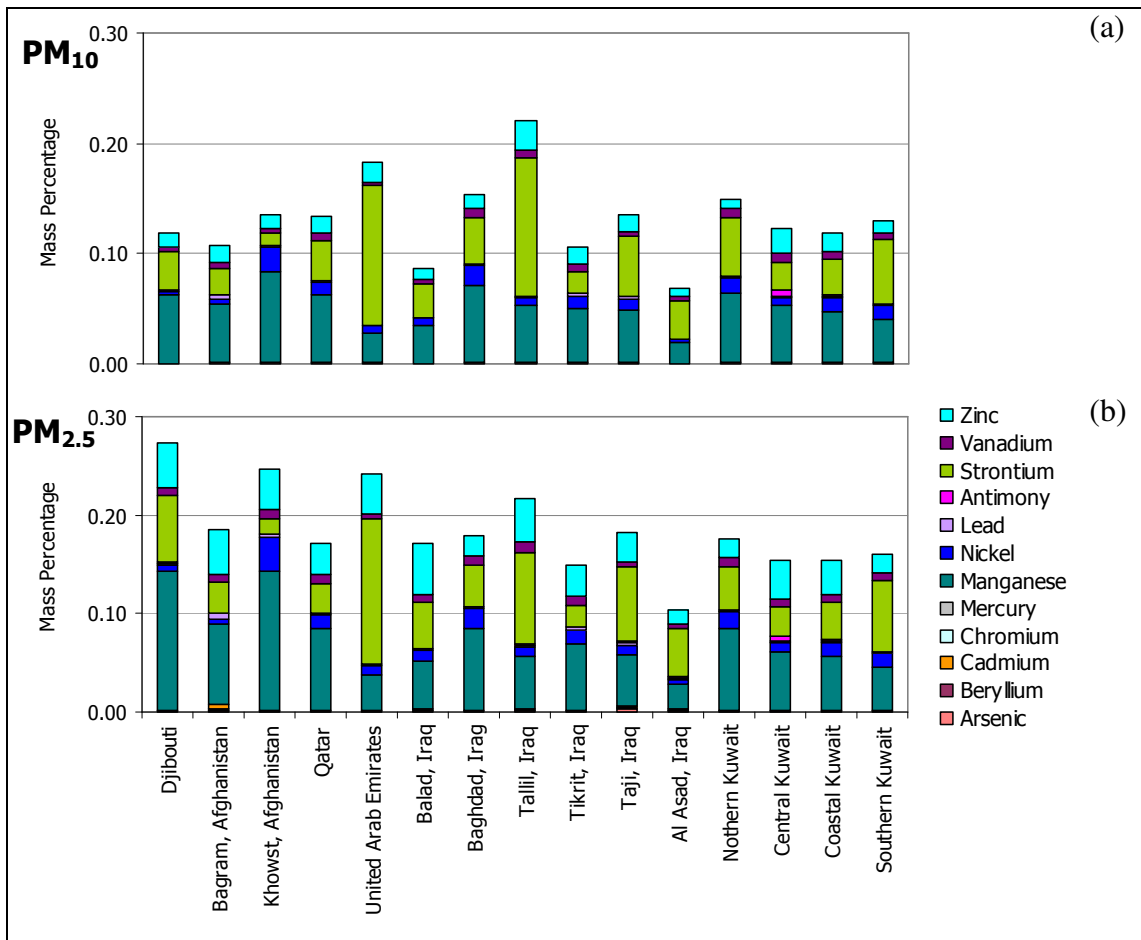


Figure 4-25. Trace element compositions of PM_{10} and $PM_{2.5}$ re-suspended samples as analyzed by P-MS for each of the 15 sites.

The 12 metal concentrations are generally below 0.1%, and only manganese (Mn), strontium (Sr), zinc (Zn), and nickel (Ni) show on the plots. Differences in trace metal chemistry among the 15 sites and two size fractions are also small. Manganese is typical of many soil types, and strontium associated with calcium in minerals such as calcite and dolomite was found in variable amounts at all 15 sites.

The distinct association of lead (Pb), zinc (Zn), cadmium (Cd), arsenic (As), and antimony (Sb) found in some ambient samples at the three Iraq sites of Baghdad, Balad, and Taji (Figs. 4-3, 4-4, 4-5) is not seen in the re-suspensions.

Higher values were found for arsenic at Taji, for cadmium and lead at Bagram, for antimony at Central Kuwait, and for zinc at Balad (Table 4-5, shown in red).

Table 4-5. Trace element compositions of re-suspended PM_{2.5} samples for each of the 15 sites, as analyzed by ICP-MS. The highest trace metal concentrations for each site are shown in red.

Site Locality	Arsenic (As)		Cadmium (Cd)		Lead (Pb)		Antimony (Sb)		Zinc (Zn)	
	Conc	Unc	Conc	Unc	Conc	Unc	Conc	Unc	Conc	Unc
	mass %	mass %	mass %	mass %	mass %	mass %	mass %	mass %	mass %	mass %
Djibouti	0.00058	0.00000	0.00012	0.00001	0.00230	0.00001	0.00029	0.00000	0.04571	0.00025
Bagram, Afghanistan	0.00227	0.00007	0.00544	0.00009	0.00639	0.00004	0.00030	0.00001	0.04651	0.00037
Khowst, Afghanistan	0.00089	0.00042	0.00018	0.00001	0.00291	0.00002	0.00090	0.00000	0.04139	0.00030
Qatar	0.00091	0.00009	0.00014	0.00002	0.00234	0.00001	0.00035	0.00001	0.03159	0.00043
United Arab Emirates	0.00120	0.00003	0.00020	0.00001	0.00080	0.00000	0.00050	0.00001	0.04168	0.00072
Balad, Iraq	0.00148	0.00025	0.00024	0.00001	0.00122	0.00001	0.00059	0.00001	0.05178	0.00046
Baghdad, Iraq	0.00140	0.00010	0.00011	0.00001	0.00144	0.00002	0.00028	0.00001	0.02090	0.00027
Tallil, Iraq	0.00174	0.00019	0.00025	0.00001	0.00175	0.00003	0.00063	0.00001	0.04456	0.00107
Tikrit, Iraq	0.00152	0.00012	0.00016	0.00001	0.00233	0.00004	0.00039	0.00000	0.03066	0.00023
Taji, Iraq	0.00360	0.00112	0.00072	0.00003	0.00314	0.00003	0.00180	0.00003	0.03000	0.00195
Al Asad, Iraq	0.00190	0.00012	0.00038	0.00004	0.00126	0.00002	0.00095	0.00000	0.01400	0.00254
Northern Kuwait	0.00137	0.00011	0.00009	0.00001	0.00157	0.00001	0.00028	0.00001	0.01848	0.00027
Central Kuwait	0.00063	0.00004	0.00013	0.00003	0.00184	0.00001	0.00474	0.00003	0.03930	0.00018
Coastal Kuwait	0.00099	0.00011	0.00011	0.00002	0.00227	0.00001	0.00029	0.00000	0.03337	0.00031
Southern Kuwait	0.00054	0.00011	0.00011	0.00000	0.00139	0.00001	0.00027	0.00000	0.01822	0.00007

4.3.3 Scanning Electron Microscopy of Re-suspended Soils

CCSEM analysis was performed on 15 re-suspended bulk samples using a PM₁₀ size cut and collection on Nuclepore® filters (Fig. 4-26). Similar to the ambient samples (Fig. 4-9 [a]), the dominant phase in 13 of the 15 samples is Si-Al-Mg, which we interpret as clay mineral coatings—masking silicate minerals such as quartz and feldspars, and, to a lesser extent, the carbonate minerals calcite and dolomite. Because of this masking effect, very little quartz was measured by CCSEM in any of the 15 samples. As with the ambient samples, high concentrations of dolomite and/or calcite were analyzed from the UAE and Al Asad, Iraq samples. Part of the dolomite measured on samples from the UAE is assumed to be dolomitization on the surfaces of calcite particles.

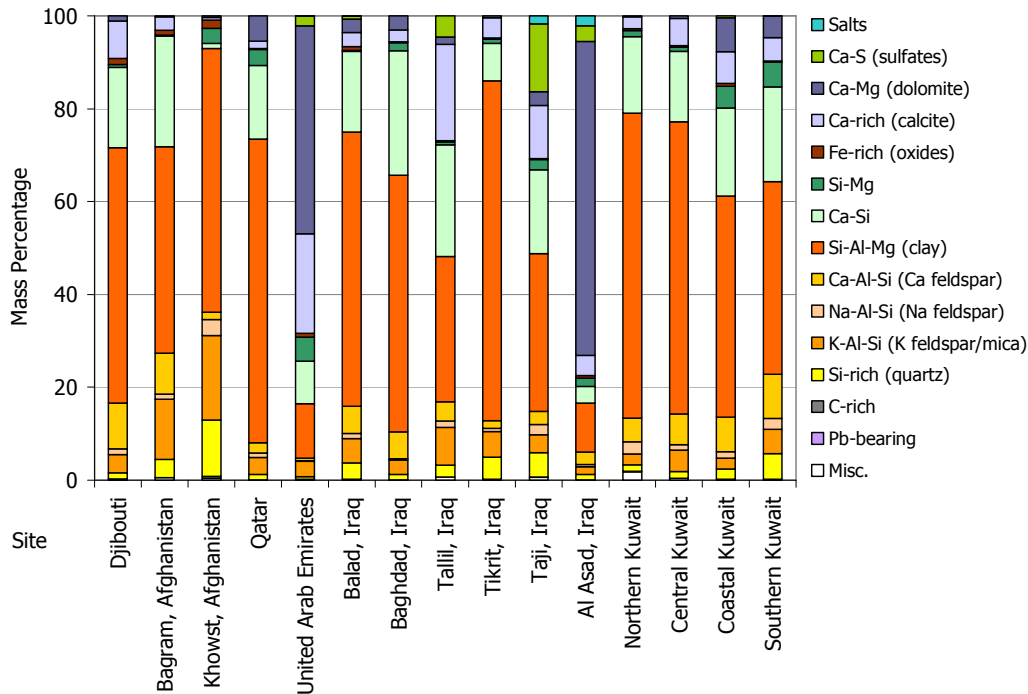


Figure 4-26. CCSEM individual particle analysis on PM₁₀ Nuclepore® filters of re-suspended soils.

4.3.4 Bulk Soil Chemistry

DRI's bulk soil chemical results are presented in APPENDIX D. XRF elemental analysis of the <1000 μm sieved soil samples (Fig. 4-27) points to mineral constituents representing a range of depositional environments found in the Middle East. The SiO_2 contained in quartz, and to a lesser extent in feldspars and clays, ranges from 13% (Al Asad) to 87% (Coastal Kuwait), with 55% as a mean concentration for all 15 sites. All samples were collected close to the air sampling sites and show elemental concentrations largely reflective of regional geology and soils. The Tallil sample is chemically and mineralogically similar to the four Kuwait samples, all taken within 250 km of each other. Djibouti lies in a rift zone, with surrounding plateaus, largely of basaltic volcanics. The Fe_2O_3 and TiO_2 from this sample are contained in the minerals magnetite and ilmenite, both typical of such parental rocks. This sample bears a distinct mafic signature, with low SiO_2 (37%), high Fe_2O_3 (16%), TiO_2 (5%), and CaO (16%).

Loss on ignition (LOI) measures change in mass when the sample is heated to 1050 $^\circ\text{C}$, due to decomposition of carbonates and clay minerals with loss of carbon dioxide, molecular water, and other volatiles. LOI values in the range of 3% to 40%, indicate decomposition of hydrated minerals, carbonates, and salts. The UAE sample has high calcium (42%), and loss-on-ignition (LOI) values (36%); together indicating a large calcitic limestone content. The Al Asad sample has a high LOI value (40%) with less CaO (29%) and more MgO (15%), reflecting abundant dolomite in that region of Iraq.

Similarities in the <1000 μm sieved soil chemistry (Fig. 4-27), re-suspended soil samples (Fig. 4-24), and ambient sample sets (Fig. 4-7) is evidence that a portion of the ambient dust may be from local soils. The <1000 μm fraction contains a much larger proportion of SiO_2 than the finer (PM_{10} , $\text{PM}_{2.5}$) re-suspensions or than the ambient samples because of the large fraction of relatively hard quartz sand and silt in the coarser size fraction.

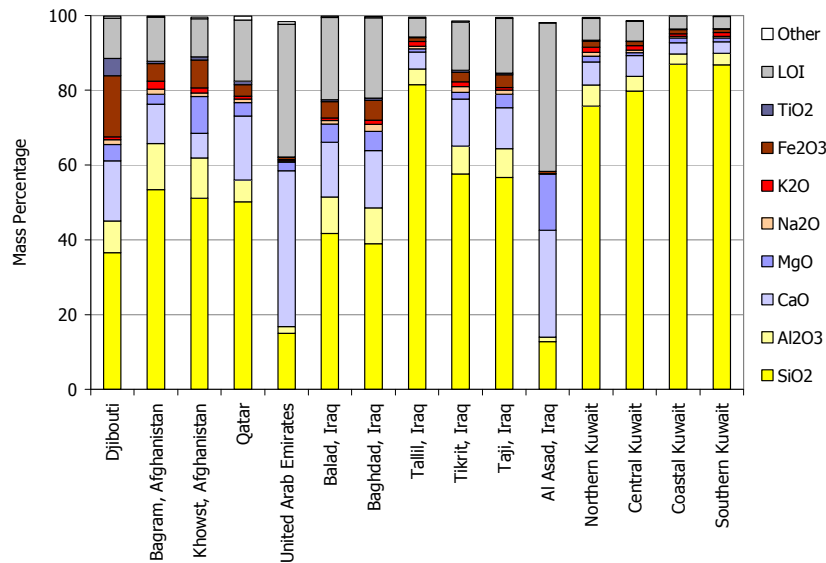


Figure 4-27. Compositional plot showing major elemental chemistry of fifteen <1000 μm sieved bulk samples.

All except UAE and Al Asad contain high concentrations of SiO₂ (quartz). UAE and Al Asad contain substantial amounts of CaO in calcite and dolomite, and Al Asad MgO in dolomite.

5 SUMMARY AND CONCLUSIONS

- This EPMSP demonstrates benefits of integrating analytical results obtained from different measurement techniques, in our understanding of the relative contributions of mineral dusts and other aerosols, as encountered at deployment locations within the USCENCOM AOR. This study includes comparative analysis of TSP, PM₁₀ and PM_{2.5} filter samples collected during a period of one year. It also includes analysis and comparison to 15 bulk samples from each of the military bases throughout the Middle East.
- Aerosol characterization included chemical analysis by XRF, ICP-MS, IC, ICP-OES, and thermal TOT, mineral analysis by XRD, as well as individual particle analysis by CCSEM. Similar chemical and mineralogical analyses were carried out on re-suspended surface soils collected at each site that have the potential to become airborne during high wind events or from human activity.
- The above analyses as well as particle-size distribution, carbonate, pH, electrical conductivity, and XRF analysis also were carried out on the 15 bulk dust samples for the <1000 μm size fraction.
- After validation, all analytical results were compiled on spreadsheets; grouped by sampling site, analytical technique, and chemical species; and posted on the password-protected EPMSP Web page managed and maintained by the DRI.
- Although only about 7% of the days during the 2006/7 year were sampled on Teflon® filters (same percentage for quartz fiber), background levels and areas of concern were identified. Therefore, statistics such as annual averages do not have the same level of confidence as for IMPROVE and STN monitoring programs, where both Teflon® and quartz fiber filters are sampled on 1-in-3 day or 1-in-6 day sampling schedule, giving 33% or 16.7% of the days per year sampled.
- Short-term dust events—exacerbated by dirt roads, agricultural activities, and disturbance of the desert surface by motorized vehicles—are largely responsible for exceedance of PM annual exposure guidelines and standards (Table 4-2). The highest annual average for PM₁₀ was recorded at Tallil (PM₁₀ of 303 μg/m³), followed by Tikrit, and Central Kuwait. All sites exceed the USACHPPM 1-year Air-MEG value of 50 μg/m³ for PM₁₀ and the 1-year Air-MEG value of 15 μg/m³ for PM_{2.5}. The USEPA annual NAAQS of 50 μg/m³ for PM₁₀ (revoked 2006-12-17) and of 15 μg/m³ for PM_{2.5} subsequently were both exceeded at all sites.
- In comparison, average particulate matter and PM_{2.5} mass and chemical concentration levels from the Middle East deployment sites are—except for a few instances such as nitrate, sodium, and rubidium—up to as much as ten times greater than those from five rural (IMPROVE) and five urban (STN) sites in the southwestern U.S.
- In general, we do not consider dust from studied areas in the Middle East to be out of the ordinary. Comparison of dust samples from the 15 Middle East sites to dust from the U.S., Sahara, and China shows similar chemical and mineralogical constituents in most cases. Generally, all dust samples contain mixtures of silicate

minerals, carbonates, oxides, sulfates, and salts in various proportions. Differences lie in the relative proportions of these minerals and chemical components in different soils. In comparison to the Sahara, China, U.S., and world dusts, Middle East samples had lower proportions of SiO_2 and higher proportions of CaO and MgO . The last two components are contained in carbonates, such as calcite and dolomite in the soil, more evident at UAE and Al Asad. Fe_2O_3 and MnO occur as iron and manganese oxides in greater concentrations in the Sahara, China, and U.S. dust compared to the 15 Middle East sites.

- Mineralogical content (Fig 4-21), chemical composition (Figs. 4-24, 4-27), and to a lesser extent individual particle analysis (Fig. 4-26) of sieved and re-suspended dust as well as ambient samples (Fig. 4-7) from each site, bear the signature of that region's geology to some extent. Examples include high quartz content of the four Kuwait sites, high percentage of calcite in the UAE samples, high dolomite content of the Al Asad samples, and titaniferous magnetite dust from Djibouti. Dust events subsequently result in short-term elevated levels of soil-forming elements (Fig. 4-6) including magnesium (Mg), aluminum (Al), silicon (Si), potassium (K), calcium (Ca), titanium (Ti), vanadium (V), manganese (Mn), iron (Fe), rubidium (Rb), strontium (Sr), zirconium (Zr), and barium (Ba).
- Events at Baghdad, Balad, and Taji not corresponding to dust storms resulted in elevated trace metal concentrations at these sites (Figs 4-3, 4-5). The metals that vary simultaneously with each other (Fig. 4-4) include lead (Pb), arsenic (As), cadmium (Cd), antimony (Sb), and zinc (Zn)—all concentrated in the $\text{PM}_{2.5}$ size fraction. CCSEM results (Fig. 4-9 [b]) also indicate that lead (Pb) concentrated in the fine size fraction (0.5–1.0 μm). Comments on field data sheets imply that these smoke events are from burn pits impacting the monitoring sites but may also be ascribed to meteorological conditions prevailing during the winter months or a combination of these two factors.



Figure 5-1. Open burn pit typical of Forward Operating Bases and Forward Operating Sites (FOB/FOS) where trash, human and medical waste, and plastic are often burned acknowledgement: Major Dennis S. Palalay, USACHPPM, unclassified presentation, 15 May 2006). Tires, oil, and metal objects (e.g., batteries, electronic circuit boards, and ammunition) also can be burned resulting in emission of trace metals into the atmosphere.

- In addition to the burn pits, a major potential source of lead (Pb) and associated zinc (Zn), cadmium (Cd), arsenic (As), and antimony (Sb) in the Baghdad-Balad-Taji region are emissions from secondary lead smelters (<http://www.cpa-iraq.org/business/industries/Battery%20Co.xls>.) and related battery manufacturing facilities impacting on the population. Since Iraq uses leaded gasoline, vehicle emissions are a contributing source of lead in the atmosphere. Lead from vehicles previously deposited on dirt roads is also continually being re-suspended and may for many years thereafter be a source of aerosol lead. Exploded ordnance also may be a minor contributor of heavy metals in the air during events. Under fall to spring meteorological conditions, heavy metal pollutants may be trapped within the boundary layer and impact military bases at Baghdad, Balad, and Taji as well as the Iraqi population living along at least a 75 km stretch of the Tigris River valley. Secondary lead smelting facilities also were reported at Fallujah (<http://minerals.usgs.gov/minerals/pubs/country/2001/izmyb01.pdf>). Lead smelters were found to be major sources of lead in Cairo's ambient atmosphere [Abu-Allaban, 2007]. Melting down of old circuit boards and other electronic components for their metals content was shown to expose communities to extremely high levels of dioxins and metals such as lead, cadmium, and mercury [Carroll, 2008].
- CCSEM results and secondary electron imagery (Figs. 4-13 to 4-16) show that quartz and other silicate minerals and, to a lesser extent, dolomite and calcite particles are coated by a thin Si-Al-Mg layer, possibly the clay minerals palygorskite and/or montmorillonite/illite.
- Carbon chains (Figs. 4-12 [a], 4-14[c]) are from combustion sources, possibly burn pits or diesel vehicle emissions.
- Further research areas included looking for freshly fractured shards of quartz. Several hundred SEM secondary electron images of individual particles from all 15 sites provided no evidence of such freshly fractured quartz grains. In all instances, quartz grains had rounded edges and were generally coated by clay minerals and iron oxides.
- Transmission Electron Microscope (TEM) measurements for airborne asbestos were performed on one Nuclepore® filter from each site. No asbestos fibers were found.
- CCSEM analysis of several million individual particles showed not more than 2.5% carbon by mass on average at any of the sites, with the highest average carbon abundances measured on PM_{2.5} at Bagram and Baghdad.

6 RECOMMENDATIONS

Recommendations are two-fold in nature: first, for remediation (which is already taking place in theater), and second, for future investigations.

6.1 Remediation

This study characterized three main air pollution sources: geological dust, smoke from burn pits, and until now unidentified lead-zinc smelters and battery-processing facilities. Although some remediation issues are currently being addressed by DoD, they were further identified by this study:

- Geological dust. Little can be done about dust from regional dust storms. Dust at FOB/FOS, however, can be mitigated using best management practices (e.g., watering, spraying with dust suppressants, application of gravel, restricting movement, minimizing disturbance) to lower the local dust emission potential. Of health concern are elevated PM_{2.5} levels. We recommend that continuous PM_{2.5} monitors (beta gauges or similar) be installed at each of the military sites, also those sites not included in this study. This will provide information on the relationship between PM_{2.5} levels, potential health effects, and effectiveness of dust-containment practices.
- Burn pits. Open burning contributes to a cloud of smoke hanging over military bases, especially during winter months. New incinerators were installed at Balad (Anaconda Times, June 20, 2007) to take care of garbage. Toxic metal objects and other combustible products, however, such as wood, paint, plastic, tires, batteries, electronic circuit boards, ammunition, and petrochemical products may still end up in burn pits. To prevent emissions of dioxins, polycyclic aromatic compounds, volatile organic compounds, and toxic metals, we recommend stopping use of burn pits. A solution which is already being followed in theater is to bury open waste by covering it with dirt. This also will prevent spontaneous combustion and smoldering of the dump.
- Although challenging in these difficult times, it is important to locate lead smelting and battery manufacturing as well as electronic component smelting facilities in the Baghdad-Balad-Taji region of the Tigris River valley. The impact of heavy metal and dioxin fumes on peoples' health should be pointed out to Iraq authorities. When found, battery manufacturing or electronic component smelting facilities should be moved downwind and outside residential areas to minimize human exposure. If practical, aerosol monitoring at and in the vicinity of lead smelters will provide information on the contribution of this source type to ambient air quality.

6.2 Future Investigations

- A review of the EPMS database to assess data gaps that need to be filled, to provide information required by the U.S. Department of Defense.
- This report summarizes analytical results through graphical representations and tables, and provides information obtained directly from these. To better understand interrelationships among sites, seasonal, and chemical parameters, further data analysis including Principal Components Analysis (PCA), Factor Analysis (FA), Multiple Linear Regression, Analysis of Variance, and Cluster Analysis are recommended. Use of receptor models, such as Positive Matrix Factorization (PMF) and Chemical Mass Balance (CMB), may provide further information on source types impacting each site.

- We recommend further analysis of TOT data for elemental (EC) and organic (OC) carbon to assess artifact contribution and perhaps generate results that can be useful in further studies.
- The OC artifact problem remained unresolved throughout this study. This is largely ascribed to the way in which filter packs were shipped, stored, and handled in the field. A month-long intensive study during the winter, including collection and analysis of new sets of quartz fiber and Teflon® filters at one or more of the sites (e.g., UAE, Qatar, Balad, Taji and Northern Kuwait), should be considered. This will provide better information on combustion processes (including oil combustion, gasoline and diesel vehicle emissions, gas field flares, and burn pits) impacting these regions.
- Source characterization of burn pits and secondary smelting operations, including measurement of trace metals, dioxins, PAHs, and VOCs.
- Identification, source characterization, and quantification of emissions from battery smelting, manufacturing facilities, and electronic circuit board smelting operations to better understand their potential health impact.
- Detailed mineralogical investigation of dust coatings on mineral grains to understand their capability of absorbing trace metals and organic compounds, and potential health impact.
- Assessment of results from this study of dust storms as well as burn pit and high trace metal events, in terms of 10-hour NIOSH and 8-hour OSHA health standards and short-term CHPPM Air-MEGs.
- Toxicological study of dust including that collected in the ambient atmosphere as well as re-suspended dust of the 15 soils. For such experimental studies, approximately two-to-three grams of respirable dust needs to be collected.
- Gravimetric data from collocated continuous PM samplers such as beta attenuation monitors can be correlated with both the Teflon® and glass fiber filter mass measurements from this EPMS study, to assess relationships among various mass measurements.
- For each site, evaluate chemical and mineralogical results in conjunction with meteorological data, to better understand their relationships and impact on human health at the military bases.
- Regular one-in-six day monitoring of particulate matter (PM₁₀ and or PM_{2.5}) at bases which operate for periods greater than one year.

7 ACKNOWLEDGEMENTS

1. We acknowledge contributions by the military public health soldiers, sailors, and airmen whose efforts were necessary to complete the Enhanced Particulate Matter Surveillance Program (EPMS). The dedicated effort shown by all participating units in the field, with operating the sampling equipment and collecting filter and grab samples, is greatly appreciated.

Participating units included:

- 61st Medical Detachment (Preventive Medicine) (MED DET (PM))
- 223rd MED DET (PM)
- 224th MED DET (PM)
- 227th MED DET (PM)
- 452nd MED DET (PM)
- 790th MED DET (PM)
- 898th MED DET (PM)
- 903rd MED DET (PM)
- 981st MED DET (PM)
- 1437th MED DET (PM)
- 379th Expeditionary Medical Group (EMDG)
- 380th EMDG
- 386th EMDG
- 4th Infantry Division
- 10th Mountain Division
- 82nd Airborne Division
- Combined Joint Task Force Horn of Africa Surgeon Cell
- Forward Deployable Preventive Medicine Unit (FDPMU) - North
- FDPMU-South
- US Central Command Surgeon's Office
- Combined Forces Land Component Command Surgeon's Office
- US Central Command Air Forces Surgeon's Office
- US Navy Central Command Surgeon's Office
- Multi-National Corps - Iraq
- Combined Joint Task Force (CJTF) - 76
- CJTF – 82

2. We acknowledge major contributions from the two collaborating laboratories:

- RTI International, specifically Dr. R.K.M."Jay" Jayanty and Edward Rickman for the filter processing and chemical analysis.
- RJ Lee Group Inc., specifically Gary Casuccio and Traci Lersch for the CCSEM and SEM individual particle analysis.

3. Thanks also are due to several researchers at DRI who contributed their expertise to the analyses and this report:

- Michał Skiba for the XRD analysis.
- Todd Caldwell for analysis of the 15 soil samples.
- Steve Kohl for the XRF, ion and carbon analysis of the 30 re-suspended filter samples.

4. Finally, three individuals deserve special recognition for their contributions:
- Many dedicated hours spent by Greta Engelbrecht on data validation, compilation of results, and providing graphical representations.
 - Support by James Sheehy and John Kolivosky of USACHPPM, from the inception of project to its completion, is greatly appreciated.

8 GLOSSARY

8.1 Acronyms and Mnemonics

1-Year Air-MEG	1-Year Military Exposure Guideline
AOR	Area of Responsibility
BEI	Backscattered Electron Image
CAS	Chemical Abstracts Service Registry
CCSEM	Computer Controlled Scanning Electron Microscopy
DoD	Department of Defense
DOEHRS	Defense Occupational and Environmental Health Readiness System
EDS	Energy Dispersive Spectroscopy
EDXRF	Energy Dispersive X-ray Fluorescence Spectrometry
EPMSP	Enhanced Particulate Matter Surveillance Program
FOB/FOS	Forward Operating Bases and Forward Operating Sites
IC	Ion Chromatography
ICP-MS	Inductively Coupled Plasma Mass Spectrometry
ICP-OES	Inductively Coupled Plasma Optical Emission Spectrometry
IMPROVE	<u>I</u> nteragency <u>M</u> onitoring of <u>P</u> rotected <u>V</u> isual <u>E</u> nvironments
IPA	Individual Particle Analysis
LOI	Loss on Ignition
MEG	Military Exposure Guideline
NAAQS	National Ambient Air Quality Standards
NIOSH	National Institute of Occupational Safety and Health
NWA	National Wildlife Area
NWR	National Wildlife Refuge
OEHS	Occupational and Environmental Health Surveillance Portal
OSHA	Occupational Safety and Health Administration
PAH	Polycyclic aromatic hydrocarbons
PM ₁₀	Particulate matter less than 10 micrometer (µm) in aerodynamic diameter
PM _{2.5}	Particulate matter less than 2.5 micrometer (µm) in aerodynamic diameter
PSD	Particle Size Distributions
REL	Recommended Exposure Limit
SEI	Secondary Electron Images
SEM	Scanning Electron Microscopy
STN	Speciation Trends Network
TEM	Transmission Electron Microscope
TOT	Thermal Optical Transmission
TSP	Total suspended particulate matter
TWA	Time weighted average
UAE	United Arab Emirates
US EPA	U.S. Environmental Protection Agency

USACHPPM	U.S. Army Center for Health Promotion and Preventive Medicine
USCENTCOM	U.S. Central Command
VOC	Volatile organic compound
WHO	World Health Organization
XRD	X-ray Diffractometry, X-ray Diffraction
XRF	X-ray Fluorescence Spectrometry
$\mu\text{g}/\text{m}^3$	Micrograms per cubic meter

8.2 Geological Terms

Amphibole	Group of chain silicate minerals – calcium magnesium iron sodium silicate
Basalt	Dark colored volcanic rock containing high percentages of calcium, magnesium, iron and aluminum minerals
Ca feldspar	Calcium aluminum silicate mineral - also plagioclase, anorthite
Calcite	Calcium carbonate mineral
Chlorite	Group of sheet silicate minerals – magnesium iron aluminum silicate mineral
Clay	Mineral group of layered aluminum silicates - including kaolinite, illite, montmorillonite, and palygorskite
Dolomite	Calcium magnesium carbonate mineral
Evaporites	Water-soluble mineral sediments (salts) resulting from the evaporation of bodies of surface water
Feldspar	Cleaved crystalline calcium sodium potassium aluminum silicate mineral group
Gypsum	Calcium sulfate hydrate mineral
Halite	Table salt – sodium chloride
Hematite	Iron oxide mineral
Hornblende	Member of amphibole group of chain silicate minerals – calcium magnesium sodium iron silicate
Igneous rock	Rock formed by solidification and crystallization of cooled molten magma
Illite	Clay mineral – potassium aluminum silicate
Ilmenite	Titanium iron oxide
K feldspar	Potassium aluminum silicate mineral - also orthoclase or microcline -
Kaolinite	Clay mineral – aluminum silicate
Limestone	Sedimentary rocks that are composed largely of the mineral calcite
Loess	Non-stratified deposit of silt (sediment with particles 2-64 micrometers in diameter) laid down by wind action
Mafic	Dark colored igneous rock containing high percentages of calcium, magnesium, iron and aluminum silicates
Magnetite	Iron oxide
Mica	Group of sheet silicate minerals - potassium aluminum silicate mineral, also containing iron, magnesium and calcium
Montmorillonite	Clay mineral group – calcium sodium magnesium iron aluminum silicate - also smectite

Na feldspar	Sodium aluminum silicate mineral - also plagioclase, albite
Olivine	Magnesium iron silicate occurring in silica poor basaltic rocks
Palygorskite	Clay mineral – magnesium aluminum silicate - also attapulgite
Plagioclase	Calcium sodium aluminum silicate - also albite and anorthite
Pyroxene	Group of chain silicate minerals – calcium magnesium sodium iron silicate – occurring in many basaltic rocks
Quartz	Silicon oxide mineral - common component of most sands, silt, sandstones, quartzite and granites
Sandstone	Sedimentary rock composed mostly of sand-sized grains cemented by clay, silica, carbonate, or iron oxide
Silt	Sediment of fine quartz particles, <0.075 mm diameter
Wadi	Valley or dry riverbed that contains water only during times of heavy rain.

8.3 Sampling Sites, USCENTCOM AOR

<i>Site No.</i>	<i>Site ID</i>	<i>Site Locality</i>
1	DJI_LEM	Djibouti
2	AFG_BAG	Bagram, Afghanistan
3	AFG_SAL	Khowst, Afghanistan
4	QAT_UDE	Qatar
5	UAE_DHA	United Arab Emirates
6	IRQ_ANA	Balad, Iraq
7	IRQ_VIC	Baghdad, Iraq
8	IRQ_ADD	Tallil, Iraq
9	IRQ_SPE	Tikrit, Iraq
10	IRQ_TAJ	Taji, Iraq
11	IRQ_ALA	Al Asad, Iraq
12	KUW_BUE	Northern Kuwait
13	KUW_AAS	Central Kuwait
14	KWT_SHU	Coastal Kuwait
15	KUW_ARI	Southern Kuwait

9 REFERENCES

- Abu-Allaban, M., D.H. Lowenthal, A.W. Gertler, and M. Labib (2007), Sources of PM10 and PM2.5 in Cairo's ambient air, *Environmental Monitoring and Assessment*, 133, 417-425.
- Al-Awadhi, J. M. (2005), Dust fallout characteristics in Kuwait: a case study, *Kuwait Journal of Science and Engineering*, 32, 135-151.
- Al-Juboury, A. I. (2006), Authigenic palygorskite in the Middle Miocene rocks of Iraq: environmental and geochemical indicators, *Geophysical Research Abstracts*, 8, 01584.
- Buringh, P. (1960), Soils and soil conditions in Iraq, Directorate General of Agricultural Research and Projects, Ministry of Agriculture, Baghdad, Republic of Iraq.
- Çagatay, M. N. (1990), Palygorskite in the Eocene rocks of the Dammam Dome, Saudi Arabia, *Clays and Clay Minerals*, 38, 299-307.
- Caquineau, S., M.-C. Magonthier, A. Gaudichet, and L. Gomes (1997), An improved procedure for the X-ray diffraction analysis of low-mass atmospheric dust samples, *European Journal of Mineralogy*, 9, 157-166.
- Carroll, C., and Essik, P. (2008), High-tech trash, *National Geographic*, 213, 64-81.
- Chung F. H. (1974), Quantitative interpretation of X-ray diffraction patterns of mixtures. I. Matrix-flushing method for quantitative multicomponent analysis, *Journal of Applied Crystallography*, 7, 519-525.
- Clarke, F. W. (1916), *The data of geochemistry*, 3rd edn., United States Geological Survey, Washington, D.C.
- Engelbrecht, J. P., L Swanepoel, J.C. Chow, J.G. Watson and R.T. Egami (2001), PM2.5 and PM10 Concentrations from the Qalabotjha Low-Smoke Fuels Macro-Scale Experiment in South Africa., *Environmental Monitoring and Assessment* 69, 1-15.
- Esteve, V., J. Rius, L. E. Ochando, and J. M. Amigó (1997), Quantitative x-ray diffraction phase analysis of coarse airborne particulate collected by cascade impactor sampling, *Atmospheric Environment* 31, 3963-3967.
- Esteve V., et al. (1997), Quantitative x-ray diffraction phase analysis of coarse airborne particulate collected by cascade impactor sampling, *Atmospheric Environment* 31, 3963-3967.
- Goudie, A. S., and N.J. Middleton (2006), *Desert Dust in the Global System*, 287 pp., Springer.
- Kahlaf, F. I., A. Al-Kadi, and S. Al-Saleh (1985), Mineralogical composition and potential sources of dust fallout deposits in Kuwait, *Sedimentary Geology*, 42, 225-278.
- Labban, R., J.M. Veranth, J.C. Chow, J.P. Engelbrecht and J.G. Watson (2004), Size and Geographical Variation in PM1, PM2.5, and PM10: Source Profiles from Soils in the Western United States, *Water, Air, and Soil Pollution*, 157, 13-31.

- Olson, D. A., and G.A. Norris (2005), Sampling artifacts in measurement of elemental and organic carbon: Low-volume sampling in indoor and outdoor environments, *Atmospheric Environment*, 39, 5437-5445.
- Potter, R. M., and Rossman, G.R. (1977), Desert varnish: The importance of clay minerals, *Science*, 24, 1446-1448.
- Rietveld H.M. (1969), A profile refinement method for nuclear and magnetic structures, *Journal of Applied Crystallography*, 2, 65-71.
- Sturges W.T., et al. (1989), Semi-quantitative X-ray diffraction analysis of size fractionated atmospheric particles, *Atmospheric Environment*, 23, 1083-1098.
- Sturges, W. T., R.M. Harrison, and L.A. Barrie (1989), Semi-quantitative X-ray diffraction analysis of size fractionated atmospheric particles, *Atmospheric Environment*, 23, 1083-1098.
- Yamate, G., S.C. Agarwal, and R.D. Gibbons (1984), Methodology for the Measurement of Airborne Asbestos by Electron Microscopy, *EPA Contract No. 68-02-3266*.